Determination of safe mooring windows based on wind predictions

C. J. Eggermont

Determination of safe mooring windows based on wind predictions

Student number: 4357892

Graduation committee:

Dr. Ing. M.Z. Voorendt	Hydraulic Structures
Dr.-Ing. S. Schreier	Ship Hydromechanics
Ir. A.J. van der Hout	Ports and waterways
Dr. Ir. A.F.J. van Deyzen	Royal Haskoning DHV

Picture front cover: Port of Rotterdam, 2020

Preface

Before you lies my master thesis "Determination of safe mooring windows based on wind predictions" investigating mooring forces caused by wind forcing on large container vessel. It has been written to fulfill the graduation criteria for the masters degree in Hydraulic engineering at the Technical University Delft. This study lasted from November 2020 until July 2021.

The project was executed based on a request from Royal HaskoningDHV to find a more time efficient and scalable method to obtain mooring force predictions for their clients. Being a combination of many input parameters and different areas of theory, this determination was not easy. However, I have managed to propose a solution which, under certain conditions, can be applied to determine the peak line forces.

My interest in data analysis and Python modelling combined with my passion for large port operations, were essential to bringing this research to a positive end. I am happy that after my graduation I can continue working in this very interesting field at RHDHV.

I want to thank my supervisors for their help in grasping the relevant theories and their guidance in my first real research project. The positive reactions and critical quality assessments helped creating a better study.

Finally, I want to thank my parents for their support and spelling checking abilities, my friends for talking through the challenges of the graduation process and helping me relax on the side and my girlfriend for helping me stay motivated even during the ,not so stimulating, circumstances caused by the covid-19 lockdown.

Enjoy your reading,

Coen Eggermont

Rotterdam, July 2nd, 2021

Summary

Over the last few decades, the increase in size of container vessels has led to massive vessels carrying up to 24,000 twenty foot equivalent units. With lengths up to 400 meters and widths of over 60 meters, these giants present new challenges on port operations and infrastructure. For ports it is essential that they can accommodate these vessels to stay up to date with developments in global shipping. However, to make sure these large vessels can be moored, quays must be adjusted or new quays must be built. As these developments take much time, a short term solution can lie in the use of under-designed quays during mild weather, wave and current conditions, as in these cases the mooring force limits are not exceeded. To determine these safe mooring windows, an accurate determination of the mooring forces is required.

The large stacks of containers on top of the vessels create large vertical areas susceptible to wind forcing. The large masses reduce the resonance frequencies of the moored vessel systems. As wind fluctuations in time are predominantly low frequency fluctuations, and wind forcing is transferred through the large wind areas, dynamic mooring analysis for these vessels is especially important when they are subjected to strong winds. Given the fact that these vessels are often moored at quays mostly sheltered from current and waves, this study focuses solely on wind as the excitation force. Currently, these dynamic mooring analysis projects require experts investigating the situation and using dynamic mooring analysis software packages to find responses of the system for different cases. This is a time intensive and therefore expensive process. Quicker calculation could be achieved using frequency domain analysis. However, this requires a linear system. As line elongation curves and line angle fluctuations result in non linearities a numerical approach is necessary.

Finding a less time intensive method for approximation of these responses will lead to a more widely used safety assessment based on the dynamic response of a moored vessel system. In this study the focus lies on the occurring line forces as these are governing for the ultimate limit state of the system. When these forces become too large, failure of lines, winches or bollards may occur.

The goal of this study is to determine how safe mooring windows based on maximum mooring forces due to the dynamic response of a moored container vessel, subjected to time varying wind forcing, can be approximated without using full case specific dynamic mooring analysis simulations.

To do this a number of steps are executed:

1. The relevant input parameters are derived from the real life moored vessel situation and related to different terms in equations of motion for a dynamic system.

2. The dynamic response is modelled using a self made conceptual Python model. In this model the different spatial data and input parameters are combined with a numerical solver to find the response of the system in the time domain, along with the generated line forces.

3. An extreme value analysis method is chosen and used to create comparable peak line force values for different simulated cases.

4. The industry standard assumptions currently in use are analysed and their influence on the occurring peak line forces is determined.

5. The influence of the relevant parameters is investigated and first or second order influence relations are determined to measure the relative influence of these parameters

6. The different influence relations are combined to form a first proposal for a peak line force prediction formula. The acquired polynomial is compared to a number of simulated cases to determine its performance.

7. The shortcomings and assumptions in the modelling and data analysis are discussed and the uncertainties in real life values for the input parameters are discussed.

Using this approach and the proper extreme value analysis method, the occurring maximum line forces generated by the dynamic response of a container vessel subjected to wind forcing can be approximated by analysis of a dataset of peak line forces for different mooring cases. The dataset is generated using a dynamic mooring analysis model and its accuracy compared to real life situations is therefore limited by the accuracy of the model. The influences were based on deviations from a certain reference case to create a time efficient method to investigate influence of different parameters without a need for too many simulations, which would result in very large computation times. The acquired first proposal for a line force approximation polynomial performs reasonably well, compared to the results of the conceptual model, for mooring cases in which especially the mooring line angles are relatively close to the used reference case situation. For these cases, a first analysis of accuracy resulted in maximum deviations from the conceptual model results of less than 15%. For these cases this polynomial could be implemented in combination with a safety factor to use in operational decision making, provided the used conceptual model provides acceptably accurate results. The maximum peak line forces for large container vessels in time varying wind fields can be estimated using the proposed polynomial combined with input information on wind area, wind coefficients, predicted mean wind speed, mooring configuration, line types, damping, mass and moment of inertia including the added mass and moment of inertia. For cases which are not similar to the reference case, errors in the polynomial performance of more than 15% occur.

Further research using different mooring cases and a more advanced dynamic mooring analysis model, also investigating the covariance between parameters, will lead to better overall performance of the polynomial. The accuracy of the used models, and the resulting polynomial, can be better assessed if more real life measurements were executed. Furthermore, additional research in the spatial and temporal variance of the wind field at the quay is recommended as this proved to be an important influence parameter which is currently neglected in industry standard methods. As this information is currently often unavailable, the polynomial is based on input that is currently used in dynamic mooring analysis methods.

Table of Contents

1. Introduction

As modern developments in shipping result in larger and larger container carriers, one of the challenges in future port development is creating quays with sufficient capacity for the largest container vessels to moor. The size of container ships is usually expressed in TEU (Twenty foot Equivalent Unit), and relates directly to the amount of cargo that can be shipped at once. To indicate the rapid growth in ship sizes one can look at the ships with the largest TEU over the past decades. Figure 1.1 gives an overview of the developments in ship sizes up to 2017. From the figure it can be clearly seen that the growth in container vessel sizes is significant at the least.

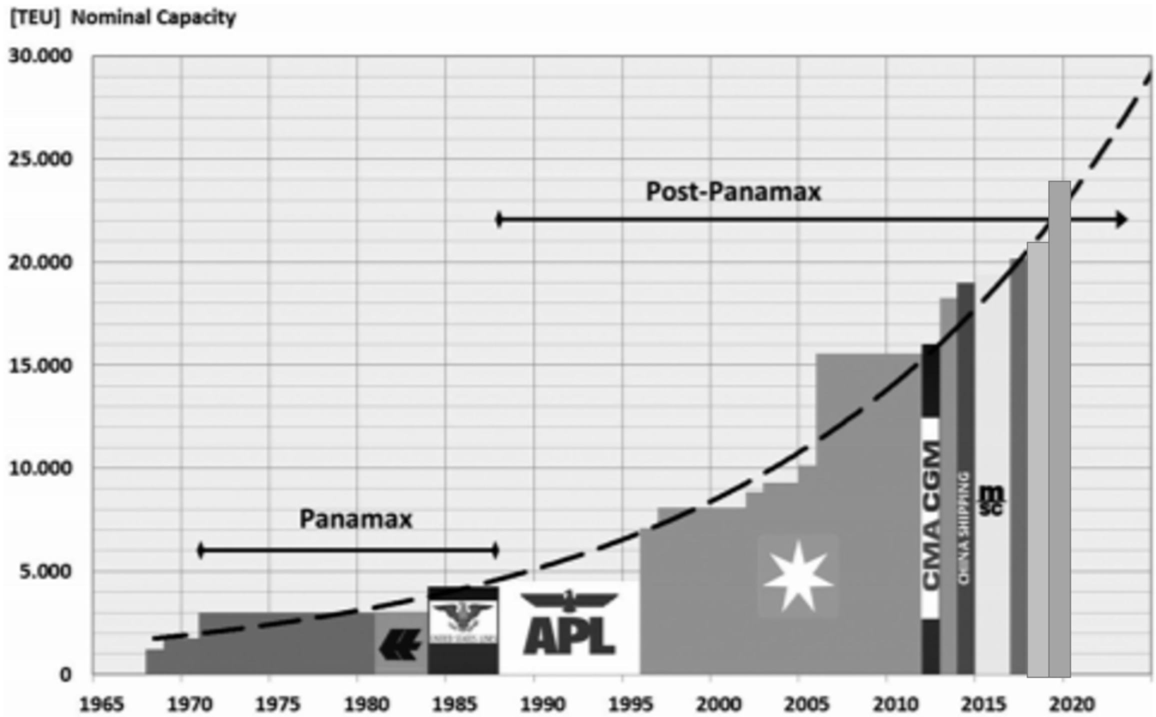

Figure 1.1: Record breaking ship sizes and their initiators (Malchow, 2017, (Modified from source))

For a port to remain relevant for container operations, having sufficient mooring capacity for these giants is a must. However, development of new berths and quays or the upgrading of older quays to the newly posed requirements is a time consuming exercise. How can a port deal with the increase of both the maximum size and frequency of visit of these giants? To facilitate mooring possibilities for large container vessels while maintaining safety, an accurate determination of the mooring forces is essential. This report studies how these mooring forces can be determined and how this can be used to facilitate the forecast of safe mooring conditions.

2. Problem analysis

An overview of the subject is presented, presenting its place in the larger system in section 2.1. Some general information on mooring and relevant forces is given in Section 2.2 and the focus of the study is presented in Section 2.3. Important theory is described in Sections 2.4 and 2.5. Finally, current approaches for determination of mooring forces are discussed in Section 2.6 and the theoretical gap is presented in Section 2.7

2.1 Place of this study in a port system

From a port planning perspective the increasing size of the container vessels requires larger waterway and berth dimensions. The increase in draught results in more dredging maintenance and revaluation of quay wall design. Finally, the large masses and dimensions influence the dynamic behaviour of a moored vessel. This behaviour poses two types of challenges.

Firstly, the actual movements of the vessel and their influence on the operability of a container terminal. At a container terminal, containers are lifted from or placed on the vessel using cranes. When vessel movements or their velocities become too large this cannot be safely executed and the operations come to a halt. Periods during which this is the case are called "downtime". The downtime of terminals depends on the movement of the vessel and the ability of a crane driver or automatic crane to carry out their work safely under increasingly challenging circumstances. This does not only require a physical assessment of vessel behaviour but also a study into crane driver performances and safety. Guidelines suggest the maximum movement conditions for a 95% efficient operation as given in Table 2.1. The different principle motions used in this table are the general movement directions of vessels, which are presented in Figure 2.1.

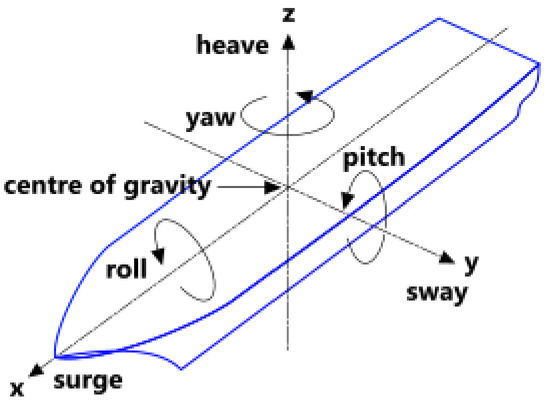

Figure 2.1: Principle motion directions (RAO)

Principle motion	Maximum allowable significant motion amplitude	Unit
Surge	0.2 to 0.4	m
Sway	0.4	m
Heave	0.3	m
Roll	1.0	°
Pitch	0.3	°
Yaw	0.3	°

Table 2.1: Operational vessel movement limits for 95% efficiency (PIANC 2012)

Apart from the operational limits, movement of a vessel generates forces in the lines and fenders. The line forces are transferred to the vessel via the winches and to the quay via bollards whereas the fender forces are transferred directly via the contact area. Determination of these forces is important to ensure none of the components fail. If failure occurs, large damages or life threatening situations may occur.

Figure 2.2 presents an overview of the different aspects relevant to the mooring of large container vessels. It indicates the different challenges that play a part in the increase in size of container vessels. From the design and port planning to maintenance, quay design, dredging and finally operational decisions regarding safety and operationality.

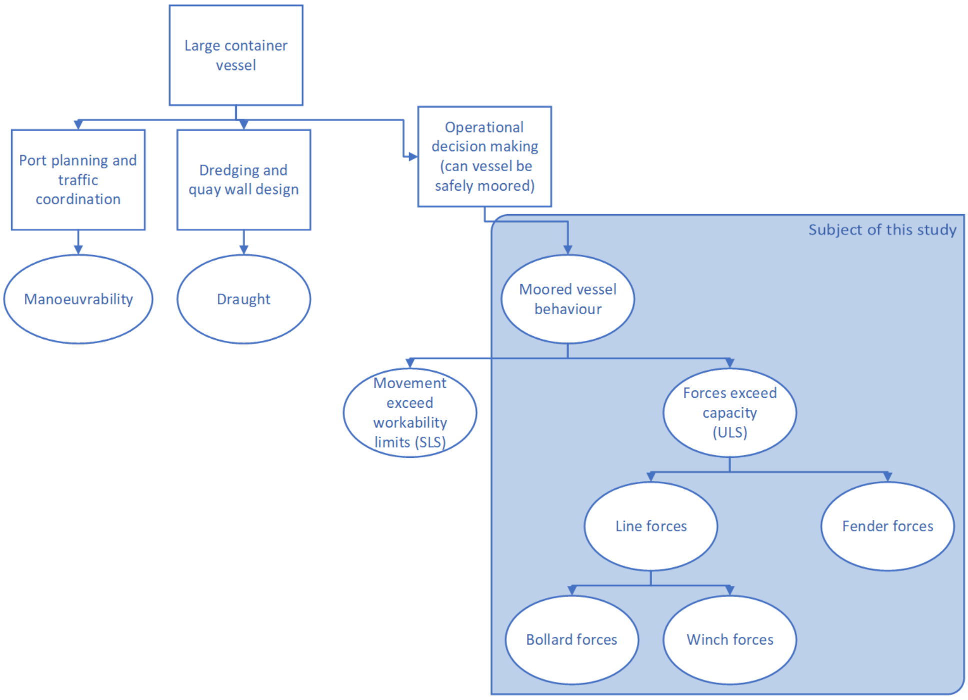

Figure 2.2: Overview of different aspects of large vessel mooring (RHDHV)

Current quays are often not designed for such large container vessels. Building new or updating old quays to fit the new design criteria takes months or years. A short term solution can lie in finding a way to solve problems in the suitable quay availability by using older quays under specific conditions. If the mooring forces do not exceed the design forces during certain hydro-meteo conditions, this can lead to time frames during which mooring of the vessels is safe. To determine these time frames, moored vessel behaviour must be assessed in order to determine the mooring forces exerted on the quays and their bollards.

2.2 Moored vessel behaviour

If a ship can successfully reach a berth or quay, the conditions at the quay become relevant. An indication of the important conditions is given in Figure 2.3

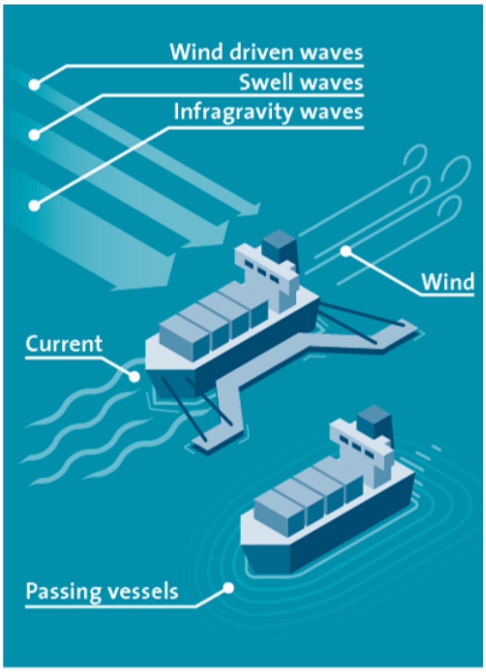

Figure 2.3: Influential conditions to moored vessel behaviour

1. **Mooring procedure**

   Once a ship reaches the quay, large mooring lines are used to secure the ship to the quay. These lines are connected to the winches on the ship and fed through fairleads before being connected to the bollards. These bollards distribute the mooring forces to the quay. Once a vessel has been successfully moored, it is at rest provided that no other forcing is influencing the vessel. In practice however, there are always forces acting on a moored ship. These forces can be split into the following 4 types: current, wave, wind and restraining forces.

2. **Current forcing**

   One of the forces occurs as a result of currents passing the vessel. Current can be tide induced, river discharge related or a combination of the two. Even propulsion of other vessel can cause currents which affect the vessel. Flow forces against a ship and resulting turbulence can cause the ship to start moving. In general, the larger the current velocity, the larger the forces on the ship.

3. **Wave forcing**

   Another influencing factor are the waves acting on the ship. These waves cause, often harmonical, forcing on the ship which will result in movement of the ship. In general, the larger the wave energy, the larger the forces on the vessel.

4. **Wind forcing**

   Wind also influences the moored vessels as a part of these vessels is above water and therefore susceptible to wind influences. Especially container vessels have large above water areas on which wind forcing is possible. In general, the larger the wind velocities, the larger the wind forces.

5. **Restraining forces**

   If forces work on a vessel it will move in the direction of the force. To make sure vessels do not move away from the quay they are moored using mooring lines. These mooring lines provide resisting forces to the vessel. These forces are distributed to the ship via the fairleads and winches and to the quay via bollards. Forces in the direction of the quay are counteracted by the fender forces which distribute the force to the ship and to the quay over their contact areas.

Mooring forces should not exceed certain capacity values as this will lead to failure of the lines, winches or bollards. If failure of one of these components occurs, dangerous situations are created. As forces are enormous, a breaking mooring line can cause snap back which can be fatal on impact. Failure of the bollards might cause the vessel to break loose and become (partly) adrift, risking collision with other ships or the present infrastructure. Failure of bollards will severely damage the quay which will cause much economical damage and often downtime for the quay until it is repaired. Also failure of the fender capacity can occur, causing damages to the hull of the ship and the quay.

2.3 Sheltered quays in strong winds

The influence of waves and current is often considered in traditional port design and therefore often quays are mostly sheltered from these influences. Figure 2.4 shows an example of this sheltering from wave and current in port design.

Considering these sheltered quays, one important forcing factor remains: wind. Given the large vertical areas, or wind areas, of container vessels, this wind influence is important and should not be underestimated. Currently, wind influence is often considered a static load for which a determination of a static response is considered sufficient. However, the large masses of these container vessels result in large natural sway motion periods for the moored vessel system of up to 300 seconds. In wind fluctuation theory, these periods correspond to the peak in spectral energy which indicates a chance of resonance causing the dynamic response to exceed the mooring forces determined by static analysis. Therefore, incorporation of these dynamic properties in the assessment of safe mooring conditions is very important, neglecting it may cause unsafe estimates. However, evaluating the dynamic behaviour is much more complicated than a static approach.

Figure 2.4 shows the Maasvlake II of the port of Rotterdam. The quays are enclosed by the constructed land sheltering them from waves from sea. The dimensions of the basin also result in negligible currents inside the basins.

Figure 2.4: Overview of Maasvlakte II with wave and current sheltered quay. The quay is sheltered on all sides by land so large wave influences are not expected. Furthermore, the short basin characteristic of the area prevents large currents. Therefore, waves and current can be neglected

2.4 Principles of rigid body dynamics

To determine the dynamic response of a moored vessel system, some information in dynamics is needed.

2.4.1 Motivation to use rigid body dynamics

To determine the maximum occurring mooring forces, the dynamic vessel behaviour under fluctuating wind forcing must be determined. This is achieved using rigid body dynamics as the flexibility of the vessel itself is not significant compared to the flexibility of the mooring lines and fenders. In order to determine this response, multiple fields of theory come into play. To understand these fields and their roles in the determination of moored vessel response, first it is important to develop an idea how such a dynamic response can be found.

2.4.2 Definition of position, velocity and acceleration

The first step to determine a dynamic response is determining a coordinate system and its origin. Using such a coordinate system, all movements of a body can be described in this coordinate system by three translations and three rotations. These translation directions (sway, surge and heave) and rotation directions (yaw, roll and pitch) are called degrees of freedom. The derivative of the location in these six degrees of freedom results in the velocities, three translational velocities and three rotational velocities. Again differentiating the velocities results in the accelerations in the six degrees of freedom. Now, knowing the shape and dimensions of the rigid body, the position, velocity and acceleration of all points within the body are known. Important to remember is that all above described positions, velocities and accelerations are described relative to the chosen coordinate system.

2.4.3 Determine response to forcing

Using a chosen coordinate system, the dynamic response of a rigid body to the external forcing can be determined. This is most principally described by Newton's second law. This simple relationship, stated in Equation 2.1, is the essence of the rigid body dynamics used in moored vessel behaviour modelling. If the mass and forcing are known, the acceleration can be computed. Knowing the initial position and velocity, the new position and velocity can also be determined. Therefore, to determine the dynamic response of a moored container vessels in wind forcing, all relevant masses and forces must be determined. In determining these masses and forces, the different relevant fields of theories quickly arise.

$$F = ma \tag{2.1}$$

2.5 The theoretical fields

Four theoretical fields are relevant to determine the vessel behaviours in wind forcing. These are displayed in Figure 2.5.

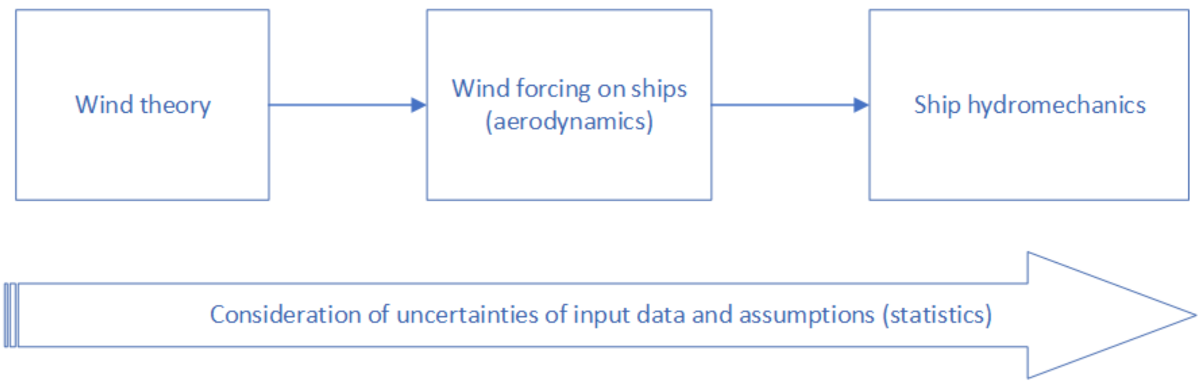

Figure 2.5: Four theoretical areas of interest

2.5.1 Wind theory

To determine the wind forcing on a vessel, the wind input must be defined. This wind input is predicted by meteorological institutions using different predictive models. The accuracy of these predictions is relevant as this should be considered when safe mooring windows are determined. For instance, a margin of safety can be applied considering uncertainties in wind prediction. Such an approach can be used for relatively small inaccuracies in the predictions in the order of one or two m/s. When large deviations are likely to occur, an error of safety approach in the solutions is not workable. Such large wind speed deviations can occur when a front with high wind speeds is expected to pass by a location but in reality it passes over the location. However, the modelling of these predictions is a meteorological process and therefore not included in this study. Nevertheless, assessment of the quality of the wind predictions is relevant when evaluating the real life accuracy of the line force predictions. A meteorological wind speed prediction does not hold all relevant aspects of the wind-field.

The wind profile is variable over the height. As friction with ground or water causes the lowest layers of a vertical wind field to slow down, the local wind velocity increases over the height. Earlier research has shown that the profile of the wind velocity can be described by the power law given in Equation 2.2 (Blocken et al. 2008) .

$$U(z) = U_{ref}(\frac{z}{z_{ref}})^{\alpha} \tag{2.2}$$

Where:
U(z) = The wind velocity over the height z
U_{ref} = The wind velocity at the reference height z_{ref} (usually 10 m)
α = A fit parameter, (on sea approximately between 0.11 and 0.14 (Janssen et al. 2017) up to 0.34 for neutral air over human inhabited areas (Kaltschmitt2007)

Another representation of the vertical field is given by Equation 2.3 (Coelingh A' et al. 1996)

$$U(z) = \frac{u_\star}{\kappa} * ln(\frac{z}{z_0}) \tag{2.3}$$

Where:
z = height above field or waterline
κ = Von Kármán constant (approximately 0.4)
$u_\star$ = friction velocity
z_0 = roughness length

Both depend on the roughness of the terrain (water, grass, etc.). As container terminals are assessed here, the container stacks, cranes and other wind distorting obstacles will complicate the situation severely. In general however, the decrease of wind velocity near the ground surface due to friction will remain valid. Currently, studies into the modeling of wind fields in more complex situations are being executed. In the Joint Industry Project Windlass, wind measurements are executed using Lidar by Marin. These measurements are analysed and models are developed to successfully predict these local wind velocities around structures and obstacles. However, for this study the aerodynamics of wind fields in built environments are not further investigated. The angle relative to the ship is considered along with the shielding effect of the quay (when the wind comes from the land, the area of the ship below quay level will be shielded by the quay.) In future, results of the Windlass studies can be used to determine the relative size of the fluctuations in the wind field due to object interference.

As the exact wind field over the length, beam and height of the vessel is in practice often unknown, in current practice, a uniform wind field is used based on u_{ref} at 10 meters height and wind coefficients, which is further explained in Subsection 2.5.2. Additionally, it should be noted that "when the real wind profile is non-uniform while the set of wind coefficients is based on tests performed with a uniform profile, the simplified use of the wind pressure at 10 m height as the reference one will lead to a large underestimation of the total wind force." (Zwijnsvoorde et al. 2019) The influence of spatial variations in the wind field must be assessed to determine if more precise approaches are needed.

Apart from spatial fluctuations in a wind field, the fluctuation in time of the wind fields is also relevant. These gusts are a form of turbulent velocity which are often decomposed into a mean velocity term and a random fluctuation term as displayed in Equation 2.4 (Boettcher et al. 2003). Both components are important to determine the dynamic response of a vessel in wind.

$$U(t) = \bar{u}(t) + u(t) \tag{2.4}$$

Where:
U(t) = total wind velocity as a function of time
$\bar{u}$(t) = average wind velocity as a function of time
u(t) = random wind fluctuation as a function of time

Different methods are available to determine these fluctuations. Each method provides a variance density spectrum of the energy which can be translated to a time-series of the wind speed. The choice of the spectrum and its influence will be further investigated.

2.5.2 Wind forcing on ship

Once the wind velocity field is determined, the actual forcing on the ship should be calculated. Determining the wind forcing on a container vessel from a known wind field has been the subject of several studies over the last few decades. The first studies mainly focused on the longitudinal forces which decrease efficiency in propulsion of vessels (Andersson , 1978 and van Berlekom, 1981). The importance of the container stacks and their spatial configuration was first realised by Blendermann (1994). Later on, wind tunnel tests were executed to determine wind resulting forces on scale models (Andersen 2012). The development of Computational Fluid Dynamics (or CFD) led to the investigation of wind-resistance of a 2800 TEU container vessel measuring the longitudinal and lateral forces as well as the velocity streamlines and pressure contours. As vessel sizes grew, larger ships were modelled. CFD simulations were executed for a 20,000 TEU vessel in two studies using the same CFD method. (Watanabe et al., 2016 and Nguyen et al., 2016) This was still focused on reduction of wind resistance in head winds but the methods are also appropriate for lateral forcing. The influence of the level of detail applied in the ship modelling for CFD was investigated and found to be substantial. (Janssen et al. 2017) For the investigated vessel, a simple block model led to an average overestimation with respect to the found forces and moments on the detailed model of almost 38% for the total forcing on the vessel. In comparison, a detailed model of the vessel led to an average overestimation of 0.4% (with an average absolute difference of 5.9%, indicating also underestimation at some wind directions.) Therefore, the chosen vessel shape is of significant importance to the forcing calculations.

Applying CFD simulation or wind tunnel tests for each vessel that is assessed results in a very time-consuming and therefore expensive process. To simplify this, tables with significant ships and their wind coefficients are available. Matching the ship under investigation to the most similar significant ship, results in a set of usable coefficients. However, case specific CFD or wind-tunnel tests will hold more accurate results. These wind coefficients determine the relation between the wind speed, wind surface area and experienced force. This is described in Equation 2.5.

$$F_i = C_i(\phi) * 0.5\rho A_i U^2 \quad \text{and} \quad M_i = C_i(\phi) * 0.5\rho A_i L_{pp} U^2 \tag{2.5}$$

Where:
i = the degree of freedom e.g. surge or yaw
C_i = wind coefficient for force or moment in the particular direction, depend on the angle of wind direction relative to the ship.
ρ = density of air
A_i = influence area in the particular direction
L_{pp} = length between perpendiculars
U_{ref} = reference wind velocity as described in Subsection 2.5.1

In most dynamic mooring analysis software, these wind coefficients are used to determine the wind forcing on the ship at known wind velocities. In this study, the coefficients and their directionality are essential for determination of the wind forcing.

2.5.3 Ship dynamics and hydromechanics

The dynamic response of the moored vessel can be modelled using the equations of motion. In principle, six degrees of freedom are present in such a dynamic system. However, it is wise to investigate which degrees of freedom are actually relevant to avoid overcomplicating the system. As described in Section 2.3, wave and current influences are not incorporated in this study resulting in only one external forcing: wind. This wind forcing is a horizontal forcing acting on the moored vessel system. Therefore horizontal responses in surge and sway direction are expected, these degrees of freedom are essential for this system. Horizontal wind forcing can also lead to yaw and roll moments and therefore these rotations can also be expected. Yaw and roll are also essential degrees of freedom for modelling a moored container vessel in wind fields.

Finally, heave and pitch must be evaluated. These motions are caused by vertical forces on the vessel. In the case of a moored container vessel in wind fields, the vertical forces come from the vertical components of the line forces. A first evaluation of the order of magnitude of the heave motions caused by the vertical line forces can be determined using a static calculation. Using a realistic case of a 250.000 tonnes container vessel moored using 16 mooring lines with a mean breaking load of 150 tonnes, equation 2.6 can be used to determine the increase in draught as a result of the vertical line force components. As stated in the Port of Rotterdam mooring guidelines, the vertical line angles should not be much larger than 30° (van Scherpenzeel 2011). Considering some margin for deviations form this guideline, a maximum vertical line angle of 45° is used to determine the heave influence of the vertical line force components. Combining the given input values with a length of 400 meters and a beam of 61 meters, the increase in draught due to the vertical line forces, in the unrealistic case that all lines are stretched to minimum breaking load, is 10 cm. In reality this will not be reached so vertical heave motions will be even smaller. Compared to expected movements for ultimate limit states of a factor 10, or more, larger and the fact that this will not significantly influence the vertical line angle given the large distances between fairlead and bollard, heave motions can be neglected. As vessels are moored with approximately the same number of lines at the front and the back, pitch moments due to the line forces are small compared to the large hydrostatic righting moments for pitch. Therefore, pitch is also neglected. In conclusion: the moored container vessel in wind fields is modelled in the following four degrees of freedom: surge, sway, pitch and yaw.

$$\Delta d = \frac{sin(\beta) * 16 * MBL}{B * L * \rho_{water} * C_{wl}} \tag{2.6}$$

Where:

Δ d = Vertical movement of vessel

β = vertical line angle

MBL = minimum breaking load of one line [kg]

B = vessel beam

L = vessel length

ρ_{water} = density of water (1025 kg/m^3 used as salt water is assumed)

C_{wl} = waterline coefficient of a vessel relating the area of the hull at the waterline to the area of a rectangle with the same length and beam. A typical 24.000 TEU vessel and the determination of its waterline coefficient is presented in Figure 2.6. The found value is 0.85.

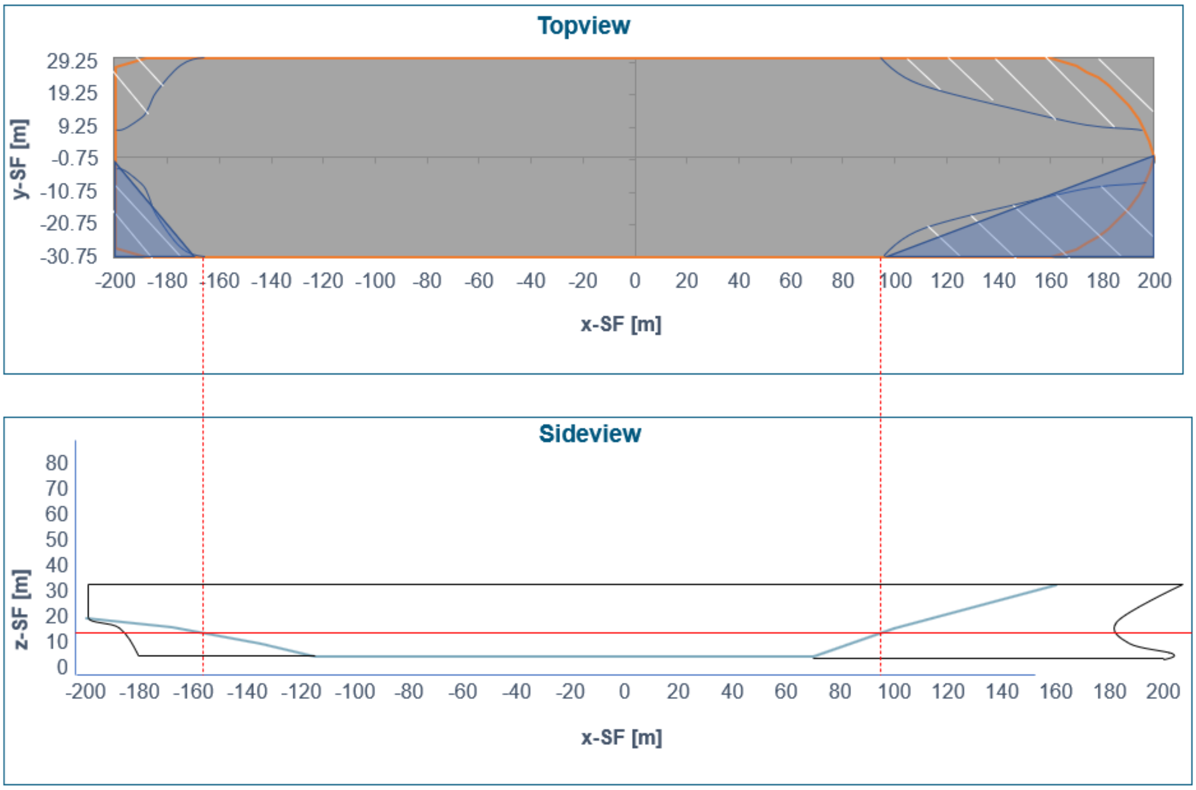

Figure 2.6: Schematization of top and side view of a 24.000 TEU vessel. The blue line in the side view represents the line where the vessel shape follows the orange line in the top view. Using a draught of 15 meters the intersect is determined and the vessel shape at waterline is approximated. Triangle approximation is used to determine the shaded areas and the waterline coefficient is determined.

For one degree of freedom (sway) an example form of the equations of motion for a vessel without external forcing is given in Equation 2.7 (Journée and Massie 2001)

$$(m + m_a)\ddot{y} + c\dot{y} + ky = 0 \tag{2.7}$$

Where:
m = mass vessel
m_a = added mass or hydrodynamic mass
y = motion (i.e. sway) of the body
c = damping coefficient
k = restoring forces coefficient (i.e. mooring line spring coefficient

Despite the fact that wave and current influences are neglected, the hydromechanics of a moored ship are still important. As the vessel starts moving, it interacts with the water surrounding it. As it moves it must move some volume of water with it. This added mass, or added moment of inertia in case of rotations, influences the sensitivity of the body to forces. The added mass increases with an increase in the draught/waterdepth ratio. The precise added mass can be computed using CFD and the Navier Stokes Equation (Gadelho et al. 2018).

Another hydromechanic influence on the system is the damping. The form of this damping differs per degree of freedom. For surge and sway the primary physical cause of damping are skin friction and flow separation. Therefore, the damping may be represented by a quadratic form, which, for no external forcing, leads to Equation 2.8 (Kriebel 1999). Furthermore, other forms of damping, like radiation damping (energy transfers into waves generated by the vessel), can play a role in the system and should be investigated when determining the damping for a mooring case. However, for low frequency movements in surge and sway directions, this radiation damping is often insignificant compared to the viscous damping generated by the combination of small under keel clearance and the presence of a quay. Especially for small under keel clearances, the linear approximations often used for determination of the damping do not hold.

$$(m + m_a)\ddot{y} + c_{NL}\dot{y}|\dot{y}| + ky = 0 \quad \text{Where:} \quad c_{NL} = C_D \frac{1}{2} \rho L_{pp} T \tag{2.8}$$

Where:
c_{NL} = the non-linear damping constant
C_D = drag coefficient for motion
ρ = density water
L_{pp} = length between perpendiculars
T = draught

The value of the drag coefficient can be determined from decay tests (Kriebel, 1999).

As roll is also a relevant degree of freedom, roll damping is important to evaluate. The roll damping is made up of 5 aspects: skin friction, eddy making damping, free surface wave damping, lift damping and bilge keel damping. (Chakrabarti 2001.) These terms incorporate both linear and non linear aspects resulting in a roll damping which is also non linear.

As the vessel is moored to a quay, the water between ship and quay must flow somewhere else when the vessel moves toward the quay. When it moves away from the quay, water flows in to fill the room left by the previous location of the vessel. This flow occurs along the bow and stern of the ship and beneath the keel. Therefore, the damping constant is also influenced by the draught/depth ratio, the smaller the under keel clearance, the larger this ratio. So the volume of water flowing through the gap between bottom and vessel keel increases relative to the area of the gap. This leads to higher flow velocities which causes larger drag forces.

Finally, a hydro static restoring moment must be incorporated for roll motions. This moment is generated by a shift in the center of buoyancy relative to the center of gravity. The moment caused by this shift restores balance to the vessel. In other words, when a heel angle is applied, the vessel is pushed back upright by the water.

The restoring force coefficient consists of the mooring line and fender forces. The line elongation and fender compression depend on the ship motion and translation, as can be seen in Equation 2.9. (Fender friction can also occur in case of surge. In that case, this will be incorporated in the damping coefficient.) To relate line elongation and fender compression to vessel motions, load-elongation (lines) and load-compression (fenders) curves must be evaluated. Two example curves are given in Figure 2.7 and Figure 2.8. As can be seen from these curves, the force response to motions is not necessarily linear. The Equations of motion as stated in Equation 2.8 therefore are slightly changed to incorporate the option for this non linearity.

$$(m + m_a)\ddot{y} + c_{NL}\dot{y}|\dot{y}| + (k_{lines} f_l(y) + k_{fenders} f_f(y))y = \Sigma F(t) \tag{2.9}$$

Where:
k_{lines} = combined spring constant of the lines
$k_{fenders}$ = combined spring constant of the fenders
$f_l(y)$ = the non linear part of the line force-elongation relation $f_l(y)$=1 if linear)
$f_f(y)$ = the non linear part of the fender force-compression relation $f_l(y)$=1 if linear)

Important to note is the fact that the fender and line relations are not continuous over the whole possible range of y, as lines can only receive tensile forces and fenders only compressive forces. When the vessel sways far enough from the quay for example, the fender will not be in contact with the vessel and will not contribute to the dynamic system at that position.

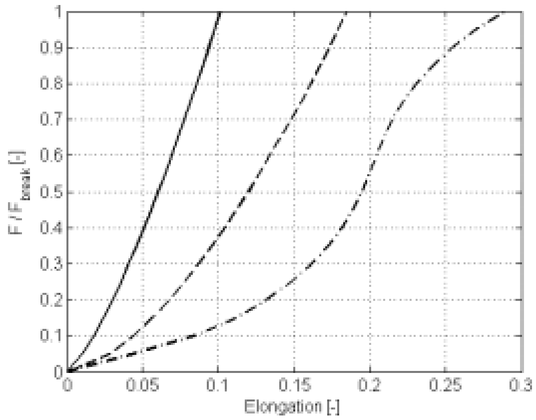

Figure 2.7: Line elongation curve for: polypropylene (–), stiff braided nylon (- -), and soft braided nylon (_._) (van der. Molen 2006)

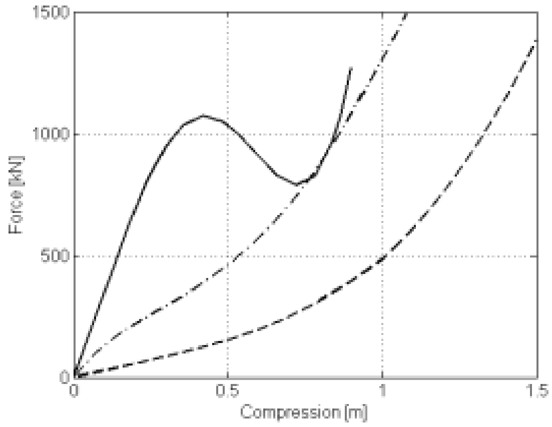

Figure 2.8: Fender compression curve for: supercone fender SCN 1200 E1.1 (–) pneumatic fender 2500 x 4000 (- -) and airblock fender 1800 x 1800 (_._) (van der. Molen 2006)

Due to the angles of mooring lines and fender influences, the degrees of freedom are coupled which results in a set of coupled equations of moment. The non-linearities in the equations of motion, caused by changing line angles and non linear force-elongation curves, require a time-domain based solving approach.

2.5.4 Regression and statistics

In this study the sought after information lies in the maximum mooring forces of a moored container vessel under wind forcing. This response depends on multiple variables. An alternative to full dynamic mooring analysis could lie in a more empirical approach of a regression based formula or polynomial. Therefore a multiple regression model must be created. As explained by Ostertagová: (2012) "Multiple regression refers to regression applications in which there are more than one independent variables. Multiple regression includes a technique called polynomial regression. In polynomial regression we regress a dependent variable on powers of the independent variables." Such a model can be described by Equation 2.10

$$y = \beta_{i,j} * x_i^j \quad \text{where} \quad i = 0, 1, 2...n \quad \text{and} \quad j = 0, 1, 2...m \tag{2.10}$$

Where:
y = Unknown value of sought after parameter
x = Known value of input parameter
β = regression constant
n = number of different influence parameters
m = maximum power of relation

However, this is only a very general form of such a model. Relations based on physical modelling combined with input parameter interaction are needed to determine the polynomial form from which regression analysis can be used to find the correct coefficients.

During discussion of the results, accuracy of the parameter value and sensitivity of the model to said parameters must be discussed. When the model has a high sensitivity to a parameter, but its value is very precisely known with very small errors, the error is less significant than that of a parameter with small sensitivity but very large errors. The sensitivity of the response to certain parameters is also important for parameter selection. If, for example, the response is very sensitive to water density, which does not vary over a very large range, this parameter may be chosen constant and its variation is not further investigated whereas line length, which may be less influencing on the response but for which the range of variation is much larger, will be included as a varying input parameter. This is an example and not yet indicative of the choices made in the study.

2.6 Current Options for determination of peak mooring forces and their disadvantage

Currently, RHDHV offers Dynamic Mooring Analysis to determine maximum mooring forces and motions for vessels in waves, wind and current. This requires on-site evaluation and measurements of the relevant input parameters and precise berth layout. This is a time consuming exercise which results in high costs for the customer. For example, a dynamic mooring analysis for one vessel case for a certain quay takes approximately one week of work when executed by RHDHV. This is only the time actually spent modelling and analysing. Including gathering relevant information, contact with the client and reporting back to the client, this takes a few weeks.

Other players in the market use different software tools to execute dynamic mooring analysis but the time intensity problem is present in all these solutions. To reduce the time required for analysis and therefore the costs, a static analysis can be chosen. However, this may lead to underestimation of the occurring forces and displacement.

2.7 Theoretical gap and advantage

A middle way producing much more accurate results than static mooring analysis without the required effort of a full dynamic mooring analysis would be beneficial. As the limit state is assessed, not the whole response is necessary to be known. If the occurring peak mooring forces can be predicted using a relatively simple assessment of a set of key parameters, this will hold a large advantage for quick assessment of berthing safety for large container vessels in wind forcing. To achieve this, a direct relation between input parameters and maximum mooring forces must be determined. This will not be fully physics based as is the case with a complete dynamic mooring analysis, but will be an empirical relation. However, as is often the case with empirical equations, the workings of the physics of the dynamic system are essential to determine such a direct relation. An empirical method for determining the maximum mooring forces of a container ship due to the dynamic response caused by wind forcing, does not yet exist. Most research currently focuses on the more detailed description of certain input parameters, for example: wind velocities as a result of disturbances by objects or ship wind interaction based on more detailed CFD simulations. (See Subsection 2.5.2 and 2.5.1.) These developments will contribute to the accuracy of a complete dynamic mooring analysis by better determination of the exact conditions at the examined site. However, this will cause more time consuming procedures instead of less time consuming ones. Not only can an empirical method increase efficiency in determination of the peak line forces, it can also be used to assess the influence of deviation of certain parameters, leading to a better feeling for the moored vessel behaviour. Finally, an empirical method will be more scalable which makes it more dynamic in its uses. It can be used for different quays and different vessel can be modelled only varying a few input parameters.

3. Objective, research questions, methodology and report outline

The research questions are formulated, the methodology is presented and the further outline of the report is given.

3.1 Research questions

The problem described in chapter 2 relates to the time intensity of the dynamic mooring analysis methods now in use. Although full case specific dynamic mooring analysis may be required for some projects, for other projects a less time consuming solution is preferred. As stated in Section 2.3, the focus for this study will lie on the maximum mooring forces occurring due to the dynamic response of large container vessels in wind fields, neglecting current and waves.

Therefore, the objective of this study is to develop a deterministic method for approximation of the maximum mooring forces of a container ship due to the dynamic response caused by wind forcing. This leads to the following research question:

How can safe mooring windows, based on maximum mooring forces due to the dynamic response of a moored container vessel, subjected to time varying wind forcing, be approximated without using full case specific dynamic mooring analysis simulations?

As the answer to the proposed research question is not easily found, it has been divided into more specific sub questions. An explanation is given as to why these sub questions have been chosen.

1. **What are the essential parameters required to compute the maximum mooring forces from a container vessel in wind forcing?**

   To determine the maximum mooring forces occurring during the response of a vessel to wind forcing, a number of parameters must be included. An overview of all influencing factors must be determined along with a decision if these will be modelled.

2. **How can the dynamic response be modelled?**

   As discussed in Subsection 2.5.3, the behaviour of a dynamic system can be approximated by a mass-spring system. All mass, inertia, damping, stiffness and external force terms should be defined so the system of second order differential equations can be solved. As non-linearities occur, a solution in the time domain must be sought. A modelling approach must be sought which can combine these aspects with a numerical solver and present and save the results for further analysis.

3. **How can the influence on the mooring forces of the different parameters be determined?**

   The input parameters like berthing configuration, wind forcing, ship draught etc. influence the dynamic response of the system. Therefore, the maximum mooring forces will also be influenced by these parameters. How can this influence be isolated and compared?

4. **What choices and assumptions must be made when describing a real life situation in a theoretical model and what are their influences on the maximum mooring forces?**

   As is often the case with modelling of physical processes, certain assumptions and choices must be made. There are some industry standard assumptions and choices that are usually made in dynamic mooring analysis. The correctness and influence of these assumptions will be investigated using, aside from literature and theory, modelling of different variations.

4.1. **Should spatial variance in the wind-field over the height and length of the vessel be considered?**

Spatial variance is usually neglected in current practice as the exact wind variance and distortion is usually unknown. However, this may have a significant influence on the vessel response and its peak mooring forces. Experimenting with different wind distributions can give insight in this influence.

4.2. **What time fluctuations (gusts) should be modelled and how can they be described mathematically?**

To model the gusts, the basis of turbulence around a mean velocity as described in Subsection 2.5.1 is used. These fluctuations should be incorporated in the analysis but as they cannot be exactly predicted, a modelling approach must be selected. Different approaches can be compared to determine their influence on the line forces.

4.3. **How does the wind forcing affect the vessel?**

As discussed in Subsection 2.5.2, the wind velocities induce force on the vessel. This interaction can be determined using wind tunnel tests or CFD. However, since wind tunnel tests and CFD are very time consuming, often wind coefficients are used. These coefficients are determined for specific vessels. One chooses one of the reference vessels most similar to the vessel under consideration and models the vessel based on these coefficients. This of course comes with certain deviations from the real situation. The influence of these deviations should be investigated.

4.4. **How do the hydrodynamic aspects, and errors in their determination, influence the line force results obtained from the model?**

As described in Subsection 2.5.3, the primary hydromechanical aspects for sway, surge and yaw are the hydrodynamic or added mass and the non-linear damping relation. The influence of these factors is introduced in the equations of motion. They are both dependent on the dimensions of the vessel, its draught and the water depth. Apart from the added mass, the righting moment is relevant for assessment of roll.

5. **How can the influence of the parameters be quantified by regression analysis of a set of dynamic mooring simulations?**

   When simulations have been executed, the results can be analysed to quantify the influence of different parameters. How can different simulations be compared and how can the influence of different parameters be isolated?

6. **How can the different influences be combined to form a peak line force prediction polynomial?**

   Finally, the combination of the different influence parameters should be evaluated to determine how a workable mooring force estimation polynomial can be created.

3.2 Methodology

To answer the research question, the sub-questions must be answered. To answer these sub-questions different steps must be taken.

1. **Determine the relevant input parameters**

   To determine the mooring forces due to the dynamic response of a container vessel under wind forcing, firstly, the relevant parameters have been determined. This is done by working from the real life situation of a moored vessel and describing the different components. Once described, a more mathematical description of each component and its influence is given. As described in Subsection 2.5.3, a dynamic system can be described by its equations of motion. Therefore, it was determined on which term(s) of the equation of motion a certain component has influence. For instance, a vessel in real life is moored using mooring lines. When looking at these mooring lines, they influence the spring term in an equation of motion. They have mass but this mass is negligible compared to, for example, the vessel mass. Losses of energy in the elongation of the line may occur. This might influence the damping in the system. In execution of this step some literature study was used in combination with a logical function analysis.

2. **Modelling the dynamic response**

   After the real life situation had been divided in different components and their global influences had been determined, the modelling of the components inside the system were executed. To do this, a step-by-step build-up approach was used. Starting from scratch and immediately building a 3-dimensional dynamic system model is difficult and may lead to errors in the logic of the model. Therefore, the first phase of modelling consisted of a simple mass spring system. To this simple model, extra components and degrees of freedom were added, resulting in a more complete model. Modelling choices and assumptions were modelled to be easily varied to allow for influence analysis. A numerical method was chosen to solve the system in the time domain and theoretical validation was applied to assess the performance of the model. These steps resulted in a simplified dynamic mooring model called the conceptual mode. The conceptual model was used for further analysis.

3. **Determining an analysis approach which can be used for simulation comparison**

   The results from the conceptual model for different simulated cases were compared in further analysis. A method to base this comparison on was chosen and motivated.

4. **Checking influences of common industry practices**

   Since the conceptual model proved usable, different modelling choices and assumptions were investigated to determine their impact on the mooring forces. Systematically evaluating this impact resulted in insight in the accuracy of current dynamic mooring analysis approaches.

   - **Influence of wind-field variation over vessel length**
     Using a spatially constant wind-field neglects influences of wind distortions along the vessel length. This influence was investigated by specifying different wind distributions over the length of the vessel using the conceptual model. Knowing this influence helped determining whether this assumption is relevant and if other combinations should be chosen.
   - **Vertical wind profile**
     As described in Subsection 2.5.1, schematization of spatially varying wind field by a spatially constant wind field requires some caution as blindly neglecting deviations in the vertical velocity profile may lead to underestimation of the forces. The influence of this vertical wind profile was investigated to determine if this is an important parameter in the determination of mooring forces.
   - **Wind fluctuation spectrum**
     The influence of choice in gust spectrum was investigated to determine its relevance. Literature was reviewed to obtain different wind spectra and the conceptual model was used to determine whether different spectra led to different mooring forces.
   - **Wind-ship interaction**
     The interaction between the wind and the vessel results in a forcing on the system. The step from wind-field to actual forcing is based on aerodynamics. Wind-tunnel testing and CFD can accurately describe the forces and moments created by this wind-ship interaction. The influence is expressed in wind coefficients, as expressed in Subsection 2.5.2. The influence of these wind coefficients on the maximum occurring mooring forces was determined to obtain insight in the sensitivity to these parameters.
   - **Hydrodynamical aspects**
     Hydrodynamical aspects like added mass can be difficult to determine accurately. The influence of these aspects was assessed to determine the sensitivity of the mooring forces to variations and errors in determination of these parameters.

5. **Create dataset and analyse results**

   The simulations were executed. Once some simulations were done, intermediate analysis was used to help further specify the simulations. Through this iterative process a dataset was created which was then used for regression analysis and polynomial fitting.

6. **Determine polynomial and regression based correlation coefficients**

   By analysing the obtained dataset and using theory of the dynamic moored ship system, a polynomial was proposed. Using regression theory as displayed in Subsection 2.5.4, this polynomial was fitted to the obtained dataset. New simulations were run to obtain a validation dataset, different from the training dataset. The found polynomial with its regression coefficients was validated and the differences were evaluated. This led to new insights which can be used in further research. Once this step was finished, a polynomial was obtained which estimates the maximum mooring forces from given values for the relevant input parameters.

7. **Determine accuracy and sensitivity to input error of the polynomial**

   Once the polynomial and its regression coefficients were determined, the sensitivity to errors and uncertainties in input was evaluated. The error of the proposed maximum mooring force polynomial was determined and a practical margin for safety was proposed.

3.3 Report outline

An overview of the report is given, relating the chapters to the different steps in the methodology and the research sub questions.

- Chapter 4, step 1 of the methodology is executed, answering sub question 1 by giving an overview of the relevant parameters for the modelling of a moored container vessel in wind. The different parameters are related to their functioning in the forcing, damping, mass and inertia or spring term.
- Chapter 5 gives an overview of the used modelling approach in accordance with step 2 of the methodology. Sub question 2 is answered by describing the used modelling approach in relation to the physics that govern the different aspects of the system.
- Chapter 6 gives insight in the influence of current industry standard practices in accordance with step 3 and 4 in the methodology. Here, the answer to sub questions 3 and 4 are found.
- Chapter 5 gives the results of the parameter influence study and presents a first proposal for a line force prediction polynomial, in accordance with steps 5 and 6 from the methodology. Here sub questions 5 and 6 are answered.
- Chapter 8 presents a discussion of the findings and relates this to real world situations with regard to uncertainties and simplifications. Here step 7 from the methodology is presented.
- Chapter 9 presents the conclusions and recommendations of this study. Here the main research question is answered.

4. Determination of relevant input parameters

This chapter elaborates step 1 of the methodology: the real life situation of a moored vessel is analysed and the different components are designated. The relation of the different components to each other is assessed and a system is defined. The response of the vessel is described in equations of motions and the different components are assigned to different parameters in the equation of motion.

4.1 The components of a moored vessel system

Starting from the system of a moored vessel in wind forcing, five different main components can be defined. The vessel, the quay, the water, the wind and the lines. Here the fenders are considered part of the quay. Figure 4.1 shows a three level decomposition of the system.

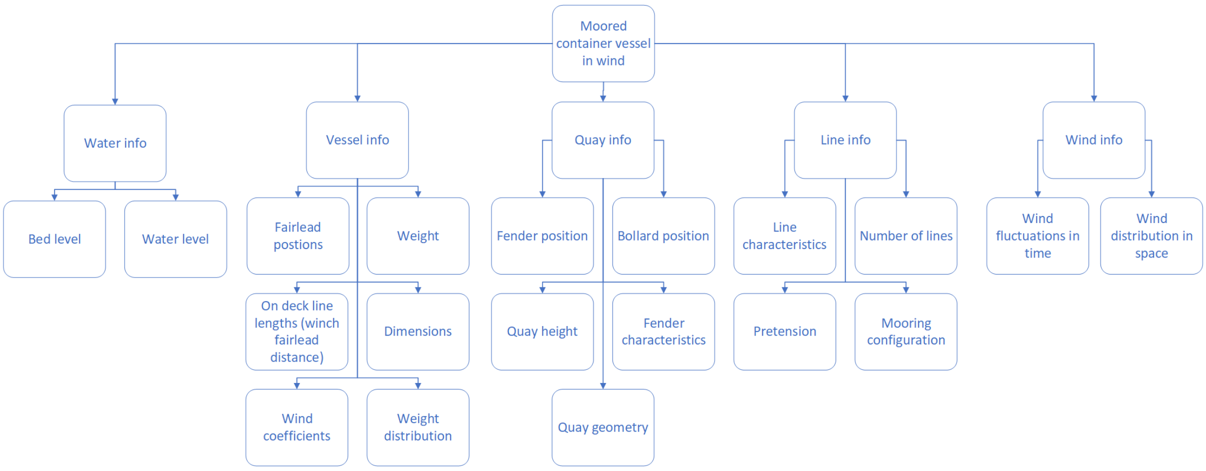

Figure 4.1: Different components of the moored vessel system

4.2 Coupling components to the equation of motion

Coupling the different components to different terms in the equation of motion helps assessing their influence. Using this method, a first view of the schematized system emerges. As described in Subsection 2.5.3 the system's dynamic response can be determined if the mass and forcing are known. Starting with the mass, two different "types" of mass can be defined: mass and moment of inertia, measured in kg and kgm^2 respectively. Furthermore, when a vessel starts moving a certain amount of water will vibrate with it. The effect of this water should be added to the mass and inertia terms to account for this in the system response, hence the name added mass. An overview of the components which affect the mass and added mass terms is given in Figure 4.2. The mass combined with the vessel dimensions can be used to determine the moment of inertia. The added mass and inertia are affected by the vessel dimension and shape as well as the presence of the quay and the amount of water between the keel and the bottom. This under keel clearance can be determined using the draught of the vessel and the water depth. As added mass depends on a hydrodynamic processes it also depends on the frequency of the vessel movement. Therefore, one could argue that all components which influence the response also influence the added mass.

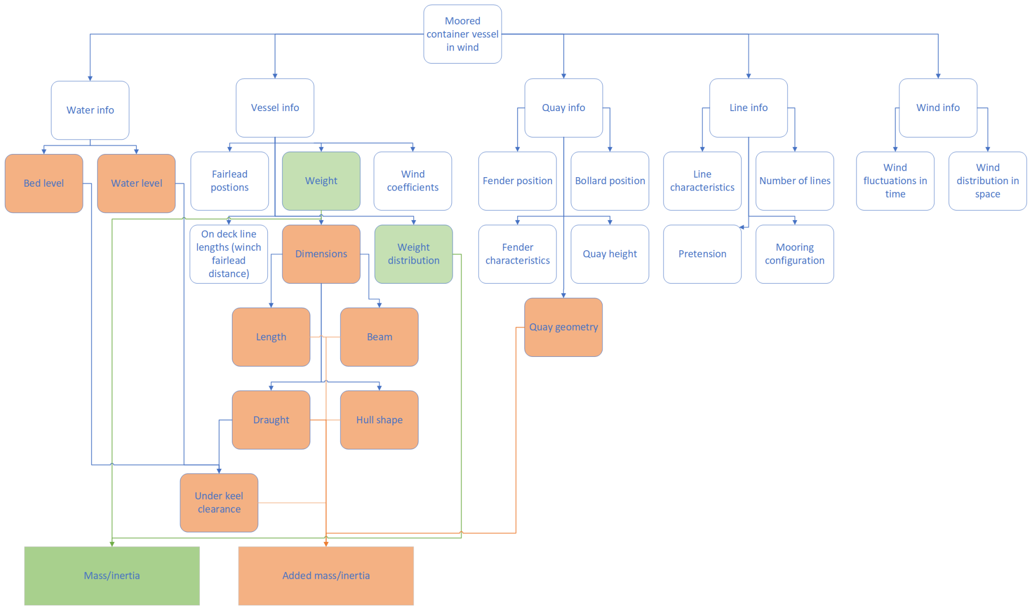

Figure 4.2: Mass term components

As described by Newton's law, the dynamic response of a system is not only based on its mass but also on the forcing in the system. These forces are divided in two types: external and internal forces. In this case the system is defined as the vessel, the quay, the water, the mooring lines and the fenders. Internal forces are forces that these internal components exert on each other, whereas external forcing in this case consists of the forcing from the wind on the vessel. In this system the internal forces can be divided into two types. The first type can be described by some sort of excitation-force relationship, which is similar to springs. Therefore, these are called spring terms. The second type relates to the velocities, either translational or angular, in the system. These terms like friction damp the response of the system and, when no external forcing is present, will bring the system to rest over time. Therefore, these forces are called the damping terms. Figure 4.3 displays the components which contribute to the spring term.

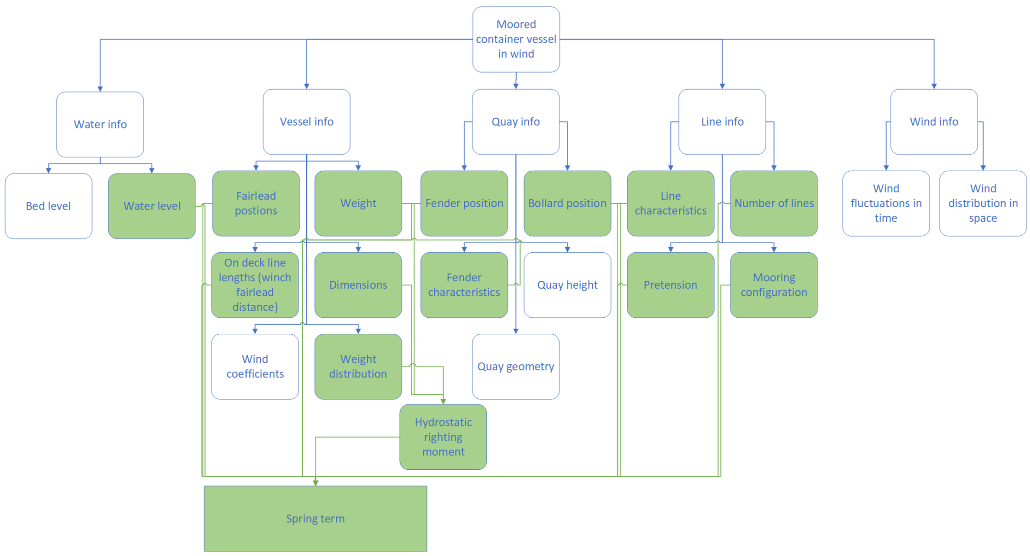

Figure 4.3: Spring term components

Motions in different degrees of freedom result in different hydrodynamic responses and with that also different mechanisms dominate the damping terms. Aside from the hydrodynamic damping energy dissipation and damping is also possible by influencing the line characteristics using, for instance, active motion dampers. As hydrodynamic processes are governed by the frequency of the vessel motions and the water-hull interactions, the influencing parameters are displayed in Figure 4.4. Here, the specific components are simplified into all vessel dimension components determining the underwater hull which interacts with the water, the under keel clearance influencing components as this influences the flow beneath the vessel and the line and mooring configuration components to account for line damping. In reality, as for added mass, all components influencing the response also influence the damping as the damping is frequency dependant.

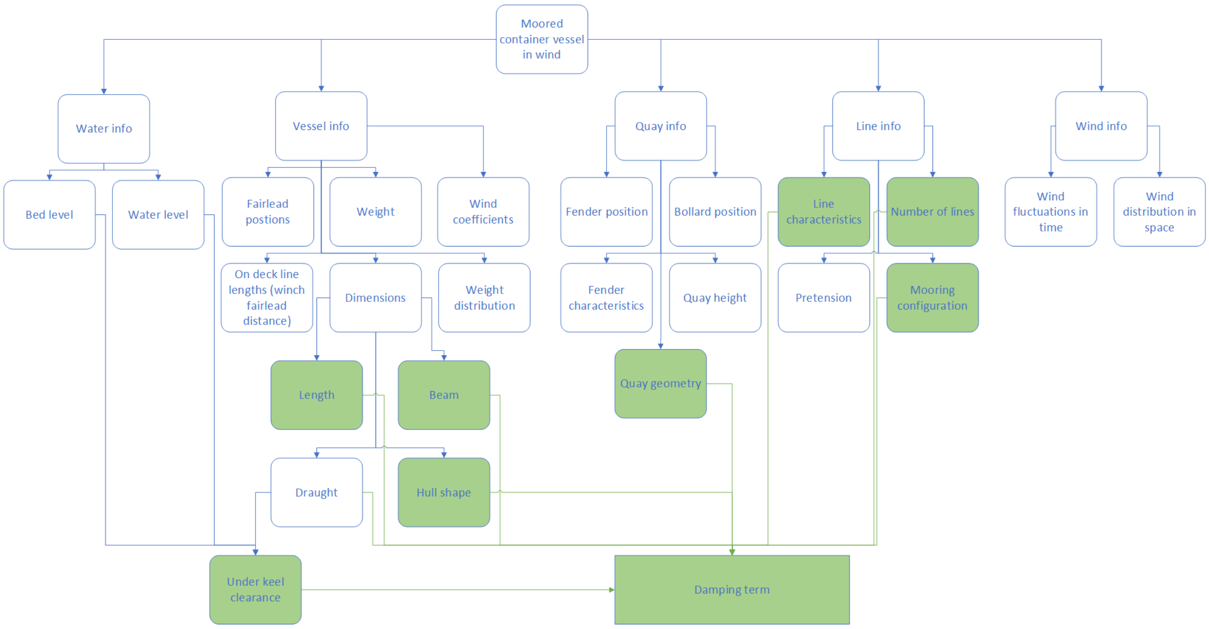

Figure 4.4: Damping term components

As all internal processes are defined, the external forcing remains. This external forcing is influenced by all wind related components, the area of the wind-vessel interaction, and the difference between quay height and water level. The part of the above water vessel that lies below the quay level is sheltered by the quay and will not experience wind forcing, for offshore winds ofcourse. Figure 4.5 displays these components. Here wind coefficients are grouped under vessel information. However, this depends both on the wind direction and the vessel layout and dimensions. Therefore, it also belongs to wind information. This is not shown in the Figure as it decreases clarity of the diagram.

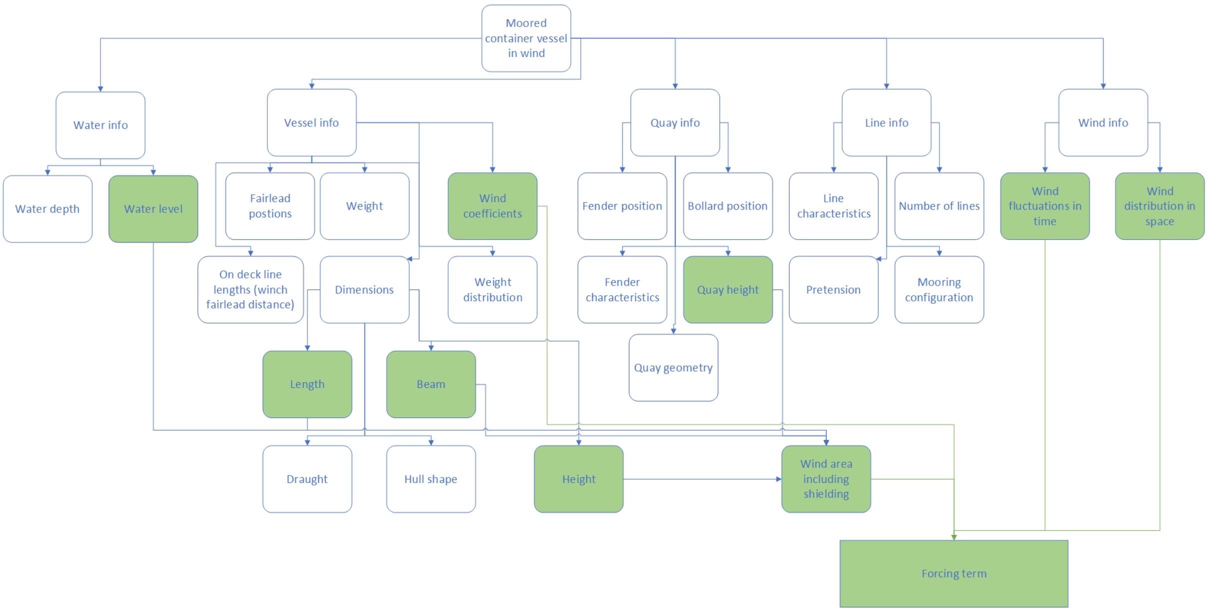

Figure 4.5: Forcing term components

5. Modelling the response of a moored container vessel in wind fields

This chapter elaborates step 2 of the methodology: using determined input parameters and the equations of motion, the response of the moored vessel due to wind excitation can be modelled. To allow for modelling some simplifications are made to the real life system. Numerical modelling is used to determine solutions in the time domain. This self made model, "the conceptual model", is used to determine the influence of different parameters on the peak line forces. In this chapter, the theory of a mass spring system response and its application in the conceptual model is discussed (Sections 5.1 through 5.4), information on numerical modelling and further modelling components are presented (Section 5.7 and the the conceptual model is verified and validated using simplified cases for which an analytical solution is determined (Section 5.11 and 5.12.

5.1 Single degree of freedom mass spring system

Firstly, the moored vessel system is simplified to a one degree of freedom mass spring system. Initially no forcing is applied and the free vibrations of the system are modelled. To do this, the simplified equation of motion is determined.

$$m\ddot{y} + c\dot{y} + ky = \Sigma F \tag{5.1}$$

or

$$\ddot{y} + 2\zeta\omega_n\dot{y} + \omega_n^2 y = \frac{\Sigma F}{m} \tag{5.2}$$

Where:
m = the mass of the vessel
c = the damping coefficient
k = the spring coefficient
and
$\zeta = \frac{c}{2\sqrt{km}}$
$\omega_n = \sqrt{k/m}$

Using the notation from Equation 5.2, the free vibration can be analytically described as shown in Figure 5.1 when the mass damping and spring coefficients are known along with certain initial conditions.

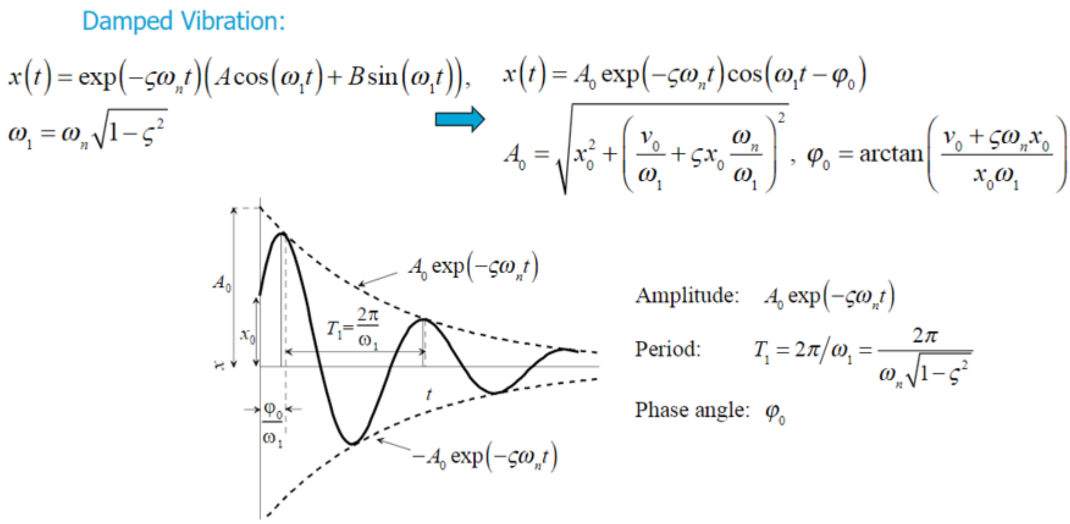

Figure 5.1: Free vibrations of 1 DOF system (Metrikine and Tsouvalas, 2020)

5.2 Two degree of freedom modelling

To more accurately determine the vessel response, a second degree of freedom is added. The system in one degree of freedom moving towards and away from the quay is a representation of sway, the logical next step is adding surge. Now the system becomes two dimensional and vessel dimensions come into play. To consistently describe positions two different coordinate systems are defined. The first coordinate system is the earth fixed coordinate system. The earth fixed coordinate system has its origin on the edge of the quay wall with the positive y axis away from the quay. The second coordinate system, the ship fixed one, has its origin at the center of gravity of the vessel. The system with two mooring lines, one at the bow and one at the stern, is displayed in Figure 5.2. Here the subscripts EF and SF indicate the earth fixed and ship fixed coordinate system respectively. To reduce complexity and computation time, all mooring lines present are grouped into four line groups: breast line front, breast line back, spring line front and spring line back. For each group, the angles and lengths of the actual lines are combined into a single angle and line length mimicking the spring stiffness and direction of the combination of a set of parallel lines, combining the load elongation curves of the separate lines. Therefore, the response of the dynamic system is modelled realistically. However, the peak line forces occur in the most critical line in a line group. Proper investigation of the ratio between the shortest line and the average line can be used to use as a multiplication factor for the found peak line forces.

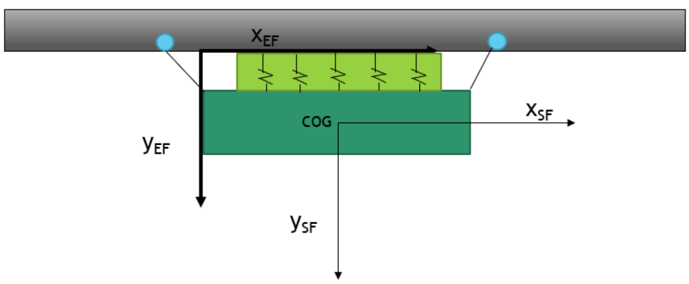

Figure 5.2: Moored vessel system in 2 DOF

As movement in the sway direction causes a change in angle of the mooring line along with an elongation, or shortening, of the line, these forces bring coupling terms between the two degrees of freedom. As the line angles change when the vessel moves, non linearities occur, provided that the change in line angle is significant. The spring terms can be decomposed to bring these terms in a classical equation of motion description. However, as more degrees of freedoms are introduced the system becomes increasingly complex, a different approach is used. Looking back at the essence of dynamics, Newton's second law states that if one can determine all forces acting on the mass at each moment, the dynamic response can be determined. Therefore the following approach is used:

1. Define the position of the bollards in the earth fixed coordinate system and the position of the fairleads in the ship fixed coordinate system.

2. Define the four initial conditions surge, surge-velocity, sway and sway-velocity (these should be taken so the system is approximately at rest). The surge and sway motions are now expressed as the movement of the ship fixed system relative to the earth fixed system, or in other words, the movement of the center of gravity of the vessel relative to the earth fixed coordinate system.

3. The length of the lines when they are slack (no tension) should be determined. To do this, the initial line lengths corresponding to the initial condition can be determined using the positions of the bollards and fairlead and the initial conditions. Next, the pretension is needed which in the provided case is 10% of the Minimum Breaking Load (or MBL). Using the line characteristics, the associated elongation can be obtained. Considering the initial line length, the fairlead-bollard distance, and the previously determined elongation that matches the 10% MBL pretension, the slack line lengths can be determined. This process is shown in Figure 5.3. Using the slack line length, the line characteristic can be determined as function of stretch relative to L_{slack} , ΔL, and by linearising, a spring constant can be expressed.

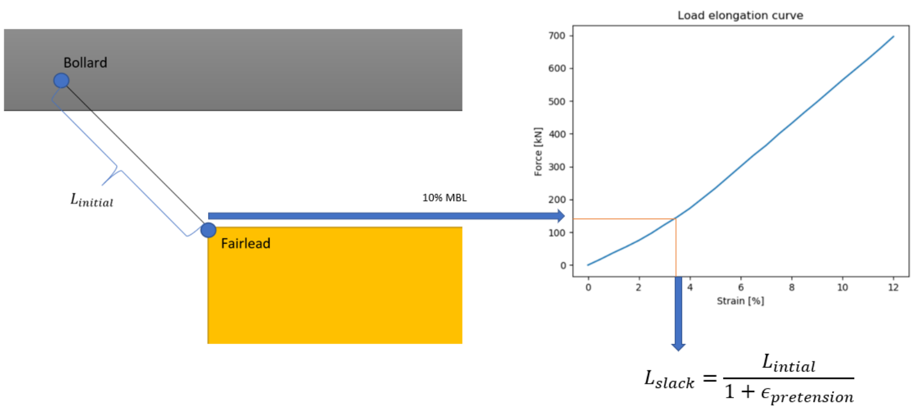

Figure 5.3: Determination of slack line lengths

4. Use the position of the vessel and the positions of the bollards and fairleads to determine the line length at t_n (first step these are the initial conditions) along with the angle α the line makes with the x-axis of the earth fixed system. Using the spring constant, the line lengths at t_n and the slack line lengths, the line forces can be determined. Using the angles α of both lines the line force can be decomposed in a surge and a sway force. This is schematized in Figure 5.4. Important here is also modelling what happens when alpha becomes 90 degrees or larger and assigning correct direction for the surge forces. Combining this with the fender compression, if any, the external forcing and the damping forces, all forces at t_n are known.

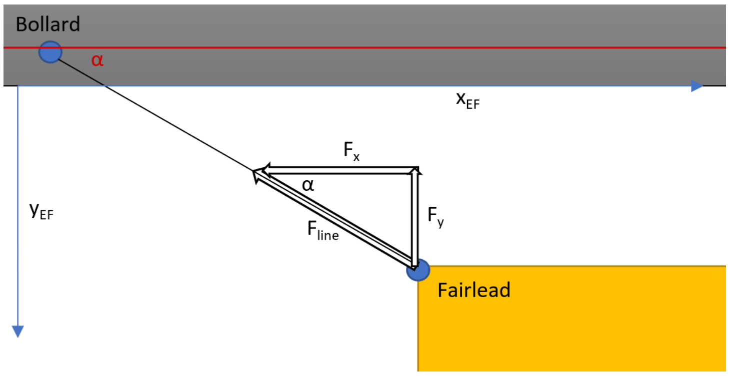

Figure 5.4: Decomposition of mooring forces

5. As all forces at t_n are known, the position and velocity at step t_{n+1} can be determined numerically. Next, the whole chain is repeated taking the position and velocity at t_{n+1} as input.

5.3 Three degrees of freedom modelling

The third degree of freedom to be introduced is the rotation around the z-axis, or yaw. The same coordinate systems are used, however, the ship fixed coordinate system becomes more relevant now. The added yaw rotation is indicated by θ and the new situation is displayed in Figure 5.5. Important here is that the fenders are now split in different discrete fenders as yaw rotation will cause differences in the response per fender.

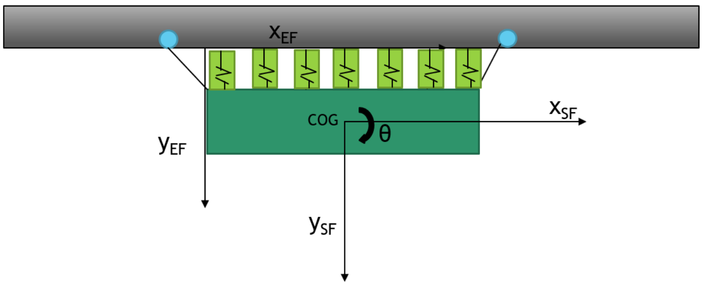

Figure 5.5: The system in 3 degrees of freedom

The yaw rotation causes all points, except for the origin, within the ship fixed coordinate system to translate in both x and y direction. This rotation and the translation of the corner of the rectangle, are shown in Figure 5.6 and the new coordinates in the ship fixed coordinate system are given by Equation 5.3 and 5.4. Using the rotated coordinates of the fairleads, the same chain as described in Section 5.2 can be executed with one addition: after the forces have been decomposed the fairlead coordinates combined with the decomposed forces are used to determine the resulting moments of the line and fender forces.

$$x_1 = x_0 \cos\theta - y_0 \sin\theta \tag{5.3}$$

$$y_1 = x_0 \sin\theta + y_0 \cos\theta \tag{5.4}$$

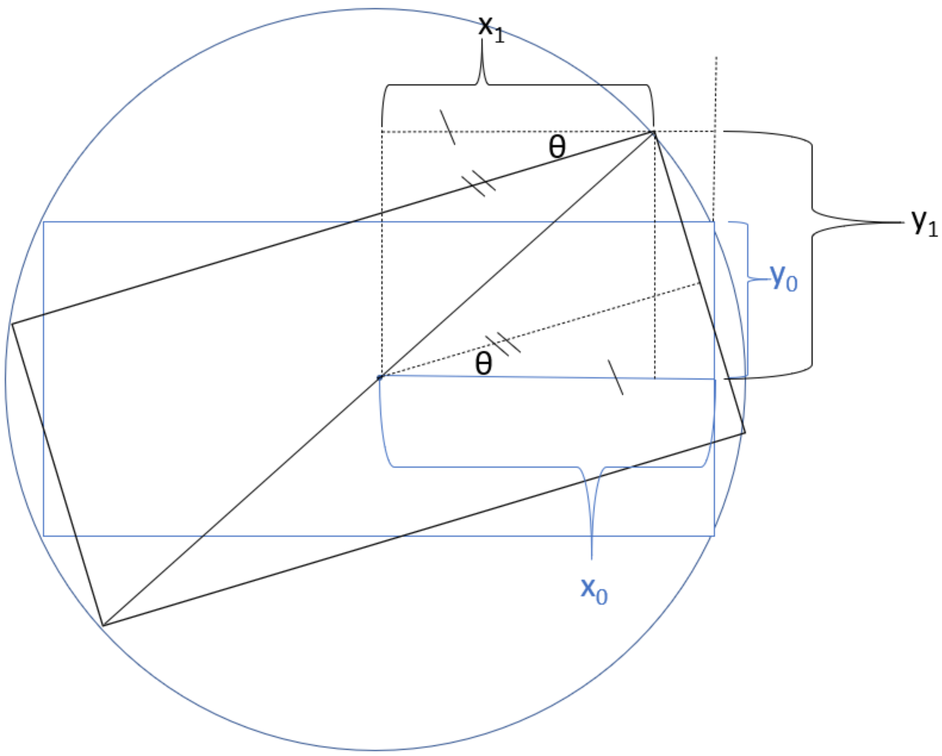

Figure 5.6: Translation of points when rotation is applied with in blue the position of the top right corner before rotation and in black after rotation θ

5.4 Four degrees of freedom modelling

Finally, the fourth degree of freedom, roll, is added to the system. This addition comes with the added complexity of a third dimension. Up to three degrees of freedom can be modelled in two dimensions but adding a fourth will also result in the requirement of a three dimensional system. This means the origin of both the ship fixed and earth fixed coordinate system must be defined. For the ship fixed system the water level is chosen as the origin and for the earth fixed system the quay level is chosen. A new line angle β is also defined as the angle between the vertical distance and the horizontal distance between fairlead and bollard. Therefore, the line forces are first decomposed in horizontal and vertical parts and then the horizontal force is again decomposed in a force in sway and a force in surge direction. Aside from the roll moment caused by wind forcing, important here is that both the line forces in y and z direction create roll moments. However, this is not the only roll moment in the model.

Roll also creates a difference in the horizontal y coordinate of the center of buoyancy and center of gravity of the vessel. Therefore the gravity and buoyancy which, according to Archimedes' principles are equal but opposite, create a righting moment counteracting the rotated position. This righting moment is relatively large and must not be neglected. The moment can be determined using the Scribanti formula which holds as long as the vertical sides of the vessel are still in the water. Once a vessel turns too far, the bottom of the hull will start to rise out of the water and the Scribanti formula will not hold anymore. An overview of the principles of the Scribanti formula is given in Figure 5.7. Using the buoyancy force (which equals the gravity and the vertical line force components) and the lever arm GZ as indicated in Figure 5.7, the moment for a certain rotation can be determined. The lever arm can be computed using Equation 5.5, 5.6, 5.7 and 5.8. The vertical components of the line forces can be neglected in the determination of the force of buoyancy as these components are not significant compared to the vessel mass. A realistic situation would consist of a vessel with a mass of 250,000 tonnes moored using

12 to 16 mooring lines with a minimum breaking load of 150 tonnes. Even in the most critical, and completely unrealistic, situation in which 16 lines are pulling straight down on the vessel, stretched to minimum breaking load, this force will still be less than 1% of the mass. Therefore, the vertical line force components are neglected in the determination of the righting moment.

$$\overline{GZ} = \overline{GN_\phi} \sin \phi \tag{5.5}$$

$$\overline{GN_\phi} = \overline{KB} + \overline{BN_\phi} - \overline{KG} \tag{5.6}$$

$$\overline{BN_\phi} = I_T/\nabla(1 + 1/2 \tan^2 \phi) \tag{5.7}$$

$$M_{righting} = \rho g \nabla \overline{GZ} \tag{5.8}$$

Where:
ϕ = roll angle
$\overline{KB}$ = distance from keelpoint to center of buoyancy
$\overline{KG}$ = distance from keelpoint to center of gravity
I_T = Second moment of area of the z-x plane of the vessel
∇ = The volume of the submerged part of the vessel

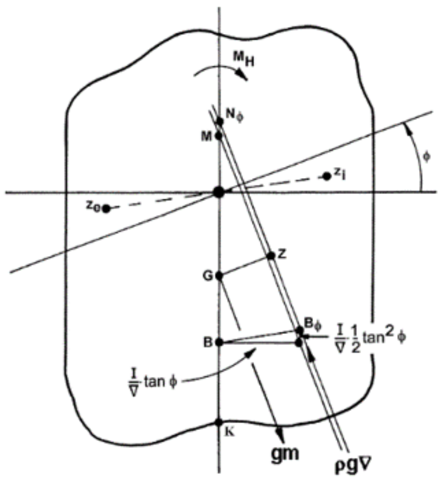

Figure 5.7: Scribanti's formula schematized

Now the righting moment can be computed. This can be added to the moments generated by the line forces in the spring term following the proper positive and negative directions as shown in Figure 5.8

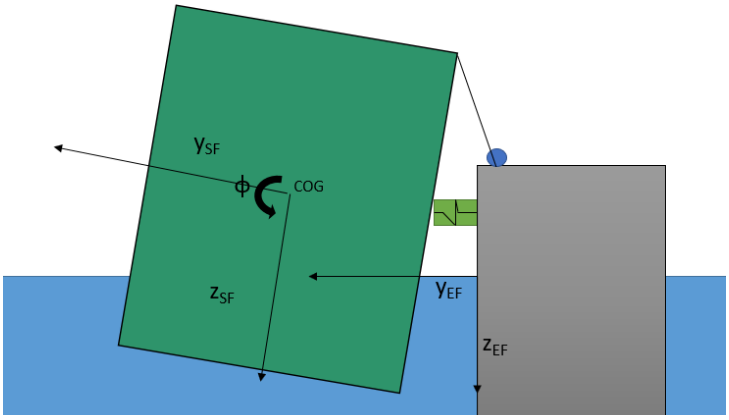

Figure 5.8: The coordinate systems in the z-y plane

5.5 Modelling a wind time-series

To properly model a time-series based on a theoretical wind spectrum, the meaning of a wind spectrum and its information must be understood. As discussed in Subsection 2.5.1, a fluctuating wind field is modelled using its mean velocity and a fluctuation in time around this mean velocity. This fluctuation can be modelled as a superposition of different waves around the mean velocity and can be expressed by a variance density spectrum which indicates the amplitude and frequency of the fluctuations. More specifically, it indicates how much fluctuation is contained in which frequencies. The fluctuation around the mean velocity η is described as a superposition of harmonics is Equation 5.9.

$$\eta(t) = \sum_{i=0}^{N} a_i \cos(\omega_i t + \delta_i) \tag{5.9}$$

Where:

a = amplitude
ω_i = angular frequency
δ = phase shift

The amplitudes matching the different frequencies, are determined by analysing the variance density spectrum. The phase shift is added randomly to each harmonic to ensure a random combination of the harmonics. Different variance density spectra have been proposed to describe the fluctuations in wind speed. The difference and their influence is investigated in Chapter 6, here a Harris wind spectrum is displayed as an example. This is also the wind spectrum that is used in the test case. Figure 5.9 displays the Harris variance density spectrum and the theory to derive a time-series from the variance density spectrum. By dividing the frequency axis in multiple small intervals of $d\omega$ and determining the area under the curve in this interval, the variance in m^2 can be determined. This variance is related to the 1/2 times the amplitude squared. Using this relation the time series of the wind is created by using the frequency-amplitude relation to determine a set of harmonics. A random phase shift between 0 and 2π was added and finally a superposition of these harmonics in the time domain was generated.

$$S_V(\omega) = \frac{7200}{2\pi}\kappa V\left[2+\left(\frac{286\omega}{V}\right)^2\right]^{-\frac{5}{6}}$$

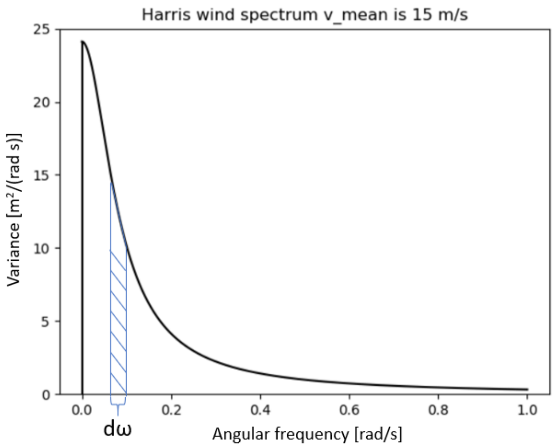

Figure 5.9: Harris wind spectrum

5.6 Modelling the excitation force due to wind forcing

When the wind speed time series are generated, this can be translated to forcing on the system. To do this, as described in Subsection 2.5.2, windcoefficients can be used. These experiment or CFD based coefficients give a coefficient for determining the force or moment generated by the wind-ship interaction in each degree of freedom. As these are discrete coefficients based on measurements of a number of attack angles, they cannot be used for each exact user defined attack angle. Therefore, it is decided to use linear interpolation between the discrete coefficients to determine coefficient for all attack angles. Using these coefficients and Equation 2.5, the forces and moments due to wind forcing at a certain moment in time can be determined. In the conceptual model, the shielding by the quay in offshore winds is incorporated in the wind area computations. Windcoefficients do not only depend on the vessel but also on the container layout and stack height. Figure 5.10 shows the windcoefficients for a fully loaded and partly loaded case, as derived from a wind tunnel study (Bartholomä 2015). It can be clearly seen that the number of container tiers does not only affect the wind surface but also the wind coefficients.

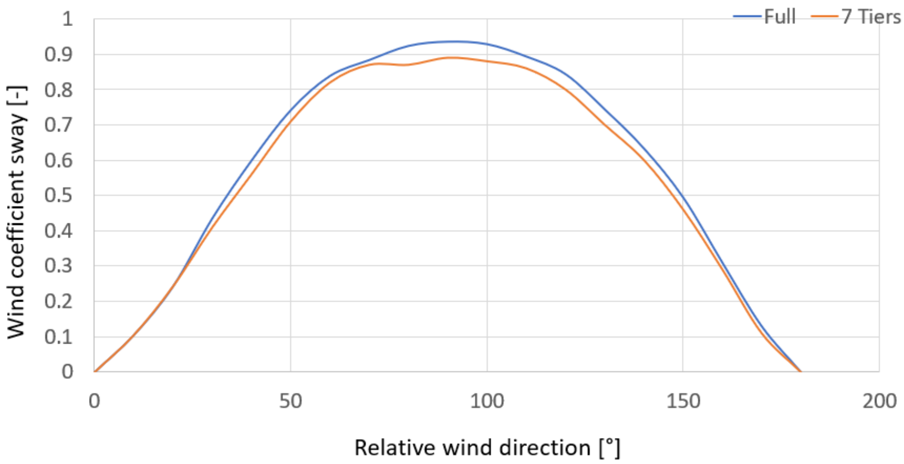

Figure 5.10: Windcoefficients for a vessel for fully loaded and 7 tiers loaded (Bartholomä 2015 modified from source)

5.7 Numerical modelling options

When using numerical modelling, a difference in implicit and explicit methods exists. The implicit methods have the advantage of being more stable for larger time steps. However, they are much more complex to program and take more computation time per step as the new state of the function is computed using, not only, the known information from the previous state but also information of the new state which is being computed. Therefore, matrix or iterative calculations are required for each step. Despite the fact that explicit methods may have some stability issues, the increased simplicity and calculation speed are preferable in such a conceptual model. As the goal of this study is not to determine which numerical model is perfect to determine the response of the vessel, the methods are assessed only globally. More detail on the process of numerical modelling and the adaptions made to model non-linear second order differential equations is given in Appendix A.

Three numerical solvers were evaluated: Forward Euler, Runge-Kutta 2 amd Runge-Kutta 4. All three numerical solvers were applied to solve a single degree of freedom mass spring system with viscous damping and harmonic forcing. To compare the computation time of each method, a base case was used to determine the step size needed for each method to achieve a root mean square error of approximately 1 mm, which is sufficiently accurate for a system which knows responses in an order of significance of decimeters. Then the computation time was measured for the execution of the numerical solving, using each method and a time series length of 100,000 seconds. This resulted in a computation time of 38 seconds for Forward Euler, 11 seconds for Runge-Kutta 2 and 43 seconds for Runge-Kutta 4. Therefore, Runge-Kutta 2 is chosen as the best solving method as it requires the least computation time to get to accurate results.

5.8 Added mass, damping and non linear line characteristics

Finally added masses and non linear line characteristics are introduced to the model. Instead of a linear spring constant for all lines, the forcing is determined based on the force-strain curve. Added masses and moments of inertia are added to the normal masses. To get realistic values of these added masses, they are set to be in accordance with those found in a reference case provided by Royal HaskoningDHV. In reality these added masses are frequency dependent. However, as small frequencies are expected, the change in added mass due to a shift in frequency within the realistic domain is relatively small. More consideration of added mass is given in Chapter 6.

5.9 Model expressed in equations of motion

Finally, taking into account all modelling choices and methods, the equations of motion in 4 degrees of freedom, as used to model the dynamic vessel response, can be written as presented in equation 5.10. Here the equations of motion are presented in matrix notation with further elaboration in equations 5.11 through 5.15. Important to note that the spring coefficients affecting the rotational responses correspond to moments and also incorporate the distance from the center of gravity to the position of application of the line and fender forces.

$$M\ddot{X} + C\dot{X} + KX = F \tag{5.10}$$

$$X = \begin{bmatrix} x \\ y \\ \theta \\ \phi \end{bmatrix} \tag{5.11}$$

$$M = \begin{bmatrix} m + m_{added,x} & 0 & 0 & 0 \\ 0 & m + m_{added,y} & 0 & 0 \\ 0 & 0 & I_\theta + I_{added,\theta} & 0 \\ 0 & 0 & 0 & I_\phi + I_{added,\phi} \end{bmatrix} \tag{5.12}$$

Where:
$m_{added,x}$ = added mass surge direction
$m_{added,y}$ = added mass sway direction
$I_{added,\theta}$ = added moment of inertia yaw direction
$I_{added,\phi}$ = added moment of inertia roll direction

$$C = \begin{bmatrix} c_x & 0 & 0 & 0 \\ 0 & c_y & 0 & 0 \\ 0 & 0 & c_\theta & 0 \\ 0 & 0 & 0 & c_\phi \end{bmatrix} \tag{5.13}$$

Where:
c_x = damping coefficient surge direction
c_y = damping coefficient sway direction
c_θ = damping coefficient yaw direction
c_ϕ = damping coefficient roll direction

$$K = \begin{bmatrix} k_{line,xx} & k_{line,yx} & k_{line,\theta x} & k_{line,\phi x} \\ k_{line,xy} & k_{line,yy} + k_{fender,yy} & k_{line,\theta y} + k_{fender,\theta y} & k_{line,\phi y} + k_{fender,\phi y} \\ k_{line,x\theta} & k_{line,y\theta} + k_{fender,y\theta} & k_{line,\theta\theta} + k_{fender,\theta\theta} & k_{line,\phi\theta} + k_{fender,\phi\theta} \\ k_{line,x\phi} & k_{line,y\phi} + k_{fender,y\phi} & k_{line,\theta\phi} + k_{fender,\theta\phi} & k_{line,\phi\phi} + k_{fender,\phi\phi} + k_{hs,\phi\phi} \end{bmatrix} \tag{5.14}$$

Where:
$k_{i,j}$ = spring coefficient for line force in direction j as a result of movement in direction i
$k_{i,j}$ = spring coefficient for fender force in direction j as a result of movement in direction i
$k_{hs,\phi\phi}$ = hydro static righting moment as result of heel angle

$$F = \begin{bmatrix} 0.5 * \rho * c_x * A_{longitudinal} * u_{wind}^2 \\ 0.5 * \rho * c_y * A_{lateral} * u_{wind}^2 \\ 0.5 * \rho * c_\theta * A_{lateral} * L_{oa} * u_{wind}^2 \\ 0.5 * \rho * c_\phi * A_{lateral} * (D - T) * u_{wind}^2 \end{bmatrix} \tag{5.15}$$

Where:
ρ = density air [kg/m^3]

c_i = relevant wind coefficient [-]
A = wind area [m^2]
u_{wind} = wind speed [m/s]
D = Vessel height [m]
T = Draught [m]

As the added mass, moment of inertia and the damping is modelled as a value, the non-linearities lie in the spring term matrix. These non-linearities exist in

1. The fender characteristics are normally non linear, therefore all fender spring coefficients are non linear.
2. The load-elongation curves for the mooring lines are non linear. Therefore, the mooring line spring terms are non linear.
3. In case of large movements the mooring line angles will change significantly, resulting in non linearities in the mooring line spring terms.

5.10 Overview of the conceptual model

Figure 5.11 displays an overview with the different modelling parts, which are different pythons scripts, and their interaction. Firstly, all relevant input parameters are defined. The mean wind velocity and angle of attack are used to generate a wind time series and use linear interpolation to determine the appropriate wind coefficients. This input is then used by the numerical solver. The numerical solver requires, for each step, all forces in and on the system. To do this, it first calculates the initial line lengths which are then used to determine the slack line lengths using the line characteristics. The fender forces are also computed and all forces and moments are returned. Additionally, the righting roll moment is computed using a Scribanti formula script. The numerical solver returns a time series record of the position and velocity in the four degrees of freedom along with time series records of the line and fender forces. The maximum line forces are used in further chapters to determine the influence of different parameters on the maximum occurring mooring forces.

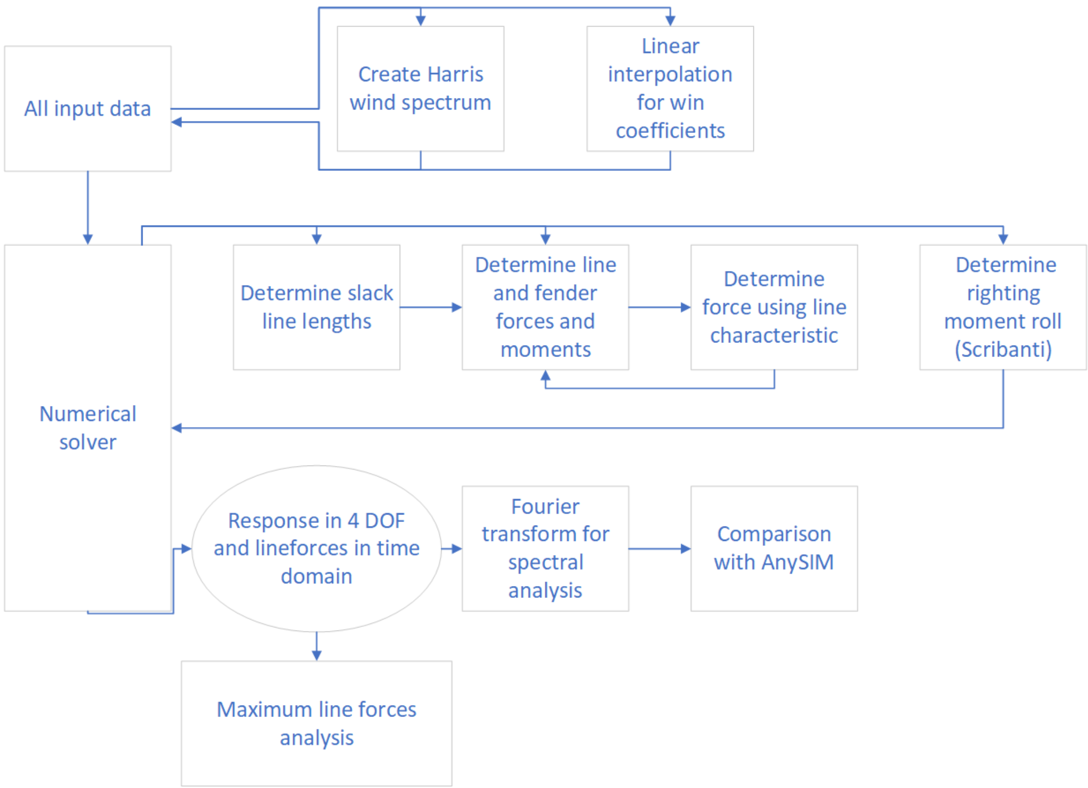

Figure 5.11: Overview of different scripts used in modelling

5.11 Verification of the model components

To verify the working of the model, each separate component can be verified using hand calculations, spectral analysis or checking of directions and coordinate systems. This is further elaborated in Appendix B. A forward Fourier transform function is used to assess the spectrum of the wind time series which matches the theoretical Harris wind spectrum from which it was generated so this functions properly. The linear interpolation of the wind spectrum is checked and found to work as expected. The line lengths, forces and moments are checked using hand calculations and excel calculations and are found to work properly. Important to note is that the fenders are simulated using linear fender characteristics and grouped in a definable number of groups spaced evenly along the relevant quay. Finally, the working of the Scribanti module is assessed which works as expected. An option is added to use the linearised method of initial stability to reduce computation time for cases where the expected roll angles do not exceed 4-7°. If the roll angles exceeds 7° Scribanti should be used.

5.12 Validation of model response for base cases

As all modules work as expected, the functioning of the model can be validated using analytical responses for a number of base cases. A validation case is used consisting of the input parameters presented in Table 5.1. In this validation, the full 4 degree of freedom model is used. Input parameters are chosen specifically to create analytically verifiable cases but the numerical solvers themselves are not manipulated. Firstly, a sway analysis is executed, positioning two complete sets of lines, one starboard and one port sided, perpendicular to the vessel and horizontal to the quay, the fenders and quay as physical barrier are removed and the line characteristics are linearised. 0% pretension is used so in the rest position all lines are slack. The system of this example case of ship spanned between two quays is displayed in Figure 5.12. Each line group in this schematization consists of 8 lines.

Parameter	Value	Unit
Length over all	400	m
Beam	60	m
Height (keel to top)	33	m
Draught	14.5	m
Mass	250,000	t
Lateral wind area	17,000	m^2
Frontal wind area	3,250	m^2
Damping ratio	0.1	-
Relative wind direction	90	°
Minimum breaking load	142	t

Table 5.1: Input parameters reference case influence analysis

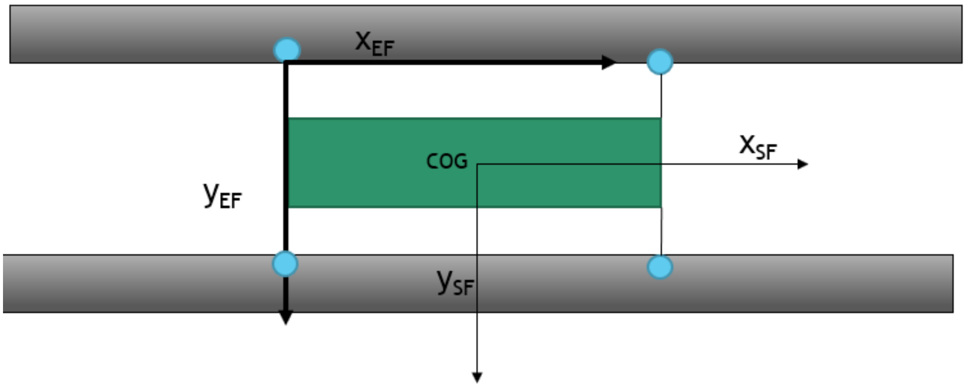

Figure 5.12: Sway validation case

As the system becomes a mass spring system which, when excited in sway direction, should only result in a response in sway direction, the spring constant and mass can be determined analytically resulting in a verifiable natural frequency. Starting with a decay test, the ship starts from an excited state in sway direction, the response is transformed to a response spectrum and the frequency of the peak is compared to the theoretical eigenfrequency determined by Equation 5.16. As the analytical solution gives a precise number, in order to have some accuracy, long time series runs are executed to increase the spectral resolution. In the neutral positions all lines are just slack. When the vessel moves in sway directions one set of lines is stretched and exerts force on the vessel while the other set of lines is slack. The transition between the slack and stretched states of the lines is modelled to be smooth and no snap loads are considered.

$$\omega_1 = \sqrt{\frac{k}{m}} * \sqrt{1-\zeta^2} \tag{5.16}$$

Where:
ω_1 = the natural frequency of the damped system
k = the spring coefficient
m = the mass including added mass
ζ = the damping ratio

As can be seen in Table 5.2, the frequencies differ for less perpendicular line angles. This is a result of the occurring non linearities when the line angles change due to the sway movements. These non linearities are considered in the numerical model, as the theoretical frequency is based on a constant spring coefficient which relates to a constant line angle, this difference is logical. As can also be seen from the fact that smaller Minimum Breaking Loads, or MBL, which cause a less stiff spring and therefore larger movements of the vessel and therefore larger line angle differences resulting in larger non linearities, result in larger differences between the theoretical and numerical frequencies.

Mass [10^6kg]	MBL [MN]	Number of lines	Line angle [°]	Theoretical frequency [Hz]	Numerical frequency [Hz]	Difference [%]
751.53	1.393	16	90	0.0121	0.0121	0
375.77	1.393	16	90	0.0172	0.0172	0
751.53	2.786	16	90	0.0172	0.0172	0
375.77	2.786	16	90	0.0243	0.0243	0
375.77	2.786	16	67.5	0.0218	0.0218	0
751.53	1.393	16	67.5	0.109	0.109	0
375.77	2.786	16	45	0.0149	0.0151	1.3
751.53	1.393	16	45	0.00747	0.00783	4.5
375.77	2.786	16	22.5	0.0062	0.0075	17.3
751.53	1.393	16	22.5	0.00310	0.00442	29.9

Table 5.2: Frequency analysis for different mass-spring ratios and line angles

For the perpendicular line case, the numerical solution should match the analytical solution of a damped mass spring system with the same mass, damping and spring coefficients. This is tested for a free vibration decay test of 5000 seconds with time steps of 0.25 seconds. These results and the root mean square error are shown in Figure 5.13

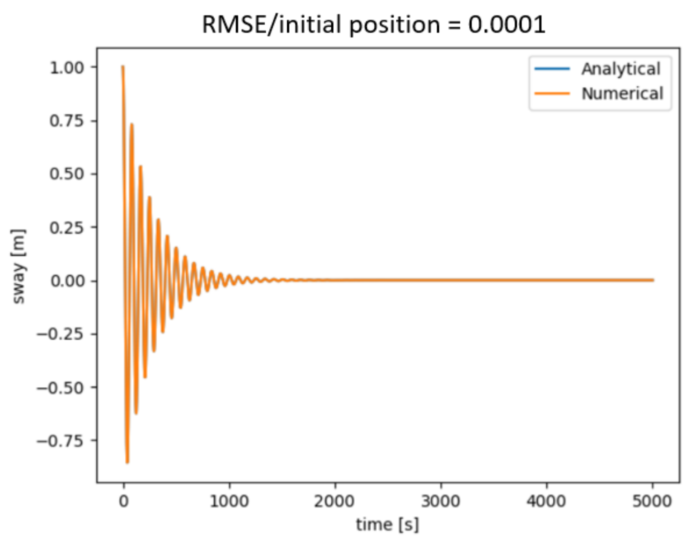

Figure 5.13: Validation of the conceptual model using the analytical solution for a decay test

As the response to external forcing and its incorporation in the numerical solver is not checked using a decay test, the same situation is simulated again but now applying a harmonic external forcing in sway direction. Again the theoretical and numerical solution are compared. This is displayed in Figure 5.14. As the numerical model only produces slight errors the numerical solver produces proper results for sway.

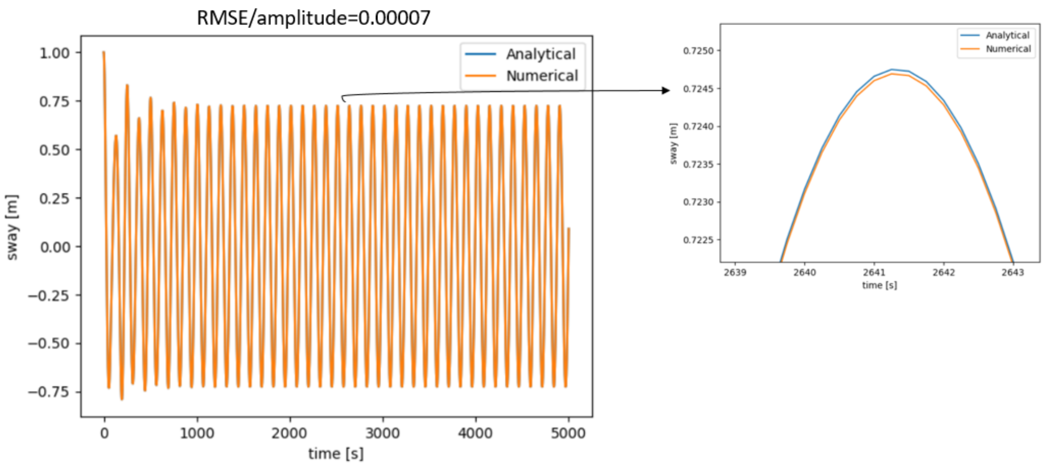

Figure 5.14: Validation of the conceptual model using the analytical solution applying harmonic forcing

Next, the fairlead and bollard positions are changed such that the lines are positioned parallel to the x axis and are connected to the bow and stern at the middle of the width of the vessel. This can be seen as a vessel spanned between two dolphins, as can be seen in Figure 5.15 . Each line group consists of 16 lines in this case.

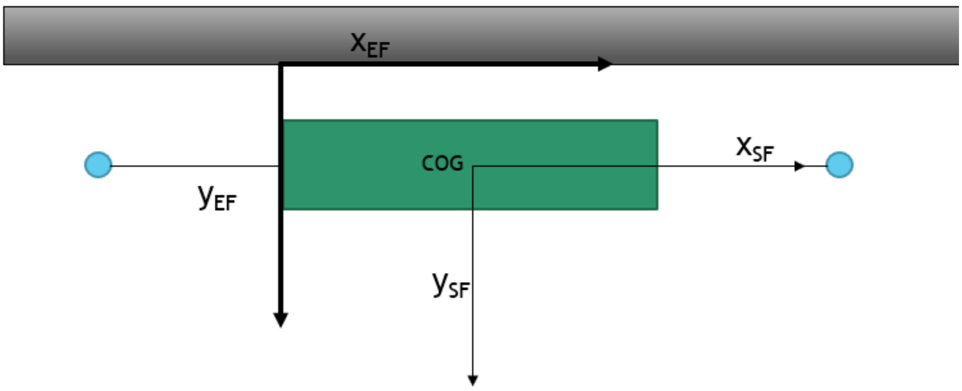

Figure 5.15: Surge validation case

Now a simple mass spring system in surge direction is obtained. Again the damped natural frequency is compared to its theoretical natural frequency and a free decay test is compared to its analytical solution. Again, also a harmonic forcing is applied to check that external forcing is also correctly assessed. The frequency produces a match and the decay comparison is shown in Figure 5.16, the harmonic excitation force response is presented in Figure 5.17

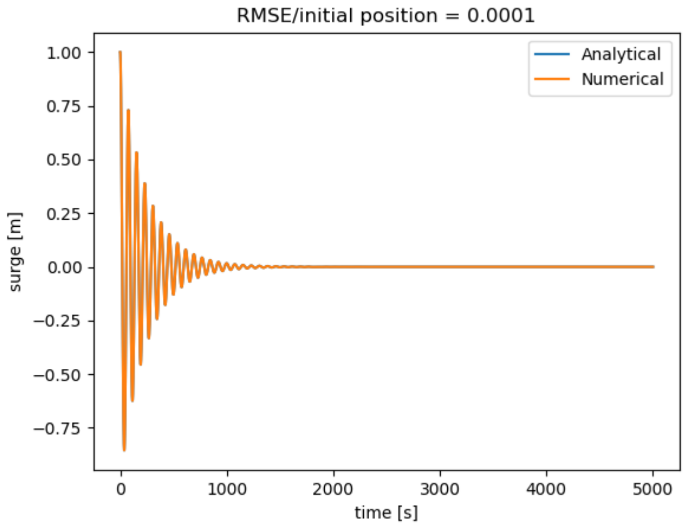

Figure 5.16: Validation of the numerical solution using the analytical solution for a decay test.

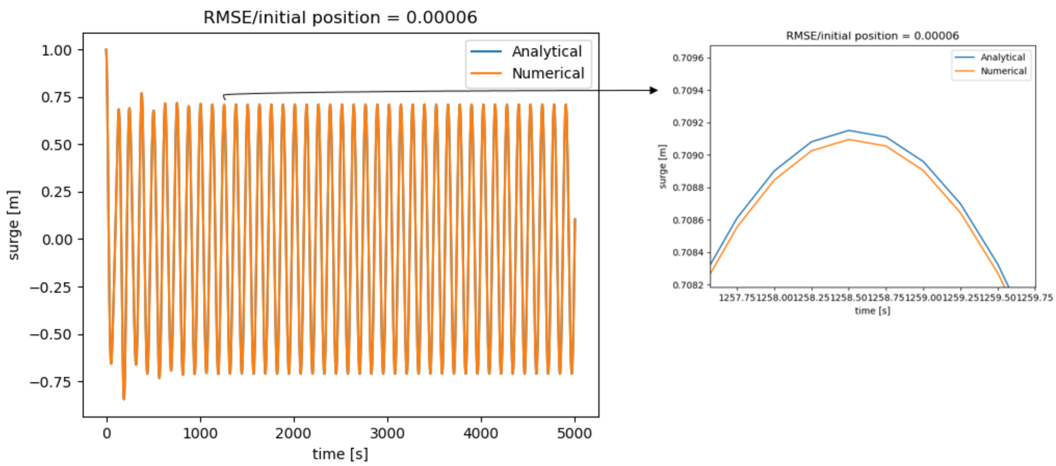

Figure 5.17: Validation of the conceptual model using the analytical solution applying harmonic forcing

Now, the same tests are executed for the configuration in Figure 5.12. However, now a initial yaw rotation is applied for the decay test and a harmonic forcing for the harmonic forcing test. Figure 5.18 displays the decay test and Figure 5.19 displays the response to a harmonic external moment.

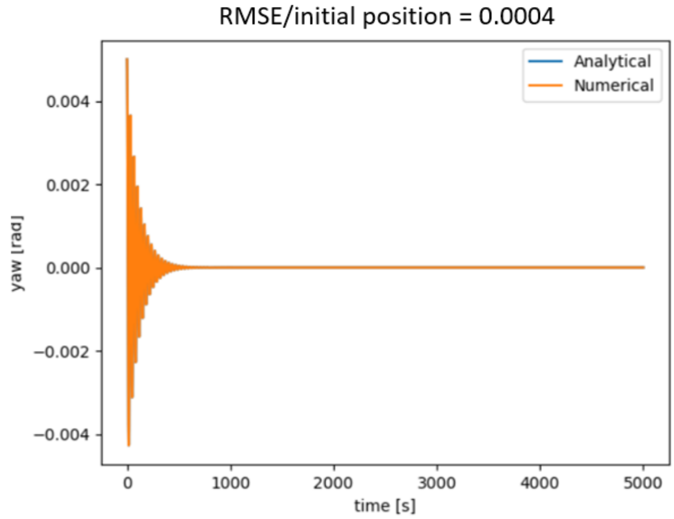

Figure 5.18: Validation of the conceptual model using the analytical solution for a decay test.

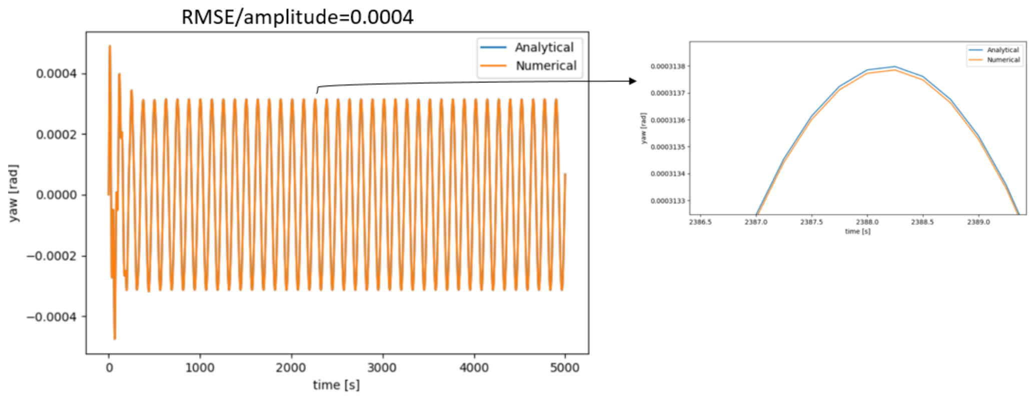

Figure 5.19: Validation of the conceptual model using the analytical solution applying harmonic moment

As the Root Mean Square errors for all cases are multiple orders of magnitude smaller than the expected significant response, the conceptual model performs well. However, the simplifications applied to the system should be kept in mind when applying the conceptual model to real world situations.

6. Checking influences of common industry practices

This chapter elaborates step 3 (Section 6.2 and 6.3) and 4 (Section 6.4 through 6.8) of the methodology: since the dynamic response of the moored vessel system is successfully modelled, relevant industry standard assumption can be checked.

6.1 Description of reference case

To check the industry assumptions, a reference case is chosen as starting position for the analysis from which certain deviations are applied to determine the influence of several assumptions on the peak line forces. The input used for the reference case is displayed in Table 6.1. When assessing influences of industry standard practices, the most thorough approach is to check these influences for many different mooring cases, wind speeds and wind angles. However, as computation time is a limiting factor, this study focuses on the aforementioned reference case and wind angles for which the peak line forces are critical. This wind angle is determined for the reference case. However, firstly an extreme value analysis method must be chosen.

Parameter	**Value**	**Unit**
Length over all	400	m
Beam	60	m
Height (keel to top)	33	m
Draught	14.5	m
Mass	250,000	t
Lateral wind area	17,000	m^2
Frontal wind area	3,250	m^2
Number of breast lines	12	-
Number of spring lines	4	-
Damping ratio	0.1	-
relative wind direction	90	°
Minimum breaking load	142	t
Line material	Nylon	-
Pretension	10	%
Mean wind speed	15	m/s
Horizontal line angle breast lines	34	°
Horizontal line angle spring lines	22	°
Vertical line angle breast lines	31	°
Vertical line angle spring lines	5	°
Simulated time	12000	s
Time step numerical solver	0.3	s

Table 6.1: Input parameters reference case influence analysis

6.2 Influence extreme value analysis

Since the modelling of wind fluctuations in time incorporates a random phase shift between the different harmonics, different simulations will result in different peak values for the line forces. Therefore one simulation is ran a certain number of times and extreme value analysis is executed to determine the relevant peak value. A relatively efficient way to do this is to fit a Gumbel distribution to the cumulative distribution of the extreme values (Stanisic et al. 2017). Using this fitted Gumbel distribution, the 90^{th} percentile value, or value that is only exceeded 10 percent of the simulations, can be found.

To determine the number of runs required to get acceptable accuracy, a convergence analysis was executed as follows:

1. For the reference case, a simulation with constant input parameters (from the reference case) is executed. The only variation is the variation in the random seed which determines the phase shifts for the different harmonics while creating the wind time series. For each run, the time series of the forces in all four modelled line groups are saved. This is executed for a total of 440 simulations
2. For each simulation, the maximum occurring line force is determined and saved.
3. A list is created containing the maximum occurring line force for each of the 440 simulations. This is called the source list
4. A second empty list, called the analysis list, and a third empty list, called the result list, are created
5. The first value of the source list is added to the analysis list. This is the peak line value achieved using only one simulation. This relates to the first coordinate on the horizontal axis of Figure 6.2. This value is saved in the result list
6. The second value from the source list is added to the analysis list, a normalized cumulative histogram is created, a Gumbel cumulative density function is fitted and the 90^{th} percentile value based on this fitted Gumbel distribution is determined. This is shown in Figure 6.1. This 90^{th} percentile value is saved in the result list For small arrays this Gumbel fit is not yet representative and the found 90^{th} percentile value coincides with the largest found value.
7. Step 6 is repeated for 3 up to 440 values in the analysis list. Each 90^{th} percentile value is saved in the result list accordingly.
8. The result list is plotted in figure 6.2 creating a line relating the number of simulations used to the found 90^{th} percentile value using a Gumbel fit.
9. The analysis list and result list are emptied, the source list is shuffled so the order of all values changes and steps 5 through 8 are repeated. The shuffling of the source list is done so the simulations are evaluated in a different order. This process is repeated 10 times and figure 6.2 is obtained.

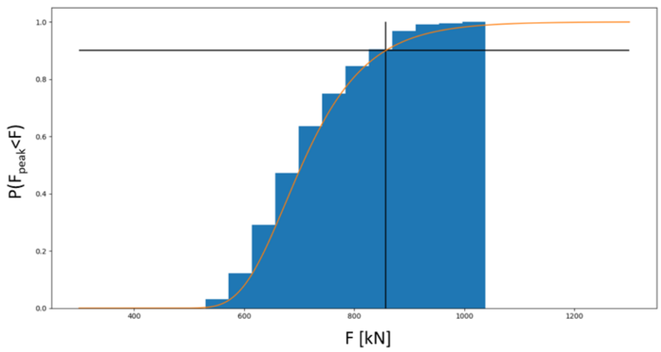

Figure 6.1: Gumbel distribution analysis with 90^{th} percentile value

Figure 6.2 is used to assess the trade off in run time (expressed in number of runs used) and the variance in the 90^{th} percentile peak line force value. A number of runs of 50 is chosen as this yields a variance of about 5% which makes it possible to assert influence relations while keeping the number of simulations relatively small. When using more than 50 runs, the rate at which the accuracy increases, decreases the more runs are used. In other words, the found values converge less quickly after 50 runs.

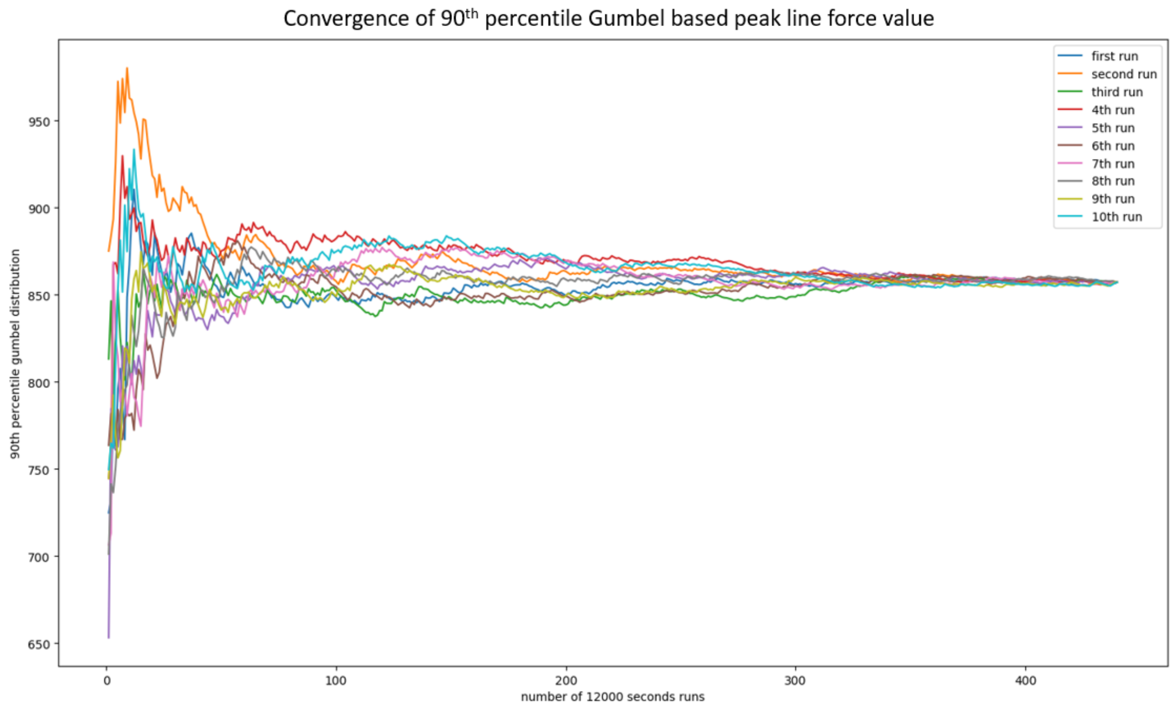

Figure 6.2: Convergence of 90$^{\text{th}}$ percentile Gumbel based peak line force value

Current dynamic mooring analysis is often executed using only one run per simulated situation. This can lead to a significant over or under estimation of the relevant peak line force. In this research, a number of 50 runs per simulation is used and the 90$^{\text{th}}$ percentile value is used to asses the peak line forces for all simulations. As it is unknown where in the 5% band width the found values lie, an uncertainty around the value of 5% higher or lower is indicated in the plots.

6.3 Critical wind angles

To determine the critical wind angle for the reference case, for the used example case, the wind angle was varied to analyse the influence on the peak line forces. This influence is presented in Figure 6.3. From these results it is clear that the critical wind direction lies between 60 and 90 degrees relative to vessel. As the used system is symmetrical, the same forces occur between 90 and 120 degrees. For this study a wind angle of 90 degrees is chosen to assess all influences.

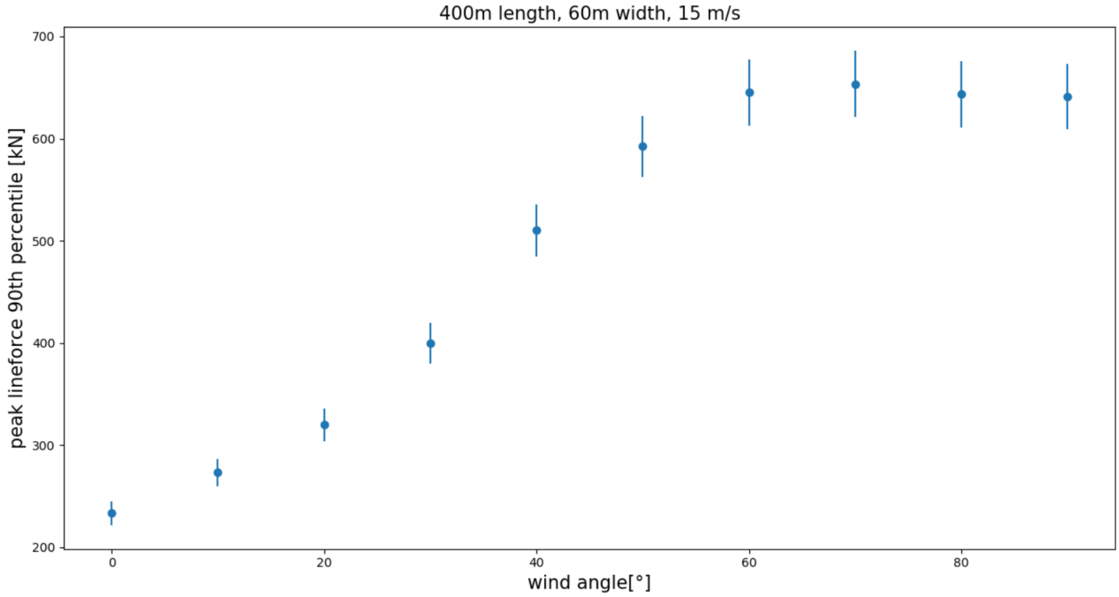

Figure 6.3: Influence wind direction on peak line force

6.4 Influence wind field variation over vessel length

At container terminals large container stacks on land can influence the wind field spatially. This can cause an extra yaw moment due to eccentricity of the resulting wind force. Currently this is often neglected as the deviation is often unknown and can also change during operations. To investigate this difference the normal yaw moment due to wind vessel interaction was neglected but instead the yaw moment was defined by the lateral wind force combined with an arm of eccentricity. To ensure only the extra yaw moment influence is analysed, the total lateral wind force was kept constant. To relate the arm of eccentricity to a real life case, an example can be used. Figure 6.4 presents an example case for which the wind field is disturbed by a stack of containers on the quay resulting in a lower wind velocity over the back part of the vessel compared to the front part. Here u_1 and u_2 are the wind velocities on the back and front half respectively and e_1 and e_2 are the distance of the resulting force with respect to the center of the vessel.

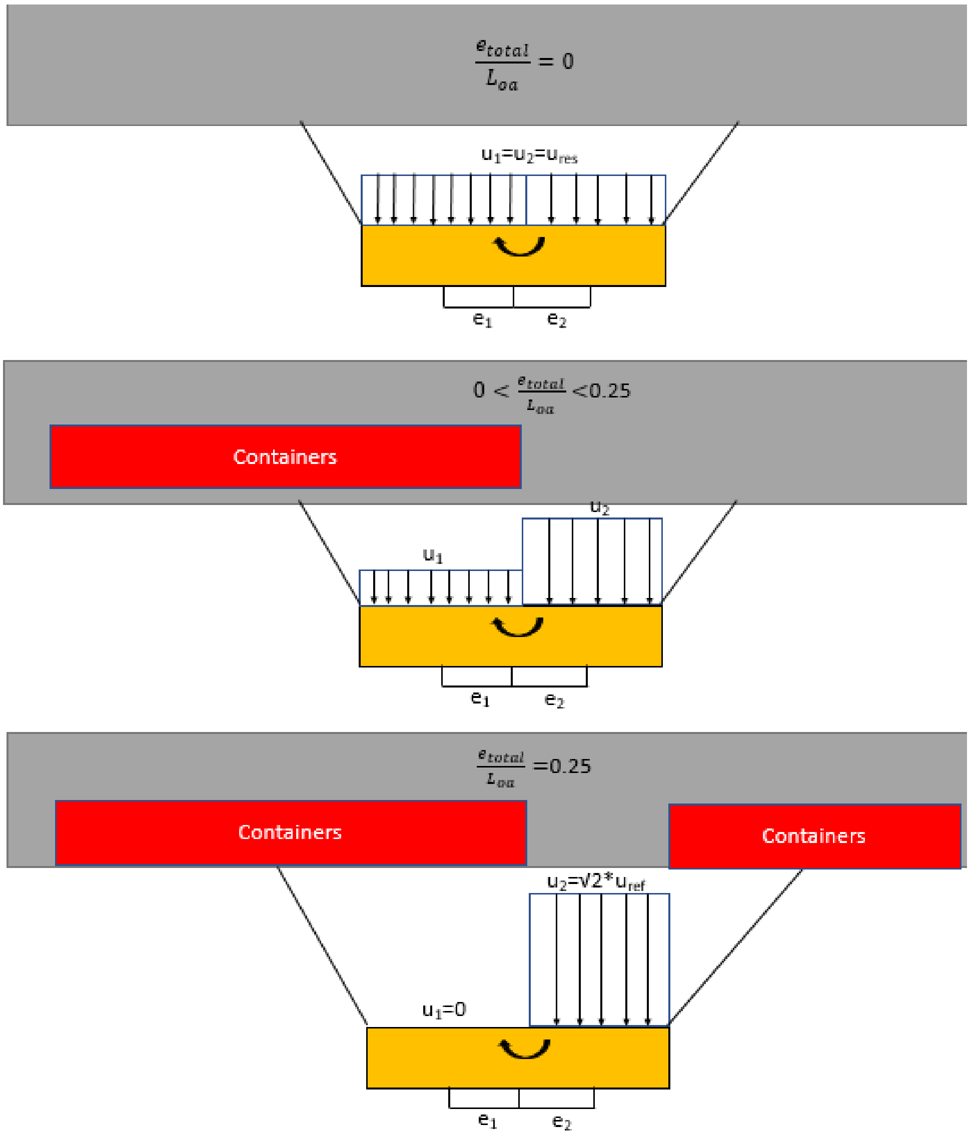

Figure 6.4: Example of a situation in which the lay out of the on land situation influences the spatial variety of the wind field over the length of the vessel

As the total lateral force is kept constant to only assess a change in the yaw moment, assuming a constant distribution of the wind area over the length and assuming a step-like transition from the one wind field to the other, the different wind speeds relate to the eccentricity arm following a logical relation. Equation 6.1 ensures that the lateral wind force stays constant which can be rewritten to Equation 6.2 to relate the wind speeds on the different parts of the vessel. The eccentricity of the total wind field is stated in Equation 6.3 and rewritten using the wind speed, force relation to Equation 6.4. Dividing this by the over all vessel length, Equation 6.5 was produced.

$$L_{oa}u_{ref}^2 = 0.5L_{oa}(u_1^2 + u_2^2) \tag{6.1}$$

$$u_1^2 = 2u_{ref}^2 - u_2^2 \tag{6.2}$$

$$e_{total} = \frac{0.25L_{oa}(-F_1 + F_2)}{F_1 + F_2} \tag{6.3}$$

$$e_{total} = 0.25L_{oa}\frac{0.5L_{oa}(-u_1^2 + u_2^2)}{0.5L_{oa}(u_1^2 + u_2^2)} \tag{6.4}$$

$$\frac{e_{total}}{L_{oa}} = 0.25\frac{-u_1^2 + u_2^2}{u_1^2 + u_2^2} \tag{6.5}$$

Combining Equations 6.2 and 6.5, the eccentricity arm can be related to the wind speed on the front half and, using the relation in Equation 6.2, the back wind speed can also be determined. This leads to Equation 6.6 which can be written to express the wind speed on the front half as a function of the eccentricity arm ratio as is defined in 6.7

$$\frac{e_{total}}{L_{oa}} = \frac{(u_2^2 - u_{ref}^2)}{4u_{ref}^2} \tag{6.6}$$

$$u_2 = \sqrt{4u_{ref}^2\frac{e_{total}}{L_{oa}} + u_{ref}^2} \tag{6.7}$$

These equations are valid under the aforementioned assumptions and until an eccentricity arm / overall length ratio of 0.25 is reached. In that case, the back half of the vessel is completely shielded and only the front half experiences wind force.

By varying the arm it was determined if spatial variety of the wind field presents significant deviations in the maximum line forces. The arm is presented as a ratio related to the over all vessel length. The results of this test are shown in Figure 6.5. From these tests it can be concluded that spatial variety can be an important factor if it causes an extra yaw moment. More detailed wind field measurements at container terminals can help in determining the real life occurrence of these spatial varieties and the associated yaw moments.

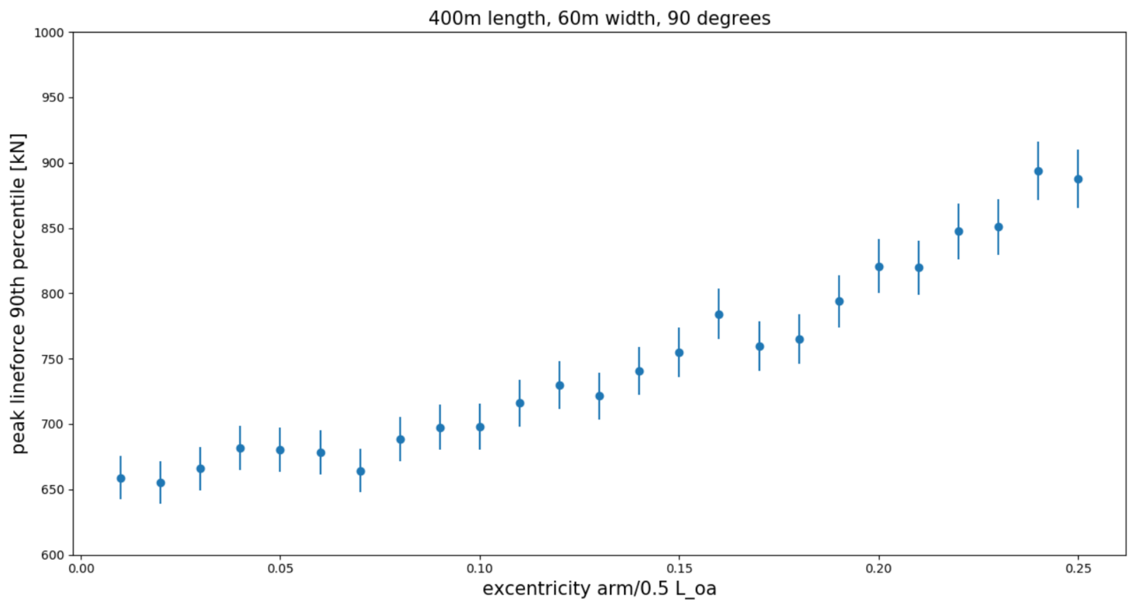

Figure 6.5: Spatial variety causing yaw moments peak line force influence

6.5 Influence roll moment due to vertical wind profile

Due to a non constant wind profile over the height of a vessel, the wind vessel interaction also produces roll moments. Currently these moments are often neglected because the location specific height profile is often unknown. A similar approach as for the spatial variety over the length was used relating the eccentricity arm to the vessel height. How wind field variety over vessel height can influence the roll motions is presented in Figure 6.6. During these simulations, like with the variety over the length, the total lateral wind force was kept constant. The representation of the total wind force at one point at quay level or at vessel top level, as seen in Figure 6.6 is unrealistic. However, for extra certainty also these impossible cases are simulated to determine if extremities approaching these limits would lead to a significant influence on the line forces.

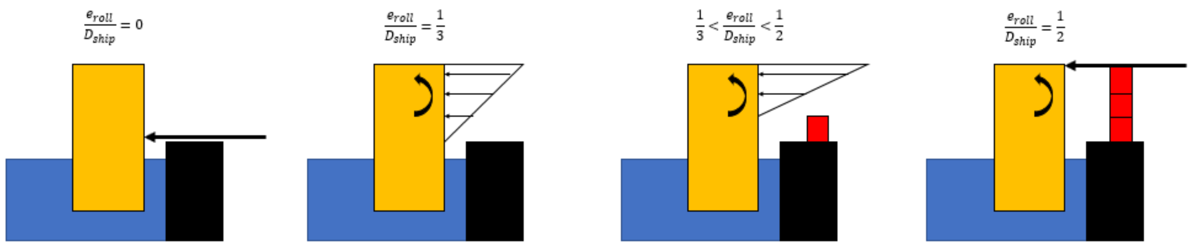

Figure 6.6: Example of how spatial variety over the vessel height creates roll moments

The results are shown in Figure 6.7. From these results it can be concluded that the spatial variety over the vessel height does not play a significant roll in the generation of the peak line forces. This has also been investigated with extremely (unrealistic) large and small vertical line angles resulting in the same conclusion, as can be seen in Figure 6.7. However, an increase in roll moment does result in an increase in roll motion, which can be relevant for operational efficiency. This is displayed in Figure 6.8. As can be seen from the case with a zero eccentricity arm, the roll motion is also influenced by line forces generated due to the other motions. The wind moment counteracts the line force moment, resulting in a shift of the mean roll angle to the positive side.

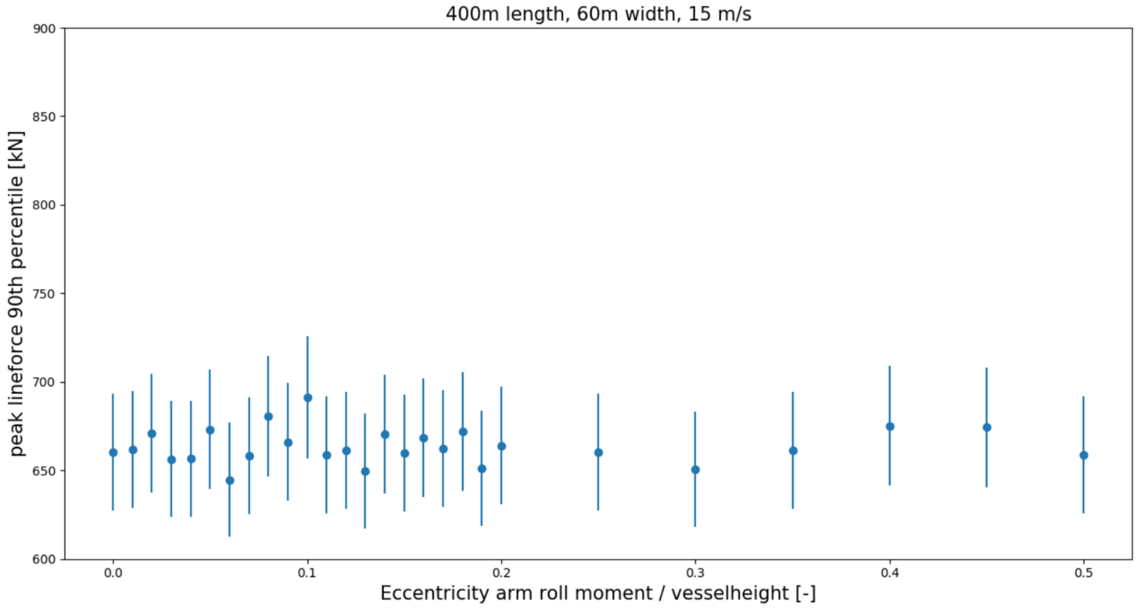

Figure 6.7: Influence vertical eccentricity causing roll moments on peak line forces

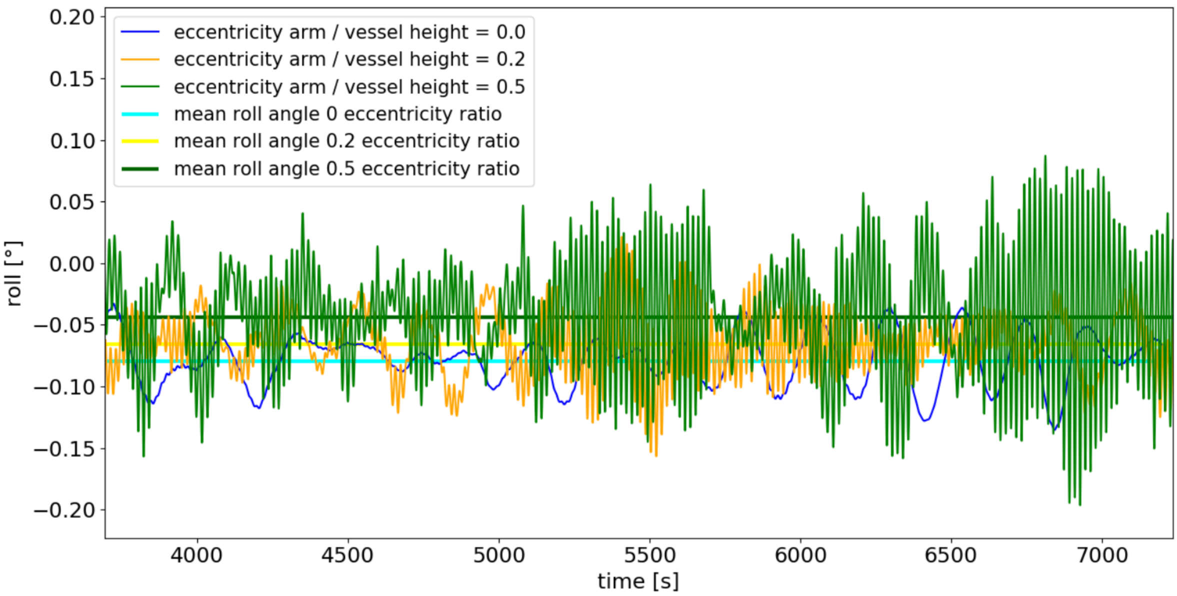

Figure 6.8: Roll movement for the reference case with different roll arms.

6.6 Choice of theoretical spectrum for the wind fluctuations in time

To describe wind fluctuations in time, different theoretical frequency spectra have been proposed. Three theoretical wind spectra are assessed here: Harris, NPD and Davenport wind spectrum. The davenport and Harris spectrum originate in wind measurements on land whereas the NPD spectrum is based on wind over sea (Kaasen 1999). As all three spectra are defined differently, this will have an impact on the wind time series and therefore, on the force on the system. The significance of this influence is investigated and presented in Figure 6.9. The choice of spectrum is a significant influence on the resulting peak line forces and which spectrum is best for the investigated situation, should be properly evaluated to achieve the best results. Which spectrum results in the largest peak line forces depends on the natural frequency of the moored vessel system, as all three spectra peak at different frequencies. For the safest estimates, the natural frequency for the relevant vessel motions must be determined and the spectrum with the most energy at that frequency must be used for the simulation.

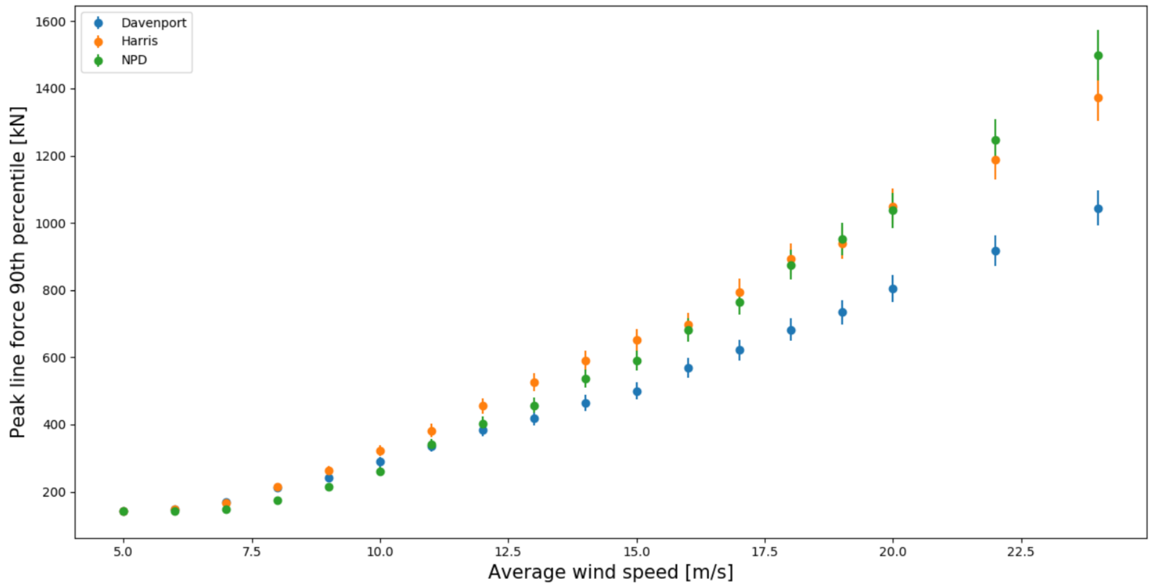

Figure 6.9: Different wind spectra influencing the maximum occurring line forces

6.7 Influence inconsistencies in the wind ship interaction coefficients

As wind coefficients are determined based on wind tunnel tests or computational fluid dynamics, the windcoefficients are not available for every individual vessel. Instead, usually the coefficients of a comparable vessel are used. This, combined with differences in different stack heights during loading and unloading can lead to deviations in the wind coefficients from the real life scenario. These wind coefficients will be further evaluated in the analysis of data and generation of peak force estimation formula. However, it should be noted that the uncertainties in these wind coefficients should be properly evaluated using the found influence relations.

6.8 Influence deviations in added mass and hydrodynamic damping

Added mass and hydrodynamic damping depend on the vessel fluid interaction. In the conceptual model this added mass is an input parameter either in ratio to regular mass or as an absolute value. However, in reality the added mass is a function of a number of input parameters like vessel dimensions, vessel draught, presence and shape of the quay, under keel clearance and water density (salt or sweet water). Furthermore, the added mass and hydrodynamic damping depend on the frequency of the excitation of the system in the different degrees of freedom. In this study the added mass and hydrodynamic damping are used as input parameters to assess their influence. When this influence is known, the relation between the input parameters and the added mass and hydrodynamic damping can be used to implement the method. However, the relation between the different response frequencies and the added mass, which in its turn again influences the response frequency, is not considered. From added mass data evaluations executed by RHDHV for numeral projects it can be derived that for frequencies that can be expected for large container vessels, the added mass frequency dependency is limited. Furthermore, an increase in frequency results in an increase in added mass which leads to a decrease in frequency, this is a stabilizing relation which makes the frequency dependency less significant. Nevertheless, further research can be executed using models which do evaluate this frequency dependant relation. This will result in a more accurate representation of the real life situation.

7. Determination of influence of different parameters and proposal of peak line force formula

This chapter elaborates step 5 (Sections 7.1 through 7.4) and 6 (Section 7.5 and 7.6) of the methodology. To determine a relationship between the different input parameters, the influence parameters are grouped by influence term: mass/inertia, damping, spring and external forcing. By evaluating the influence of the combined parameters, a first relation can be determined.

7.1 Influence of mass and inertia on peak line forces

To create a consistent damping for all variations, damping is not defined as an absolute value in the conceptual model but as a damping ratio based on the theoretical damping coefficient used for regular linear mass spring systems as presented in Equation 7.1. The spring coefficients are approximated by determining the linearised spring stiffness of the lines and decomposing them in surge and sway direction. These are combined with the appropriate mass or inertia terms and the chosen damping ratio to obtain the damping coefficient for each degree of freedom. This means that an increase in mass while keeping the damping ratio constant, results in an increase in the damping coefficient. In other words: the increase in mass with a constant damping ratio results in an absolute increase of damping in the system.

$$\zeta = \frac{c}{\sqrt{2km}} \tag{7.1}$$

Where:
ζ = damping ratio
c = damping coefficient
k = spring constant
m = mass

Checking the mass and moment of inertia influence is executed by multiplying the mass including added mass and the moment of inertia including the added moment of inertia by one factor. For this analysis the reference case form Chapter 6 is used. Only the mass and inertia are varied, while the damping ratio is kept constant. The results are presented in Figure 7.1. Here it can be seen that the mass and inertia do not significantly influence the occurring peak line forces when combined with a constant damping ratio. The same analysis was also executed under different wind angles which also did not show significant influence of mass and inertia on the peak. Therefore, the influence of mass and inertia is not an explicit input parameter for a peak line force prediction polynomial, but is used implicitly in determining the input value for the damping ratio. However, mass and inertia do influence the frequency of movement of the vessel, which can be influential for the serviceability limit state. This change in frequency is presented in Figure 7.2

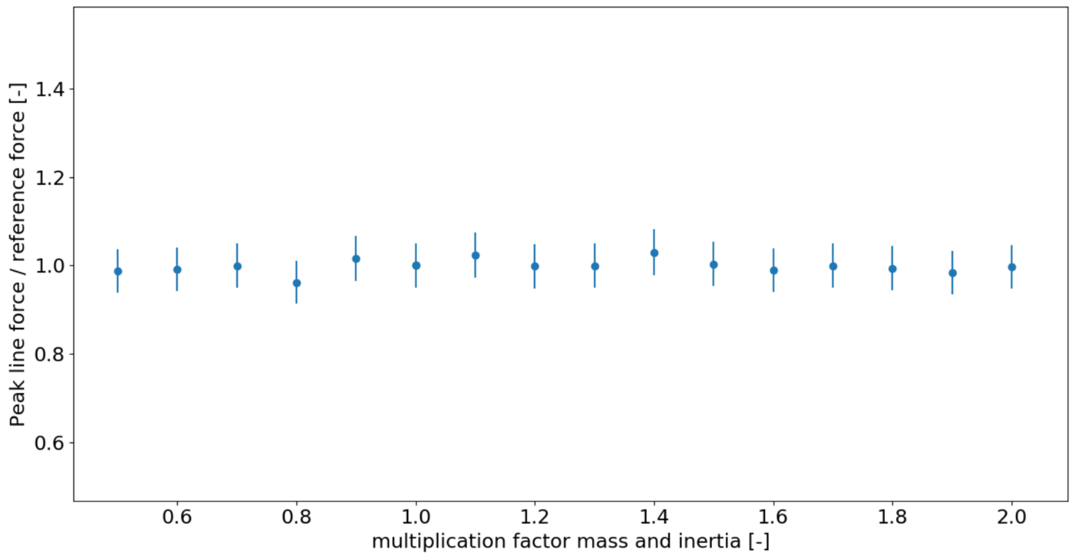

Figure 7.1: Influence of mass and inertia on the peak line forces

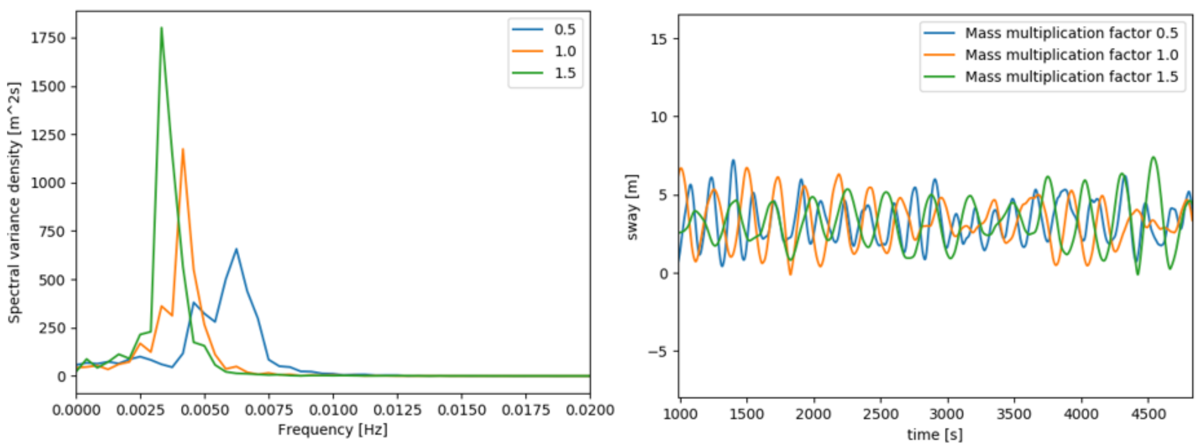

Figure 7.2: sway results for different mass multiplication factors (left: variance density spectrum, right: response in time

7.2 Influence of damping ratio on peak line forces

Now, by varying the damping ratio, the influence of the relative amount of damping can be assessed. Again the described vessel was used to assess influence from damping on the peak line forces. The results of this influence is presented in Figure 7.3. A linear relation is fitted to the results and a relation between the relative peak line force and the damping ratio is determined. To do this, the found peak force values were divided by the peak line force for the reference case, which is 660 kN. The prescribed relation is given in Equation 7.2. All influence relations in this chapter are determined using least squares fit and are displayed with a 5% uncertainty band to account for the uncertainty in the extreme value analysis method.

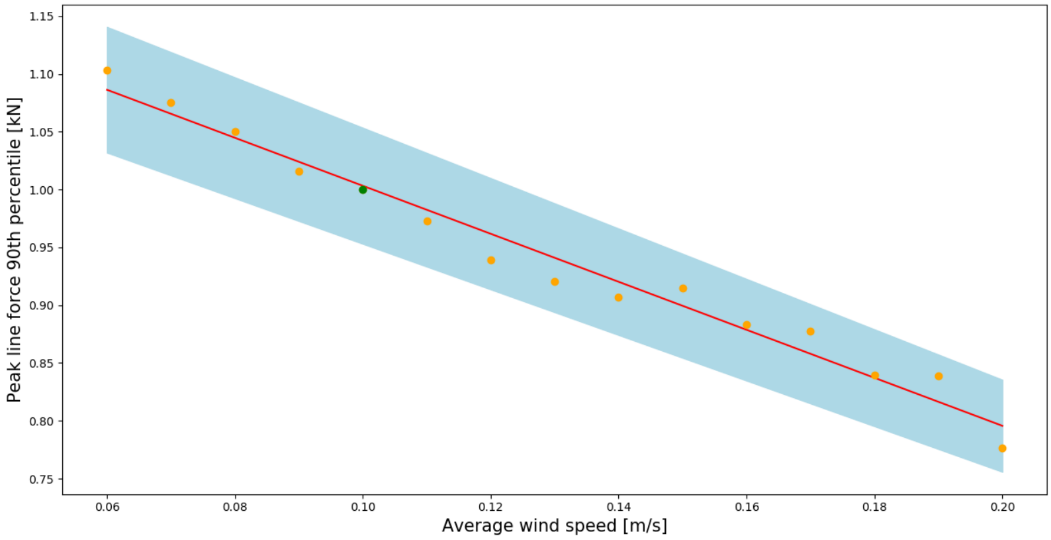

Figure 7.3: Variation of damping ratio with linear fit and 5% uncertainty band, the green dot represents the reference case.MBL

$$\frac{F}{F_{ref}} = -2.11\zeta + 1.21 \tag{7.2}$$

where:

F = 90^{th} percentile peak value
F_{ref} = 90^{th} percentile peak value reference case
ζ = damping ratio

7.3 Influence of spring term

As the conceptual model bundles all lines into 4 groups which are represented by one line each, the spring term influence can be more easily determined than with many separate lines. However, this also simplifies the response and may lead to underestimation of the actual peak line forces, as in real life there is always one line which is positioned less favourable than the "average" line. One of the key input parameters for the spring term is the minimum breaking load of the lines. The influence of this MBL relative to the reference case is investigated for Nylon and polyester lines, which have different load elongation curves. The results and the fit with 5% uncertainty band is presented in Figure 7.4.

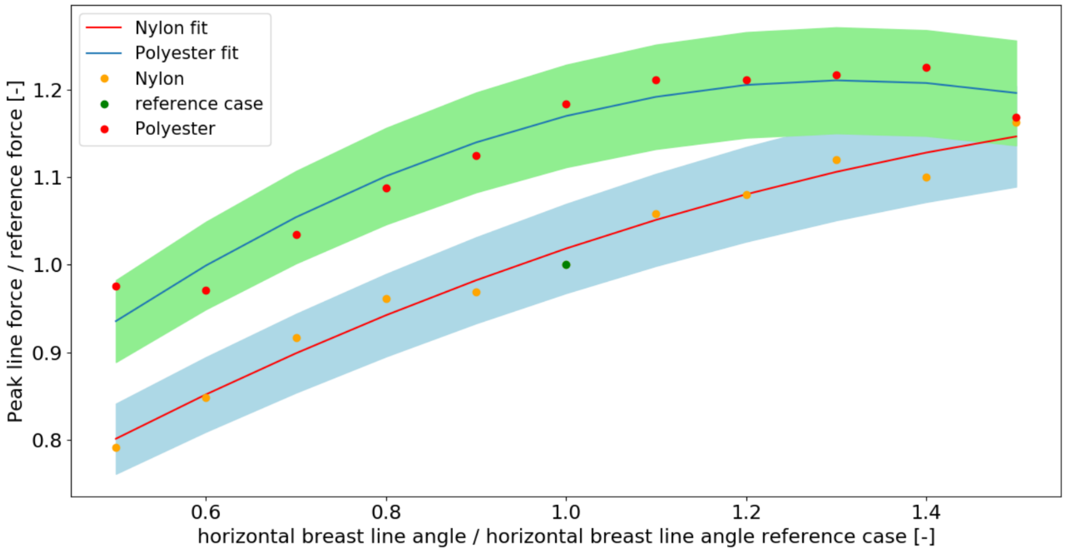

Figure 7.4: Influence of minimum breaking load on absolute peak line forces

$$\frac{F}{F_{ref}} = -0.179(\frac{MBL}{142})^2 + 0.70\frac{MBL}{142} + 0.495 \quad (7.3)$$

Where:
MBL = minimum breaking load in tonnes

Another parameter for the spring term is the line angle in the horizontal plane. To investigate this, the bollard positions were varied to create different line angles in the horizontal plane while changing the on-deck line length to ensure a constant total line length. The way this is simulated, is indicated in figure 7.5 This influence is presented in Figure 7.6. The second order polynomial is fit which results in Equation 7.4

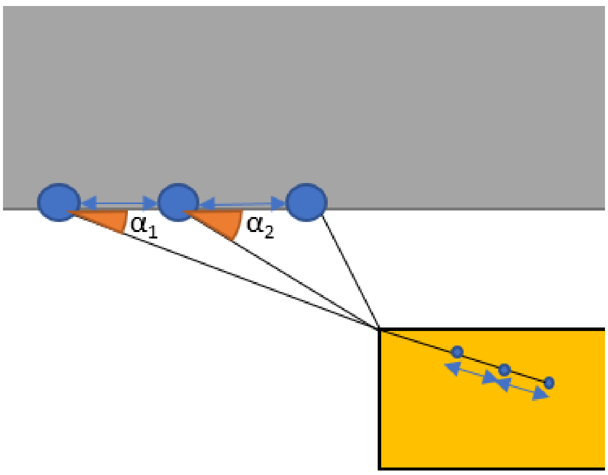

Figure 7.5: Variation of horizontal line angles and adjustment of on-deck line length

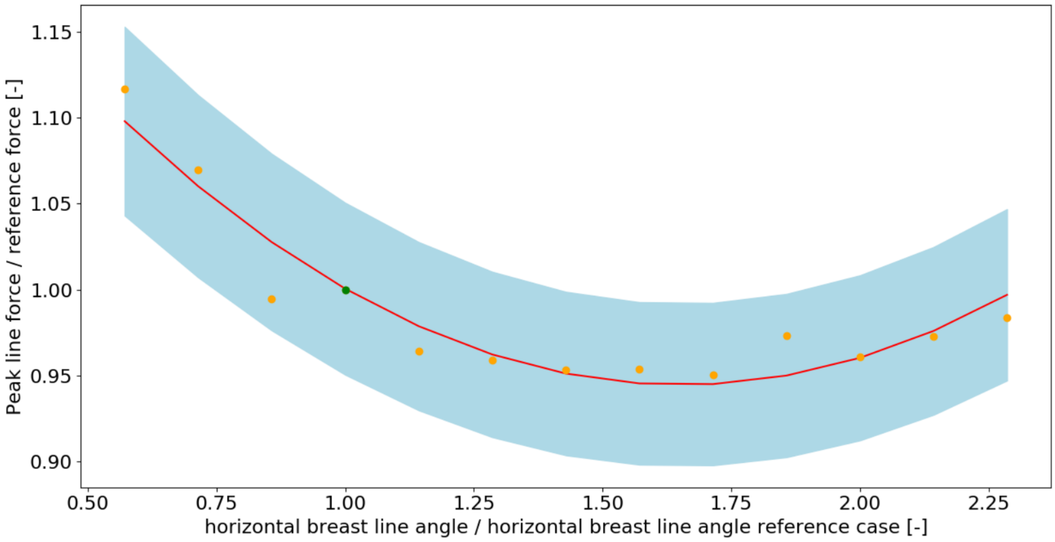

Figure 7.6: Influence horizontal line angles on peak line forces

$$\frac{F}{F_{res}} = 0.124(\frac{\alpha}{34})^2 - 0.42\frac{\alpha}{34} + 1.3 \quad (7.4)$$

Where:
α = horizontal line angle in degrees

Apart from horizontal line angles, vertical line angles are also present. The influence of these angles was again investigated by varying the bollard positions as indicated in Figure 7.7. The vertical line angle relative to the reference case is used to assess the influence of this vertical line angle. The results are presented in Figure 7.8 and the determined second order influence polynomial is described by Equation 7.5.

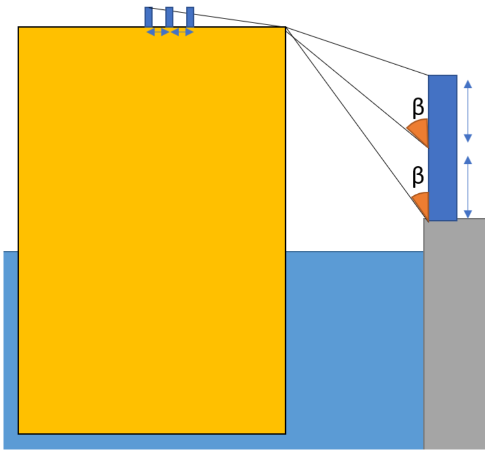

Figure 7.7: Variation of vertical line angles and adjustment of on-deck line length

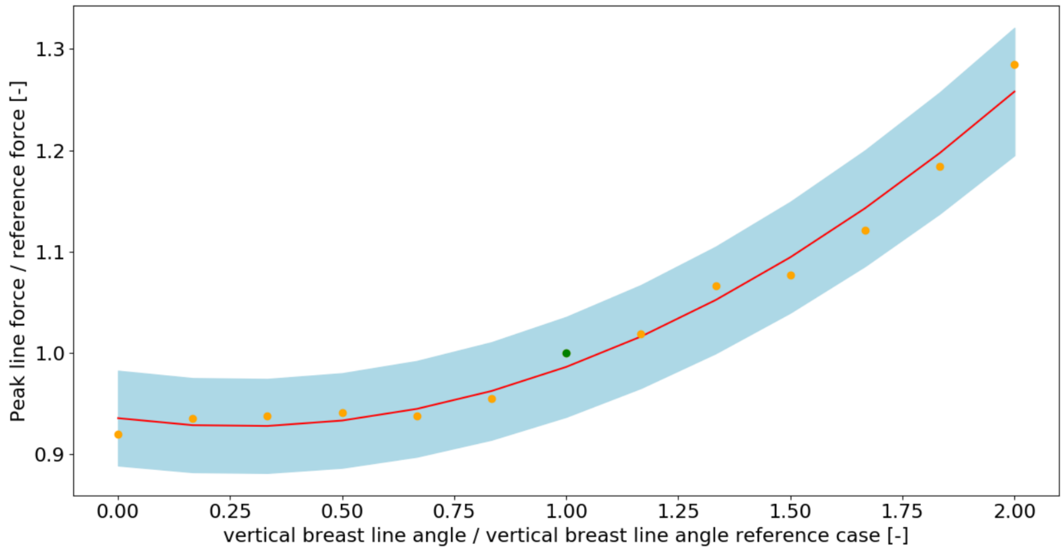

Figure 7.8: Influence vertical line angles on peak line forces

$$\frac{F}{F_{res}} = 0.11(\frac{\beta}{31.16})^2 - 0.06\frac{\beta}{31.16} + 0.94 \quad (7.5)$$

Where:
β = vertical line angle in degrees

The influence of pretension was also analysed but no significant impact on maximum mooring forces was found. The relation between the breast line length to reference line length ratio and the peak force to reference force ratio is presented in figure 7.9

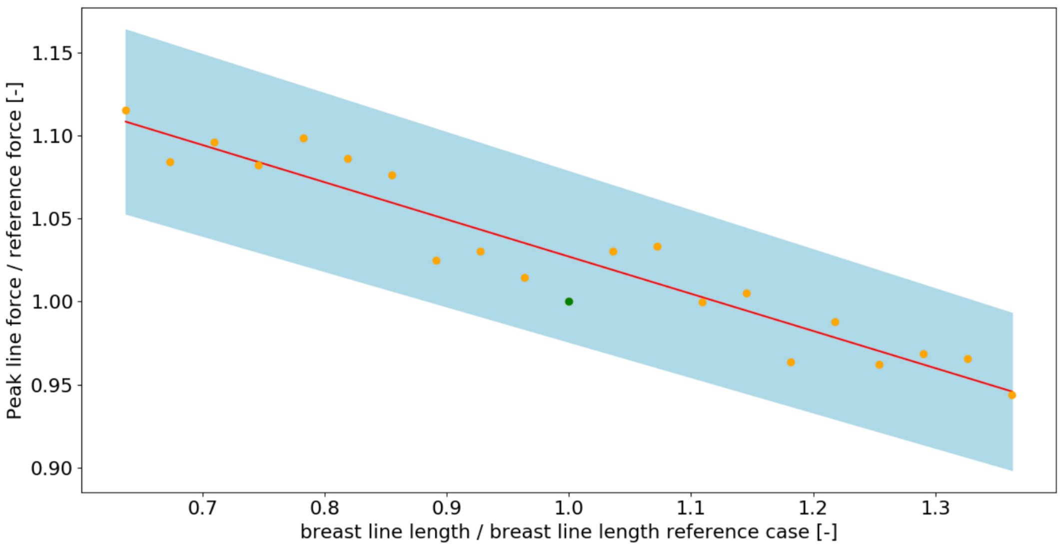

Figure 7.9: Influence of on deck line length on peak line forces

$$\frac{F}{F_{res}} = -0.22\frac{L_{breast}}{55.13} + 1.25 \quad (7.6)$$

Where: L_{breast} = length breast lines in meters

7.4 external forcing term

As the external wind forcing on the system is defined by Equation 7.7, the forcing input parameters that are assessed are wind coefficient, wind area and mean wind speed. Important to note is that the mean wind speed is an input parameter for the wind spectrum and therefore also influences the wind fluctuations around this mean velocity. Again for a vessel with length 400m, beam of 200m and wind blowing perpendicular on the vessel, the influence of these parameters is assessed

$$F = 0.5\rho c A u_{wind}^2 \tag{7.7}$$

where:
ρ = density of air
c = wind coefficient
A = surface wind area
u_{wind} = the wind velocity at a certain time.

To assess the influence of the wind coefficients, the full set of wind coefficients (sway, surge and yaw) is multiplied by a scaling coefficient. The results are presented in Figure 7.10. The found peak line forces are plotted against this factor resulting in an approximately linear relation. This relation is quite similar for 60 degrees and 90 degrees wind direction indicating no significant difference between the directions.

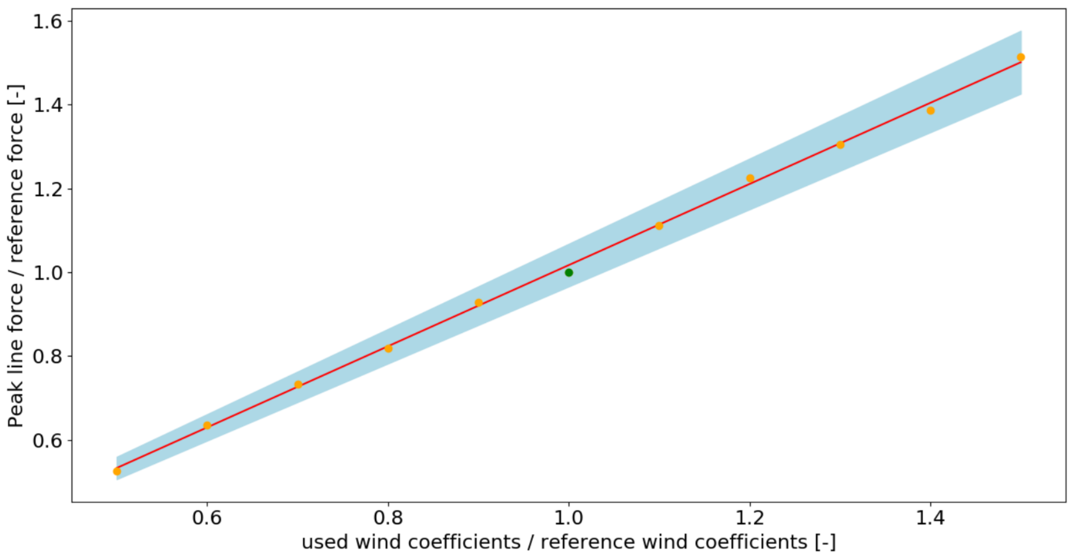

Figure 7.10: Influence multiplication factor over wind coefficients

Similar to the wind coefficients also both lateral and longitudinal wind areas are multiplied with a scaling coefficient. The results are presented in Figure 7.11. Both the wind coefficient as wind area multiplication result in similar linear fits. This is expected behaviour as the area and coefficients and wind areas are directly multiplied with each other to determine the forcing in the different degrees of freedom.

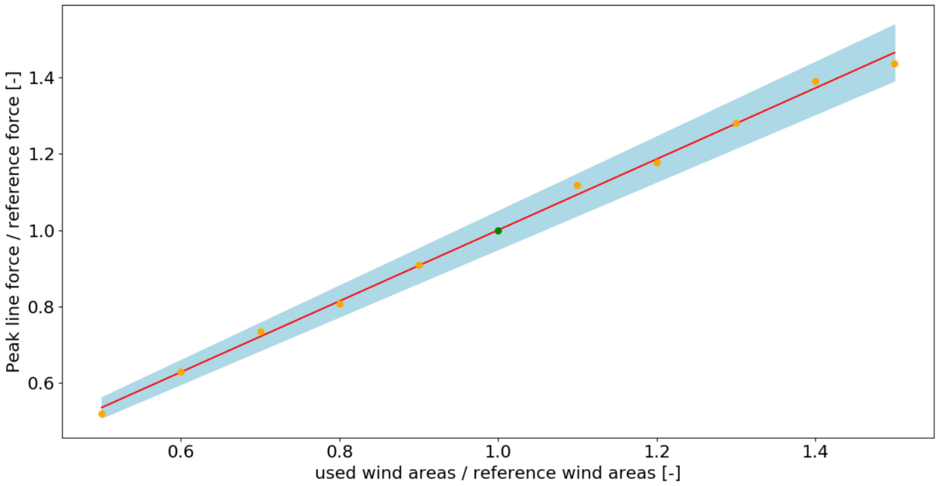

Figure 7.11: Influence multiplication factor over wind areas

Both the wind area and wind coefficient appear to be direct scaling parameters for the peak line forces. Therefore, the product of these two values can be taken as one influence parameter resulting in equation 7.8

$$\frac{F}{F_{ref}} = 0.95\frac{AC_{used}}{AC_{ref}} + 0.05 \tag{7.8}$$

As can be seen from equation 7.7, the other input parameter for the external forcing is the wind speed. This wind speed depends on the chosen theoretical wind spectrum (see section 6.6) and the modelled mean wind speed. By varying the mean wind speed, an influence relation can be found. The results are presented in Figure 7.12. The found influence relation is described in Equation 7.9

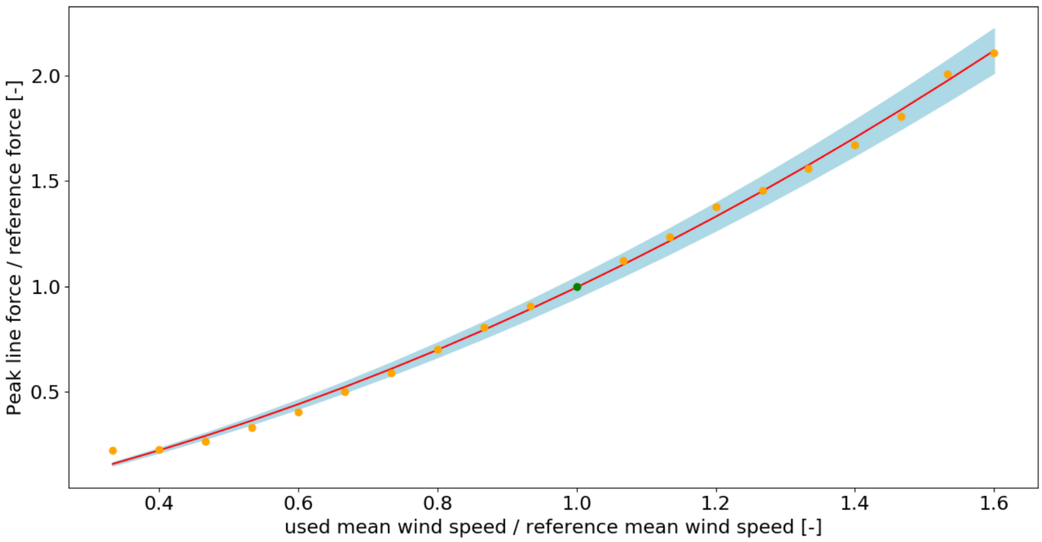

Figure 7.12: Influence of mean wind speed on peak line forces

$$\frac{F}{F_{res}} = 0.49(\frac{u_{wind}}{15})^2 + 0.61\frac{u_{wind}}{15} - 0.1 \tag{7.9}$$

Where:

u_{wind} = mean wind speed in m/s

As the wind speed, wind area and wind coefficients are multiplied in the forcing term (Equation 7.7), it is logical that the influence of these parameters is not independent. To test this, the wind speed influence is analysed for the reference case, a case where the wind areas were halved and a case where the wind areas were doubled. Instead of adding the influence relations, like is common for independent parameters, the relations were multiplied. This gave a better result compared to the actual results from the simulations, as can be seen in Figure 7.13. The deviation in the smallest area factor curves can be explained by the fact that the line forces will not reach zero in reality as there is a base force balancing the line forces due to pretension and the initial compression of the fenders.

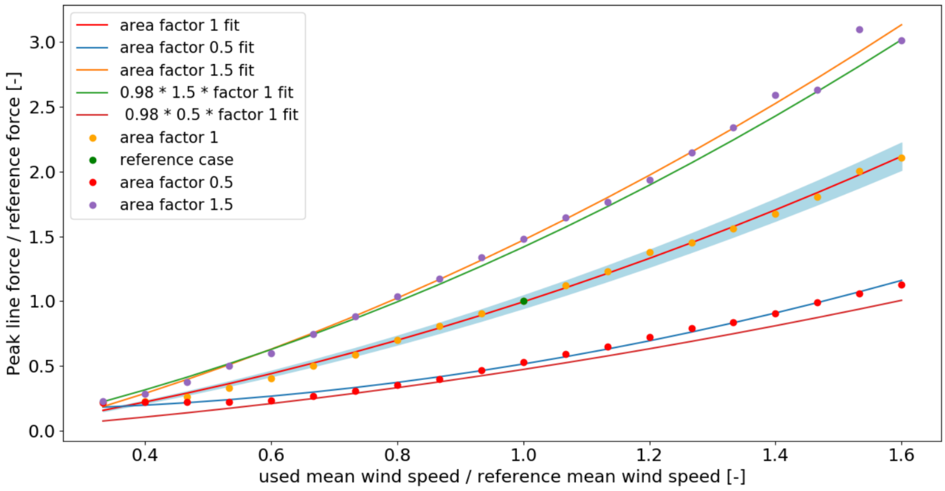

Figure 7.13: Analysis of multiplication of wind speed and area/coefficient relations

7.5 First proposal of a peak line force prediction polynomial

Now the individual influence relations are determined, a first proposal for a peak line force prediction polynomial can be put forward. If all influence parameters are completely independent, the polynomial can be written as a summation of the individual relations. However, as can be seen from the wind speed, wind area, wind coefficient relations not all parameters are completely independent. For all other parameters only individual influence relations were derived, as finding all dependencies between the influence parameters requires a lot more simulation and analysis time. Therefore, for all other parameters no covariance is assumed. This results in the polynomial described by Equations 7.10 through 7.16. From the influence relations it can be determined that the most influential parameters are the wind area, wind coefficient and mean wind speed, as described in the term ACU, and the damping ratio.

$$\frac{F}{F_{res}} = ACU + K + L^* + \zeta^* + \beta^* + \alpha^* \tag{7.10}$$

$$ACU = (0.95\frac{AC_{used}}{AC_{ref}} + 0.05) * (0.49(\frac{u_{wind}}{15})^2 + 0.61\frac{u_{wind}}{15} - 0.1) \tag{7.11}$$

Where:

$$K = -0.179(\frac{MBL}{142})^2 + 0.70\frac{MBL}{142} - 0.505 \tag{7.12}$$

$$L^* = -0.22\frac{L_{breast}}{55.13} + 0.25 \tag{7.13}$$

$$\zeta^* = -2.11\zeta + 0.21 \tag{7.14}$$

$$\beta^* = 0.12(\frac{\beta}{31.16})^2 - 0.06\frac{\beta}{31.16} - 0.06 \tag{7.15}$$

$$\alpha^* = 0.124(\frac{\alpha}{34})^2 - 0.42\frac{\alpha}{34} + 0.3 \tag{7.16}$$

Where:

F_{res} = 650 kN
u_{wind} = mean wind speed in m/s
MBL = minimum breaking load in tonnes
L_{breast} = length breast lines in m
ζ = damping ratio
β = vertical line angle in degrees
α = horizontal line angle in degrees

7.6 Testing of the polynomial with model results

Finally, the proposed polynomial is compared to different simulated cases to get a first estimate on the performance and possible areas for improvement. The results are presented in Figure 7.14. Some key cases are case 1 and case 9. For case 1, the input parameters are all chosen so that very small line forces are obtained. Here one of the shortcomings of the polynomial becomes clear: The polynomial results in negative line forces, which is impossible. However, very small values are not relevant in real life, as the critical line forces are relevant for the safety. However, this may become relevant if substantially smaller vessels are analysed. For case 9, line force increasing values for the parameters are chosen. Here, the performance is better than for case 1, but also significant differences are found. Finally, some large overestimations are found for cases with line angles very different from the reference case. This implies that the found influence relations for the line angles perform poorly when incorporated into the polynomial.

Case	Area*coefficient deviation	windspeed deviation	deviation dampin ratio	deviation breas line length	MBL deviation	deviation horizontal angle	deviation vertical angle	Model result	polynomial result	percent difference
Reference	0	0.0%	0.0%	0.0%	0.0%	0.0%	0.0%	653	662	1.44%
2	-50%	-46.7%	100.0%	27.2%	-50.0%	47.1%	-100.0%	76	-253	-432.79%
3	-40%	26.7%	40.0%	14.5%	30.0%	2.9%	-35.8%	568	532	-6.39%
4	-20%	26.7%	10.0%	10.9%	20.0%	32.4%	-35.8%	682	721	5.73%
5	-10%	40.0%	50.0%	0.0%	-30.0%	23.5%	-42.2%	747	804	7.57%
6	20%	13.3%	40.0%	0.0%	30.0%	105.9%	-61.5%	661	890	34.63%
7	30%	-26.7%	50.0%	36.3%	30.0%	61.8%	-77.5%	316	373	17.93%
8	40%	-26.7%	-10.0%	-23.6%	10.0%	76.5%	-67.9%	387	548	41.64%
9	40%	6.7%	-10.0%	-23.6%	-20.0%	67.6%	-61.5%	750	930	24.06%
10	50%	46.7%	-40.0%	-27.2%	50.0%	-11.8%	-3.7%	2368	1965	-17.02%
11	-30%	-13.3%	40.0%	9.1%	-10.0%	0.0%	0.0%	329	291	-11.69%
12	-20%	-20.0%	20.0%	-18.1%	20.0%	0.0%	0.0%	372	423	13.60%
13	0%	26.7%	30.0%	36.3%	-50.0%	0.0%	0.0%	703	715	1.72%
14	20%	13.3%	0.0%	-18.1%	-10.0%	0.0%	0.0%	983	961	-2.21%
15	20%	13.3%	0.0%	27.2%	-10.0%	0.0%	0.0%	872	892	2.25%
16	50%	6.7%	-30.0%	-27.2%	40.0%	0.0%	0.0%	1389	1232	-11.27%
17	80%	-26.7%	80.0%	-13.6%	-30.0%	0.0%	0.0%	563	542	-3.75%

Figure 7.14: 17 simulated cases compared to the polynomial results, results in blue: 0-10%, yellow:10-25%, red: >25%

8. Discussion of the conceptual model and the results

To correctly interpret the results from Chapter 6 and 7, it is important to relate the results to the real world. To do this, the different steps should be discussed. The discussion presented in this chapter relates to step 7 in the methodology.

8.1 Simplifications used in the conceptual model

To create a model that solves the dynamic system of a moored container vessel in fluctuating wind fields, certain simplifications are made to decrease the programming work required to create the model.

8.1.1 Multiple lines modelled as one

As discussed in Chapter 5, all lines are schematized using two breast lines and two spring lines. In reality many more lines are used in large container vessel mooring. Those multiple lines have different lengths and angles resulting in different spring coefficients. The used approach adds the individual lines by choosing the average length and angle and implementing the number different lines as the same number times the average line. This is based on the equivalent spring theory from basic mechanics stating that the spring coefficients of multiple parallel springs can be added to create one equivalent spring. To determine the exact equivalent spring for a given mooring case, the angles lengths and load elongation curves can be assessed to determine the best approximation for the equivalent spring However, for more exact determination of the real life peak line force, a relation between the peak line force of the equivalent line and the critical line can be added.

8.1.2 Wind angle fluctuations

In reality, wind fields do not only fluctuate in velocity but can also have deviations in direction but these were not modelled. Incorporating these fluctuations may yield better results but also incorporates an extra random factor in translating the directional spectrum to time series. This may require more extensive analysis with larger numbers of simulation to achieve the 5% or less variance in the extreme value analysis.

8.1.3 Assumptions within the Scribanti module

Determining the hydromechanic righting moment using the Scribanti formula, some assumptions regarding weight distribution are made to determine the center of buoyancy and the center of gravity for a vessel. Changing the assumed positions of these points results in an increase or decrease in the righting moment resulting in a weaker or stiffer rotational spring. As stated in Section 6.5, for the used positions, which are realistic for a loaded container vessel, the roll moment influence is not significant for the peak line force determination. However, for different assumptions for the positions of the center of gravity and center of buoyancy, different results may be obtained. In reality, the positions of the center of gravity and buoyancy shift when different degrees of loading are applied. This will result in changes in the hydro static stiffness and therefore in larger or smaller roll angles. However, as described in Chapter 6, increases in roll angles have no significant influence on the peak line forces. Here the maximum, completely unrealistic, eccentricity still does not give a significant influence on the peak line forces. Therefore, smaller rotational stiffness will have limited influence on the peak line forces.

8.1.4 lack of real life measurements to validate theoretical models

At the moment there is no large dataset present with detailed movement and line force measurements for moored large container vessels. Therefore, both the conceptual model used in this study and models used in the industry are largely based on theory. If this data would be available, it could be used to asses the performance of dynamic mooring analysis models and increase the performance of these models compared to real world situations.

8.2 Analysis method for industry standard practice assumptions

In the determination of the influence of industry standard practice assumptions, some statistics were used. The implications of the chosen approaches are important to remember.

8.2.1 Extreme value analysis

The extreme value analysis method chosen for this study is one of the possibilities and based on a trade off between computation time and accuracy. Different methods can have different increase in accuracy with an increase in number of runs and may therefore be more or less efficient. The chosen method is based on literature and not all possible methods were tested for this specific case. Furthermore, if computation time of the model could be decreased, the preferred number of runs used in each simulation could increase as a change in computation time also changes the trade-off between computation time and accuracy. Additionally, the choice for a 90^{th} percentile value means that once in every 10 runs the presented value will be exceeded. This is an important note when using these predictions in real life. The markers in the influence plots give a 5% margin above or below the found value as it is unknown where in the 5% variance a certain value is located. This could be further investigated by assessing the distribution of this variance but for these purposes the used indicators were deemed sufficient.

8.2.2 Only variations on reference case used

All influence analyses in Chapter 6 are executed based on the reference case and only varying the parameter of interest. This was done to gain insight in the influence without executing many different simulations, which ensured time efficiency. However from these analyses the influence of certain parameters cannot fully be proven to be negligible, as certain parameters might be important for significantly different vessel sizes or mooring configurations.

8.3 Analysis and polynomial proposal

In analysing the influence of different parameters and quantifying this in influence polynomials certain choices were made. It is important to realise how these choices influence the end result.

8.3.1 Limited dataset

As this study was subject to time pressure and limited resources, a fairly small dataset was created. This can decrease the accuracy of the found influence relations as the uncertainty in the results due to the chosen extreme value analysis method are less averaged out than when more simulations were added to the dataset.

8.3.2 Neglected covariance

The neglected covariance is an important factor in this study. This leads to a less accurate result as in reality the parameters which are assumed independent can in fact be interacting. The downside of the current approach can be visualised using the mean wind speed and the area-coefficient product as an example. As is stated in Section 7.4, these variables are not independent. However, if they are assumed to be independent both relations can be added together into one influence function by means of summation. This leads to a flat plane in a 3D space. As was determined in Section 7.4, a much better approximation is a multiplication of both influence relations. The difference in a 3D space is given in Figure 8.1. If independence is assumed when in fact a multiplication is the better relation, the results of the combined influence are less accurate.

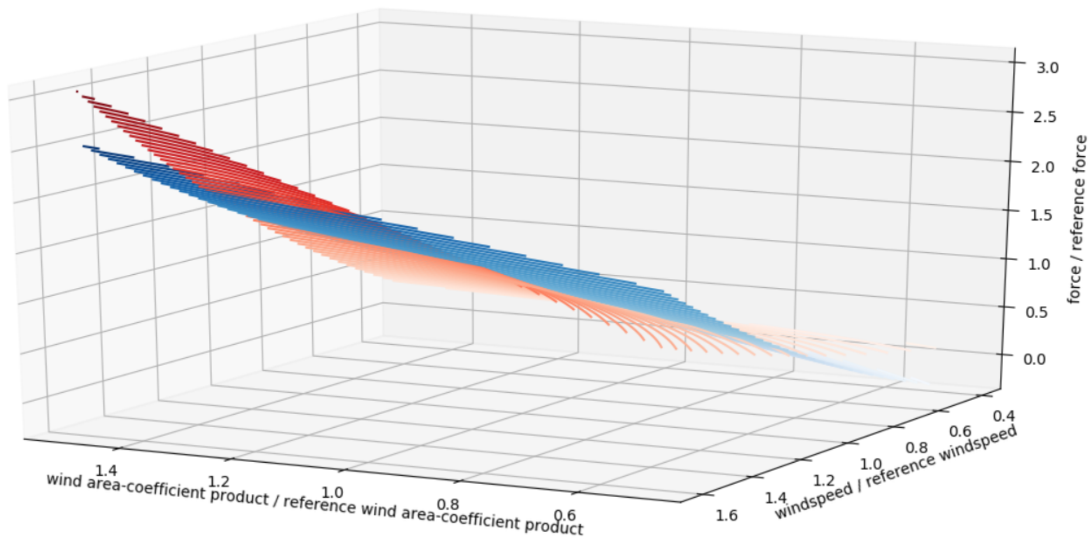

Figure 8.1: Influence of wind area-coefficient product and wind speed on peak line forces with in blue: simple summation of both influence relations and in red: multiplication of both influence relations

This principle, here described in 3d, holds for all relevant dimensions in the prediction polynomial. Given 6 terms are used in Equation 7.10 to predict the peak line forces, this results in a 7 dimensional system. In the current approach only the 2D line linking each term with the peak line force is defined using the reference case as the origin. The relation between these terms is now assumed to be a plane. Investigating the covariance between parameters would increase the accuracy of the definition of the shape of these planes.

8.3.3 Used method with constant damping ratio creates less clear feeling for influence

The chosen approach to maintain a constant damping ratio decreases the clarity of the influence of different parameters as all mass and spring related dependencies are also incorporated in the damping via the damping ratio. A more clear image could be found by defining the damping as an absolute independent variable. However, this can lead to over damped systems for certain combinations of parameters and to numerical instability for other cases.

8.3.4 Influence of wind area and coefficients may indicate largely linear system

As the influence of the wind area-coefficient product approaches a proportional relationship, questions can be asked on the influence of the non linearities on the final results of the system. If these non linearities could be neglected, the system could be investigated in the frequency domain, discarding the necessity of numerical modelling. However, this proportionality is not a direct result from the response but is based on the extreme value analysis of the peak line forces. Furthermore, this is the results for a single reference case and can vary for other cases. Therefore, based on the obtained results only, it is not wise to approximate the system as linear and switch to analysis in the frequency domain.

8.3.5 Uncertainties input parameters

Apart from all method and analysis related uncertainties there are of course also uncertainties related to the input parameter. This is important to keep in mind as they can become limiting to the performance of line force prediction methods. A method can only become as good as the input it is based on. Therefore, this can become a limiting factor for the performance of methods. The uncertainties can be divided into two groups: first order uncertainties and second order uncertainties. The first order uncertainties are uncertainties in measurable input data such as vessel dimensions and mooring configurations. The second order uncertainties relate to to the methods used to determine certain input parameters such as the mass (computed from water displacement) and damping (computed using hydro dynamical approximations.) A qualitative assessment of both types of uncertainties is given in Appendix C.

9. Conclusions and recommendations

Having discussed the results, conclusions and recommendations for further research can be formulated.

9.1 Conclusions

To determine the answer to the research question, firstly, all sub questions are answered.

1. **What are the essential parameters required to compute the maximum mooring forces from a container vessel in wind forcing?**

   As presented in Chapter 4, a number of influence parameters are used to determine the dynamic response of a moored vessel system and the occurring line forces. These parameters are related to the quay, the vessel, the water, the line or the wind. The most important influence parameters for determining the maximum occurring line forces were, as presented in chapter 7, the damping ratio, the mean wind speed, the wind area and coefficients, the force elongation curve of the lines, the horizontal and vertical line angles and the line lengths.

2. **How can the dynamic response be modelled?**

   The dynamic response of a moored vessel can be modelled in the time domain as described in chapter 5. Important here are the simplifications made to the system to allow for time efficient modelling while maintaining the important properties of the modelled system. As no real life measurements of large container vessels in wind fields were available, the validation was executed based on theoretical solution in case of particular linearised system conditions.

3. **How can the influence on the mooring forces of the different parameters be determined?**

   Important here is the fact that using wind time series generated from theoretical wind fluctuation spectra with random phase shifts between harmonics, results in a need for an extreme value analysis approach. Simply using one run per simulation will result in large uncertainties regarding the actual peak line forces. Using this method, all parameters can be kept constant while varying only one of the parameters. By doing this, and using the chosen extreme value analysis approach, the influence per parameter can be found.

4. **What choices and assumptions must be made and what are their influences on the maximum mooring forces?**

   As not all input is fully known when a situation is modelled using dynamic mooring analysis, some assumptions are needed. Their influence was investigated and described below:

   - The variation of the wind field over the vessel length is an important influence on the peak line forces.
   - Vertical variation of the wind field causing roll moments appears to have no significant influence on the peak line forces
   - The choice of theoretical wind spectrum can have a significant influence on the peak line forces
   - Possible errors in added mass/moment of inertia terms, damping and choice of wind coefficients influence the result via the influence determined in the further questions.

5. **How can the influence of the parameters be quantified by regression analysis of a set of dynamic mooring simulations?**

To determine the influence of the individual parameters, simulations were executed in which all parameters were kept constant and only the parameter of interest was varied. As described in Chapter 7, a first or second order polynomial was formed for each influence parameter based on the ratio between the used input and the reference input. In doing so, the individual influences of the parameters on the reference case are quantified.

6. **How can maximum line force be predicted without using full case specific dynamic mooring simulations?**

   Combining the separate influence relations to one prediction polynomial, a first proposal for a peak line force estimation formula can be created, as presented Equations 9.1 through 9.7.

$$\frac{F}{F_{res}} = ACU + K + L^* + \zeta^* + \beta^* + \alpha^* \tag{9.1}$$

$$ACU = (0.95\frac{AC_{used}}{AC_{ref}} + 0.05) * (0.49(\frac{u_{wind}}{15})^2 + 0.61\frac{u_{wind}}{15} - 0.1) \tag{9.2}$$

Where:

$$K = -0.179(\frac{MBL}{142})^2 + 0.70\frac{MBL}{142} - 0.505 \tag{9.3}$$

$$L^* = -0.22\frac{L_{breast}}{55.13} + 0.25 \tag{9.4}$$

$$\zeta^* = -2.11\zeta + 0.21 \tag{9.5}$$

$$\beta^* = 0.12(\frac{\beta}{31.16})^2 - 0.06\frac{\beta}{31.16} - 0.06 \tag{9.6}$$

$$\alpha^* = 0.124(\frac{\alpha}{34})^2 - 0.42\frac{\alpha}{34} + 0.3 \tag{9.7}$$

Where:

F_{res} = 650 kN

u_{wind} = mean wind speed in m/s

MBL = minimum breaking load in tonnes

L_{breast} = length breast lines in m

ζ = damping ratio

β = vertical line angle in degrees

α = horizontal line angle in degrees

The answers to all sub questions lead to an approach for the determination of a peak line force prediction formula, which can be used to approximate the occurring peak line forces for a large moored container vessel in time varying wind fields. Using such a formula will increase efficiency in the analysis of these cases. This will result in larger accessibility to include dynamic aspects in operational risk assessment, quay design and choice of mooring lines and arrangement. The acquired first proposal for a line force approximation polynomial performs reasonably well, compared to the results of the conceptual model, for mooring cases in which especially the mooring line angles are relatively close to the used reference case situation. For these cases, a first analysis of accuracy resulted in maximum deviations from the conceptual model results of less than 15%. The polynomial is especially limited for cases in which very small peak line forces occur. This limit is irrelevant in reality. Considering that this method is used to determine if the ultimate limit state of the system is exceeded, cases with very small line forces are unimportant.

Using the polynomial will decrease time per mooring case significantly. The mooring line angles and lengths can be determined based on the mooring configuration and deck plan, the added mass, moment of inertia and damping must be determined using simple hand calculations or software packages, and all values are used as input for the polynomial and a first estimate of the mooring line forces is determined based on wind predictions. This is doable within a half day excluding client contact and reporting. Compared to the one week analysis period needed for current dynamic mooring analysis as is executed by RHDHV, this is a large increase in efficiency. When a case is analysed it is also very easy to determine different variants within a few minutes by changing input values, keeping the limits of the polynomial in mind. This makes the method more easily scalable applying one vessel to different quays or different vessels to the same quay. The increase in efficiency and scalability comes at a price: time is needed for research and development of this method. Finally, main research question has been answered: **How**

can safe mooring windows, based on maximum mooring forces due to the dynamic response of a moored container vessel, subjected to time varying wind forcing, be approximated without using full case specific dynamic mooring analysis simulations?

The maximum peak line forces for large container vessels in time varying wind fields can be estimated using the proposed polynomial combined with input information on wind area, wind coefficients, predicted mean wind speed, mooring configuration, line types, damping, mass and moment of inertia including the added mass and moment of inertia. For cases similar to the reference case a safety margin of 15% should be applied. For cases which are not similar to the reference case, larger errors in the polynomial performance occur.

9.2 Recommendations

As described in the discussion and conclusion, the proposed peak line force estimation polynomial described in Chapter 7 is a first estimate. Therefore, a number of recommendations are described which can be used to further investigate the influence of the different parameters on the peak line forces as well as increasing accuracy for current dynamic mooring analysis approaches.

9.2.1 Recommendations for current dynamic mooring analysis practices

In Chapter 6, the industry standard assumptions were discussed and their influence was investigated. A number of recommendations follow from this assessment.

- Start measuring large container vessel movements at quays during strong wind conditions. A simple measuring system to easily and cheaply gain vessel movement measurements would help in different areas and create feedback to assess quality of advice. Furthermore, if measurements of the movements can be combined with the used mooring lines, mooring configuration and relevant vessel and quay information, the theoretical models now used can be validated with real life full size measurements.

- Investigate the convergence of the extreme values for different random seeds. Include an extreme value analysis method for all dynamic mooring assessment projects to obtain more stable and accurate results.

- Investigate the real life occurrences of spatial variability over the vessel length of the wind field. As described in Chapter 6, this can be an important influence on the maximum occurring line forces.

- Investigate per case which theoretical wind spectrum is most accurate. As described in Chapter 6, different theoretical spectra can lead to different peak line forces. It is possible to always choose the safest option (the spectrum which results in the largest force). However, when a less critical spectrum is more accurate for the situation, this will lead in lower limiting wind speeds and can result in less conservative estimates.

9.2.2 Recommendations for determining a peak line force prediction polynomial

For further research into peak line force predictions without using complete dynamic mooring analysis, a number of recommendations are made to find well performing and realistic line force prediction polynomials.

- Investigate possibilities of frequency domain analysis of a linearised representation of the moored vessel system. If the peak line forces can be approximated using a linearised representation of the moored vessel system, this can result in more time efficient analysis.
- Investigate use of implicit methods for the numerical solvers. As implicit methods can allow for larger time steps, while requiring more computation time per step, it is possible that overall computation time could be reduced by using implicit methods.
- Investigate more reference cases using the conceptual model used in this study to create multiple polynomials for different, often occurring mooring cases. Compare accuracy to dynamic mooring analysis and check the deviations to see if these are already usable.
- Use a more advanced dynamic mooring analysis model. By using a more advanced mooring analysis model than the conceptual model used in this study, more accurate results can be obtained. This will ensure more realistic results on which the further analysis can be based. Using more realistic models therefore result in more realistic approximations by a polynomial.
- Execute more different simulations than used in this study. Using more simulations will result in a better fit for the influence relations. Doing this not only by varying one parameter from the reference case, but by using different realistic combinations of the input parameters, a more general dataset is created for analysis.
- Investigate covariance between input parameters. Using a more general dataset it is possible to further investigate the planes between the now determined influence relations. The multivariable regression can be executed using supervised machine learning methods, using dynamic mooring analysis results as training sets. When a polynomial is found based on this training dataset, the result must be checked using a different test dataset.
- In applying both regular dynamic mooring analysis and a prediction polynomial be aware of uncertainties in input parameters like wind coefficients and wind predictions. These uncertainties can also be limiting for the performance of models and formulas. Investing time in further improvement of accuracy while the uncertainties in the input are in fact the critical limitations should be avoided.
- Keep relating the theoretical and computational world to the real world. Using expertise, possible measurements and real life experience from operational experts, keep checking model results with what is realistic.
- Determine the benefits of the use of a polynomial in efficiency and scalability and compare them to the costs of further development. From a business point of view, this cost-benefit analysis is essential. However, I think the possibilities for implementations, especially in software products presenting in one view which vessels are in danger during a predicted storm in a harbour, outweigh the costs of development.

A. numerical modelling theory

Here a more in depth explanation of the three considered numerical solvers is given. First the Forward Euler method is considered, next RK2 and finally RK4.

A.1 Numerical methods

The three assessed explicit numerical solvers are described.

A.1.1 Forward Euler

The first and most basic approach for numerical modelling is the Forward Euler method. The Forward Euler method uses the slope of the curve, or derivative, at a certain known time to predict the next state of the system. Then the new state is taken as the known state and its derivative is used to determine the next state. The Forward Euler method, also called RK1, is a first order method which means the local error is proportional to the step size squared resulting in a global error proportional to the step size.

To apply the Forward Euler method on a second order "ordinary differential equation", or "ODE", the second order ODE's must be split into two first order ODE's. In case of a 1 DOF mass spring system with viscous damping the equations of motion can be written as in equation A.1. This second order ODE's can be split in two first order ODE using Equations A.2 and A.3.

$$\ddot{x} + 2\zeta\omega_n\dot{x} + \omega_n^2 x = F(t)/m \quad \text{(A.1)}$$

$$\dot{x} = u \quad \text{(A.2)}$$

$$\dot{u} = \frac{F(t)}{m} - 2\zeta\omega_n u - \omega_n^2 x) \quad \text{(A.3)}$$

Now for each time step both first order ODE can be subjected to the forward Euler method resulting in Equations A.4 and A.5. The Forward Euler method is graphically explained for an arbitrary curve in Figure A.1

$$x_1 = x_0 + hu_0 \quad \text{(A.4)}$$

$$u_1 = u_0 + h(\frac{F_0}{m} - 2\zeta\omega_n u_0 - \omega_n^2 x_0) \quad \text{(A.5)}$$

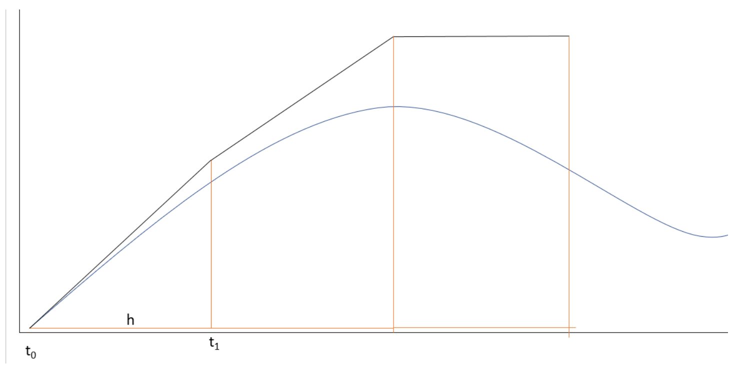

Figure A.1: Example of Forward Euler workings for an arbitrary curve

A.1.2 RK2

As can be seen from Figure A.1 the use of only the derivative at t=0 can lead to significant errors for large step sizes h. One can instead decide to add an extra step to the Forward Euler method. Equations A.4 and A.5 are used to compute the first estimates of the next state of the system. The derivative for this new state is computed and the two derivatives are averaged to obtain a more accurate estimate of the new state.

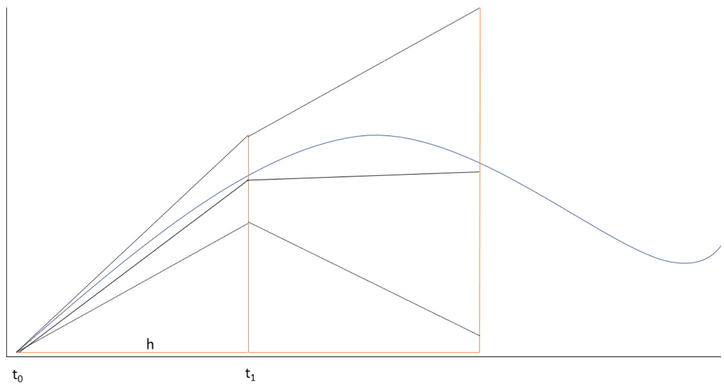

Figure A.2: Example of RK2 workings for an arbitrary curve

A.1.3 RK4

The RK4 method applies a similar technique as RK2 but using two extra derivatives at half a stepsize. The approach is schematized in Figure A.3

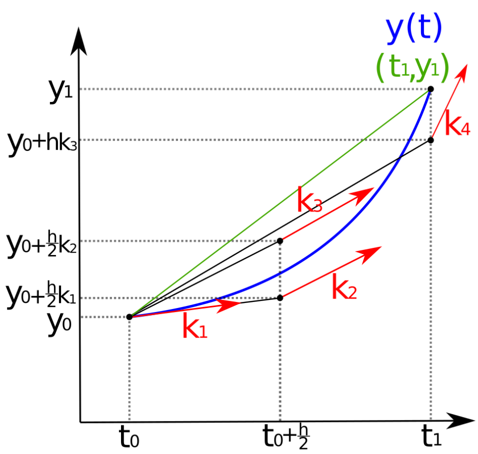

Figure A.3: Example of the RK4 method (Schmiedel 2019)

A.2 Comparison

Forward Euler, RK2 and RK4 are explicit methods which are based on the same principle: determine the derivative of a function at t_n and using a time step dt computing the state at t_{n+1}. However, RK4 iterates this process four times to increase accuracy whereas Forward Euler only considers one derivative and one time step. All three numerical solvers were applied to solve a single degree of freedom mass spring system with viscous damping and harmonic forcing. To compare the computation time of each method, a base case was used to determine the step size needed for each method to achieve a root mean square error of approximately 1 mm, which is sufficiently accurate for a system which knows responses of order of significance of decimeters. Then the computation time was measured for the execution of the numerical solving, using each method and a time series length of 100,000 seconds. This resulted in a computation time of 38 seconds for Forward Euler, 11 seconds for RK2 and 43 seconds for RK4. Therefore, RK2 is chosen as the best solving method as it has the least computation time to get to accurate results.

B. Verification of separate modules

Here the verification of the different components as shown in Figure 5.11 is presented. The verification of the numerical solvers is presented in appendix A

B.1 Verification Harris wind spectrum

A Forward Fourier Transform was executed on the time-series to check whether the time series actually matches the spectrum. This is displayed in Figure B.1. As the Harris formula is defined in rad/s this is used in Figure 5.9, whereas other spectral analysis is displayed in Hz as this gives a more direct feeling for frequency and period. The spectral analysis gives a good match with the theoretical spectrum from which it is generated. Therefore, the Harris wind time series generation performs as expected.

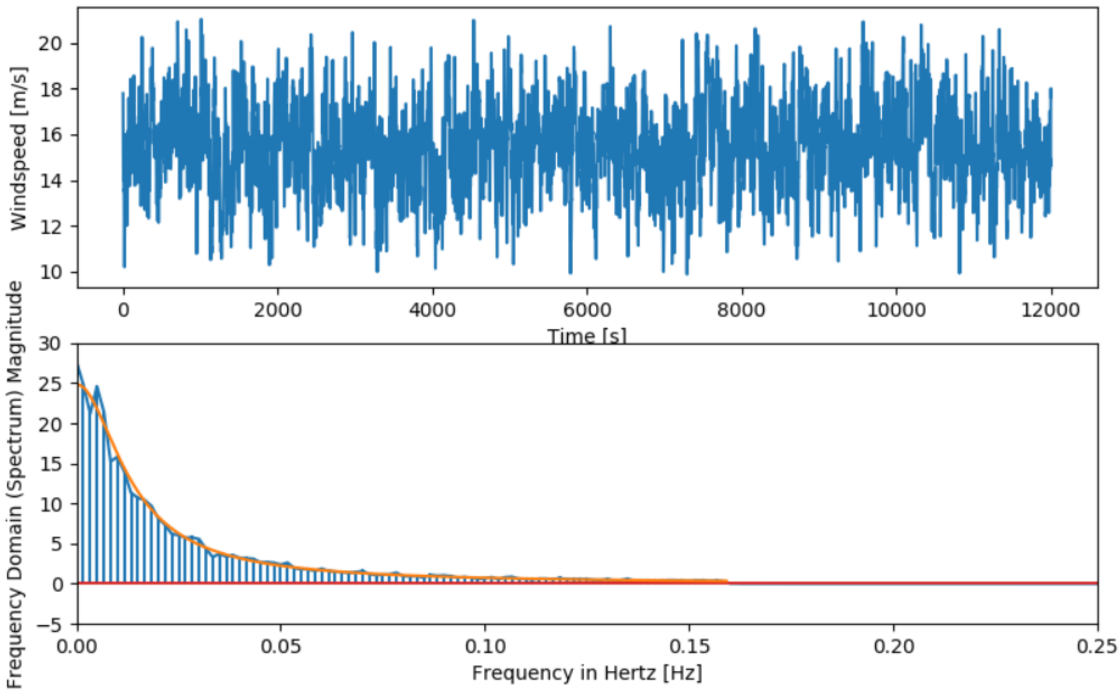

Figure B.1: Wind time series and spectral analysis

B.2 Verification wind coefficient interpolation

To verify the interpolation component for the wind coefficients, a test is executed inserting every direction with steps of 1° to check if no strange deviations occur from the curve defined by the used 10° step size coefficients. No strange deviations were found and the wind coefficient interpolation model works as designed.

B.3 Verification slack line lengths, line forces and moments

To verify the line length and force computations along with its decomposition, the different directions and the resulting moments, an excel sheet is made to determine the angles and distances between two points for different bollard, fairlead position combinations. These results are compared to the line lengths and angles at certain positions during the simulation. The values determined using the excel sheet match the model results. Therefore, the angles and line lengths are determined as expected. To translate the lengths to forces, the elongation must be determined. The slack line length determination module is checked for certain initial line lengths dependant on the initial conditions. This determination functions as expected. Important to note is the elongation related to the pretension is a hard coded value and does not change automatically with changes in the force elongation curve. To check the workings of this force elongation, a list of different elongations is put into line characteristic module and the results are plotted. This can be seen in Figure B.2. Important to note is that for negative elongations the force is 0, lines do not exert compressive force, and outside the specifically defined curve (in this case values are defined between 0 and 0.12 elongation) the curve is extrapolated linearly based on he slope at the end of the spectrum. As all angles and forces are known these can be decomposed in x, y and z forces according to the orientation of the earth fixed coordinate system. This decomposition was checked and works as expected. The fairlead positions and the ship's orientation are used to determine the moments, yaw and roll, on the vessel. These moments are checked focussing extra on the positive and negative directions. This also functions as expected. Therefore, the force and moment determination functions as expected. Important to note is that linear fender characteristics are used and fenders are grouped in a number of point fenders spaced along the relevant length of the quay equally.

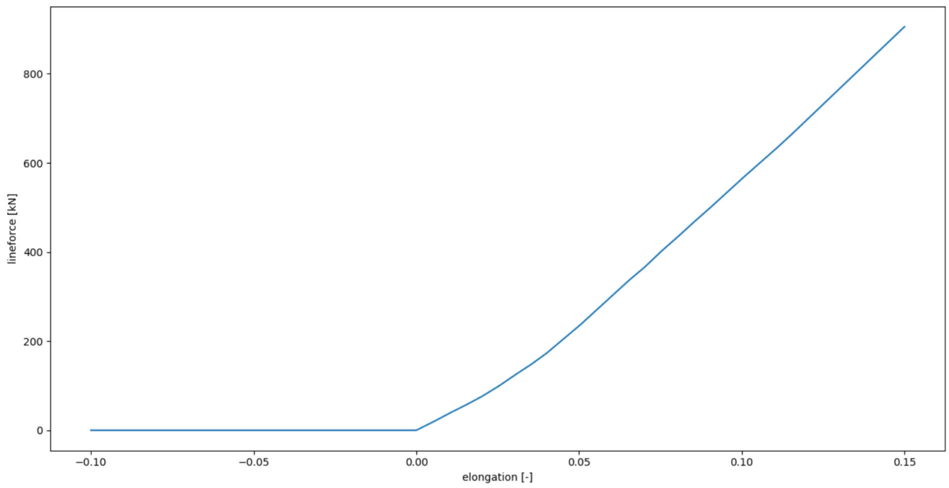

Figure B.2: Force elongation curve

B.3.1 verification of Scribanti module

The Scribanti module is checked for different input values of vessel dimensions and roll angle. This is compared to hand calculations and the results match. For small angles, the Scribanti formula can be approximated by a linear spring as can be seen in Figure B.3. This option is added to the Scribanti module so run time can be reduced for cases in which only small roll angles are expected. For angles smaller than 7° in this case, the linear approach results in an underestimation of less than 4%. In reality the vessel is not wall sided over the complete length and the waterline does not follow a rectangular shape. The waterline coefficient, described in Subsection 2.5.3, will reduce the roll stability. However because vessel becomes increasingly wider at the flares, the change in center of buoyancy is more sensitive to roll angles than for the wall sided parts. This, to some extend, counters the decrease in stability caused by the waterline coefficient.

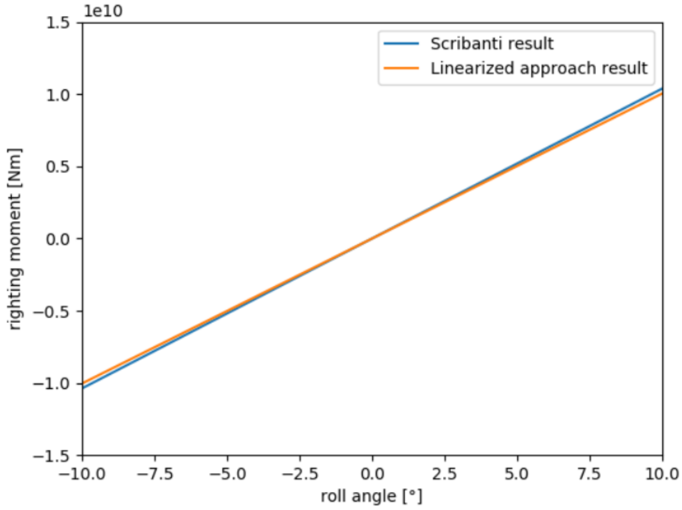

Figure B.3: Scribanti calculated righting moments as function of roll angle.

C. First and second order uncertainties

The influence and related limitations of different uncertainties is described in 8. Here a qualitative assessment of these uncertainties is given.

C.1 First order uncertainties

In this case, the first order uncertainties are the uncertainties inherent to the input parameters. These uncertainties are presented in table C.1.

Parameter	Uncertainty
Wind predictions	large
Weight distribution	large
Line info	medium
Draught	medium
Length	small
Beam	small
Water level	small
Quay lay-out	small
Deck plan	small
Mooring configuration	small

Table C.1: First order parameter uncertainties

Looking at Table C.1, some extra explanation is given.

- Mean wind speed predictions vary in accuracy over the world. Different climates call for different prediction methods and different methods result in different accuracy. Errors in both speed and direction are present and increase in more complex weather systems. As the wind speed and direction are essential parameters in the determination of line forces this is an important uncertainty to consider.
- The weight distribution on the vessel changes during the loading and unloading and requires very detailed information of container lay out and weight to determine. The uncertainty in the mass distribution is therefore quite large.
- Line information is usually available in terms of which line type is used and what its minimum breaking load is. However, the minimum breaking load is a guarantee from the manufacturer about the strength of a new line. Use of old and worn down lines can decrease the actual breaking load drastically. The line information is therefore fairly uncertain
- The draught varies during the loading and unloading and also depends on the weight of the containers. In dynamic mooring analysis, the critical draught cases are used for evaluation. However, this is often an estimate which implies some uncertainties present.
- All other parameters can be known accurately provided that proper contact between the different parties is present. The vessel captain should share its plans regarding mooring configuration and deck plan, the port authority the precise quay lay out and an accurate water level predictions should be acquired.

C.2 Second order uncertainties

The second order uncertainties are related to the calculation of parameters which depend on first order input parameters. For example: the mass of the vessel is calculated based on the dimensions and the draught of the vessel, whereas the inertia is also based on the weight distribution.

Parameter	**Uncertainty**
Wind area	small
Wind fluctuation spectrum	medium
Mass	medium
Inertia	medium
Wind coefficients	medium
Added mass/inertia	large
Damping	large
Spatial wind variance	large

Table C.2: Second order parameter uncertainties

Looking at Table C.2, some extra explanation is given.

- The wind area can be computed based on the expected loading conditions. It does vary during loading and unloading but a critical situation can easily be determined (fully loaded). The effective wind area also depends on the draught and quay height including sheltering. Therefore, some uncertainty is present but this uncertainty is generally small.
- The theoretical wind fluctuation spectrum is chosen based on the conditions at the quay such as doe the quay lie at open sea or further inland. This is always an approximation and therefore includes a significant uncertainty
- The mass is computed using the draught which varies during the loading or unloading of the vessel. Therefore, the uncertainty in draught results in an uncertainty in mass.
- Inertia is usually approximated using approximation equations relating the so called radius of gyration used to compute the inertia to the length and beam of a vessel. This are global approximations as for the precise inertia computations the exact mass distribution must be known. As this is normally not the case, significant uncertainty is present in the inertia input.
- The wind coefficients are generally based on wind tunnel studies or computational fluid dynamics for comparable vessels. In reality, the relevant vessel is not exactly equal to the reference vessel resulting in significant uncertainty.
- The added mass and inertia are based on hydrodynamic approximations which incorporate many input parameters such as water level, draught, quay shape and response frequency. The combination of all these parameters with different uncertainty results in a large uncertainty regarding the added mass and inertia. This also holds for the damping term.
- The actual spatial wind field variance at a quay is usually unknown and therefore assumed constant. The fact that the actual spatial wind variance is unknown results in a large uncertainty.

References

Bartholomä, R. (2015). Wind tunnel studies ultra large container vessels.

Blendermann, W. (1994). *Parameter identification of wind loads on ships* (tech. rep.).

Blocken, B., Stathopoulos, T., Asce, F., & Carmeliet, J. (2008). Wind environmental conditions in passages between two long narrow perpendicular buildings. *Journal of aerospace engineering - ASCE 2008 volume 21, issue 4, pp. 280-187*.

Boettcher, F., Renner, C., Waldl, H.-p., & Peinke, J. (2003). *On the statistics of wind gusts* (tech. rep.).

Chakrabarti, S. (2001). Empirical calculation of roll damping for ships and barges. *Ocean Engineering*, *28*(7), 915–932. https://doi.org/10.1016/S0029-8018(00)00036-6

Coelingh A', J. P., Van Wijk, A. J. M., & Holtslag, A. A. M. (1996). *Analysis of wind speed observations over the North Sea* (tech. rep.).

Gadelho, J. F., Rodrigues, J. M., Lavrov, A., & Guedes Soares, C. (2018). Heave and sway hydrodynamic coefficients of ship hull sections in deep and shallow water using Navier-Stokes equations. *Ocean Engineering*, *154*, 262–276. https://doi.org/10.1016/j.oceaneng.2018.02.025

Janssen, W. D., Blocken, B., & van Wijhe, H. J. (2017). CFD simulations of wind loads on a container ship: Validation and impact of geometrical simplifications. *Journal of Wind Engineering and Industrial Aerodynamics*, *166*, 106–116. https://doi.org/10.1016/j.jweia.2017.03.015

Journée, J. M. J., & Massie, W. W. (2001). *Offshore hydromechanics, First Edition* (tech. rep.).

Kaasen, K. E. (1999). *"Time Domain Model Representations of Standard Wind Gust Spectra."* (tech. rep.). Brest, France, .

Kriebel, D. L. (1999). *Added mass and damping characteristics for multiple moored ships* (tech. rep.).

Ostertagová, E. (2012). Modelling using polynomial regression. *Procedia Engineering*, *48*, 500–506. https://doi.org/10.1016/j.proeng.2012.09.545

PIANC. (2012). *Criteria for the (Un)loading of Container Vessels the* (tech. rep.).

Schmiedel, B. (2019). Runge-Kutta 4th order scheme. https://lowebms.readthedocs.io/en/latest/code/rk4.html

Stanisic, D., Efthymiou, M., Kimiaei, M., & Zhao, W. (2017). *Evaluation of conventional methods of establishing extreme mooring design loads* (tech. rep.).

van der. Molen, W. (2006). *Behaviour of moored ships in harbours.* University of technology.

van Scherpenzeel, B. (2011). *Richtlijnen Afmeervoorzieningen Rotterdam* (tech. rep.). Havenbedrijf Rotterdam.

Zwijnsvoorde, T. V., Donatini, L., Hoydonck, W. V., & Lataire, E. (2019). Wind modeling for large container vessels: A critical review of the calculation proce dure. *International Journal of Transport Development and Integration*, *3*(4), 369–381. https://doi.org/10.2495/tdi-v3-n4-369-381